A Structural and Stratigraphic Study of the Keewatin-Type and Shebandowan-Type Rocks West of Thunder Bay, Ontario

A thesis submitted in partial fulfillment of the requirements for the degree of Master of Science

Lakehead University

G. Heather Brown ©

August, 1985

Abstract

Detailed mapping was carried out in the Shebandowan Lakes area and eastward to the Kaministiquia River to study the structural and stratigraphic relationships between the Keewatin and Timiskaming rocks (herein referred to as Keewatin-type and Shebandowan-type, respectively, to avoid connotations of time-stratigraphic equivalence with type areas) of the region.

It is believed that the Shebandowan-type rocks are younger than the Keewatin-type rocks. Although no actual contact between the two has been seen in outcrop in the study area, the trend of their contact is discordant with the trend of cleavage in the Shebandowan-type rocks. This, along with the less recrystallized appearance of the Shebandowan-type rocks, and the presence of clasts of jasper in conglomerates of the Shebandowan-type sequence similar in appearance to the jaspilitic iron formation interbedded with the Keewatin-type mafic volcanics, leads to the conclusion that an unconformity separates the two groups of rocks. Recent geochronological work on some of the rocks in the region, carried out by the Ontario Geological Survey, supports this theory.

The macroscopic, microscopic and sub-microscopic structure of both groups of rocks was examined in detail. The minor structures seen in outcrop, the examination of thin sections, scanning electron microscope work, and the

determination of the magnetic fabric of the rocks all show that the rocks in the present study area contain a single, penetrative, primary cleavage, which has a consistent trend across the whole area. The regional structural picture which emerges from the data is characterized by close-spaced, isoclinal folding with sub-vertical fold axial traces trending roughly east-west. Local variations exist in the eastern portion of the study area where more widely-spaced and open folding is more common. No evidence of a second, significant period of deformation in the present study area has been found.

Acknowledgements

I would like to thank Dr. G.J. Borradaile for his supervision, advice and patience. Advice and help was also generously offered by Dr. M.M. Kehlenbeck. Dr. P. Fralick aided in some of the petrological studies of the sedimentary rocks.

I am also indebted to numerous employees of the Ontario Geological Survey for advice, discussion, help and, again, patience and understanding. These include Dr. A.C. Colvine, Dr. L.B. Chorlton, Dr. M.W. Carter, Dr. G.M. Stott, Dr. P. Thurston, Geri Atkinson, Joan Van Kralingen and Iva Sherrett.

My sister-in-law, Debbie Brown, quickly and proficiently typed the majority of this thesis, usually under extreme time constraints, for which I am extremely grateful. Susan Koski was also quick to offer typographical aid when it was needed most.

Finally, several friends and relatives must be acknowledged who helped me in various ways, not least of which was being always ready to listen and never losing faith in me; John Scollie, Patricia Perry, Karen Roche, my sisters Carol Spearn and Debbie Blakey, and my brother-in-law, Scott Blakey.

This research was supported by Dr. G. Borradaile's N.S.E.R.C. grant #A6861.

TABLE OF CONTENTS

LIST OF FIGURES

Page

Introduction

The problem addressed in this thesis concerns the stratigraphic and structural relationship between two groups of rocks that comprise part of the Shebandowan greenstone terrain, west of Thunder Bay, Ontario. This terrain constitutes part of the Shebandowan-Wawa volcanic-plutonic subprovince, or "superbelt", of the Superior Province of the Canadian Shield. One group of rocks in the Shebandowan greenstone terrain is the predominantly metavolcanic sequence of rocks generally known under the name "Keewatin", the other is the predominantly metasedimentary sequence generally known as the "Timiskaming". While these terms are in common use, and date from the pioneering work in the Shield by A.C. Lawson at the turn of the century, they do not satisfy modern international stratigraphic codes. To expand further, neither the bases nor the tops of these "formations" or "groups" are known, and the internal structure is so complex that the "groups" defy any immediate stratigraphic analysis into stratigraphic columns. Furthermore, there is little justification for correlating these rocks with the rocks, elsewhere, originally labelled "Keewatin", etc., for there is no way of tracing the rocks continuously across the Shield to the type localities, nor, of course, is there any circumstantial evidence for the correlation other than by broad lithological similarity. It should be noted, also, that even in type areas such as at Rainy Lake it has only recently been possible to evaluate the structural ordering of the sequence using modern methods (Poulsen, Borradaile and Kehlenbeck, 1980).

The areas of outcrop of the rocks in question, as they are shown in Figure I-1, were first delineated in 1965 by the Ontario Department of Mines on a geological compilation map (Pye and Fenwick, 1965). Notwithstanding the comments above, the unit marked "metasediment/metavolcanic" has been compared to the Timiskaming rocks of the Kirkland Lake area by various workers (Watson, 1928; Shegelski, 1980; Stott and Schnieders, 1983). From the literature it is true that the mineralogical and textural similarities between the rocks of the two areas seem remarkable (Shegelski, 1980). As a result, other authors have extended the assumed temporal relationship in the Kirkland Lake area (younger Timiskaming unconformably overlying older, basement Keewatin) to the rocks of the Shebandowan Lakes area as well. Clearly, the scientific basis for this is weak.

Many of the workers in the area believe that features such as large-scale truncation of Keewatin structural trends by Timiskaming structural trends

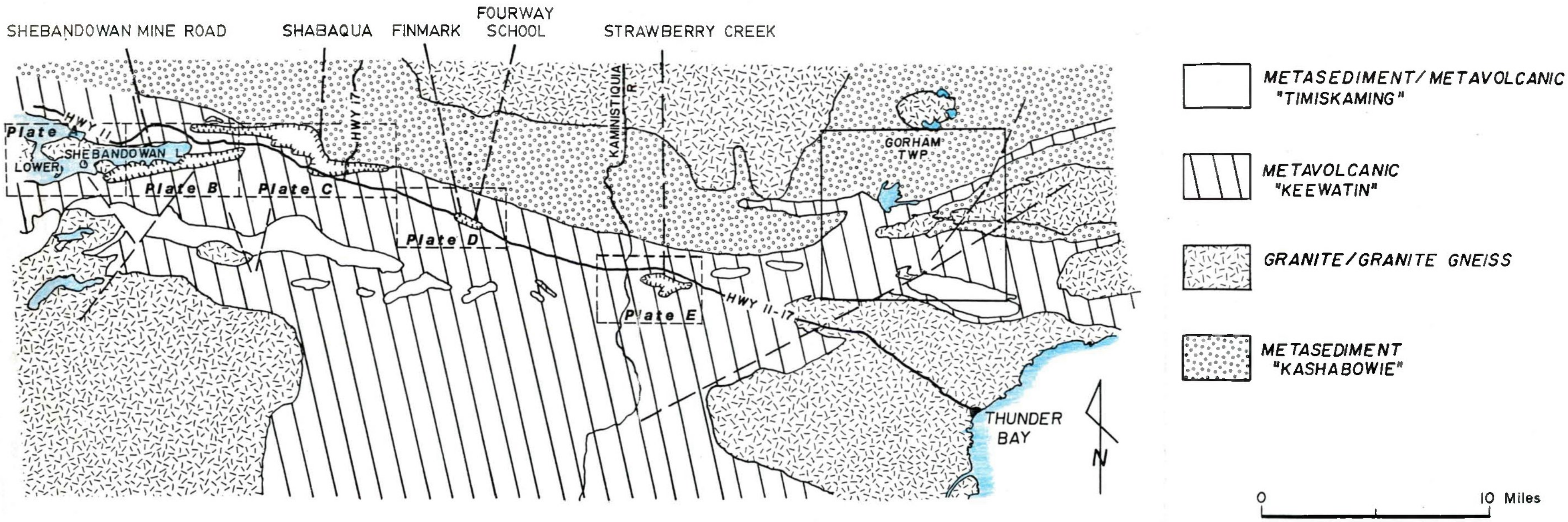

Figure I-1: General geology and location map of the study area. The rock unit left unornamented is the unit of interest. Those outcrop areas of this rock type with hachured boundaries (⊥⊥⊥⊥) denote the areas treated in this thesis. (Geology generalized from Ontario Geological Survey Compilation Map 2065, Atikokan-Lakehead Sheet, Pye and Fenwick, 1963)

(Shegelski, 1980), the relatively undeformed appearance of the Timiskaming rocks (Stott and Schnieders, 1983) and the presence in the Timiskaming conglomerates of clasts of jaspilitic iron formation similar to that interbedded with the Keewatin volcanics (Ibid) represent evidence in support of this proposed relationship. However, at least one worker considers the rudaceous and arenaceous rocks being compared to the Timiskaming, as coeval with the older metavolcanic rocks (Morton; 1979, 1982).

Another matter of controversy for some time centres on the classification of the various rock types of the area into either the older sequence or the younger sequence. One unit in particular has been consecutively called a felsic agglomerate of the Keewatin succession (Watson, 1928), a conglomerate of the Timiskaming succession (Morin, 1973), a volcanic breccia of the Timiskaming succession (Shegelski, 1980), and a laharic deposit coeval with the Keewatin succession (Morton, 1982).

Finally, the earlier views of the structure of the area being singly-deformed, isoclinally-folded sequences (Watson, 1928; Tanton, 1938; Morin, 1973) have been supplanted by the proposal that two, and possibly three, deformation events are recorded in the rocks of the area (Stott and Schwerdtner, 1981; Morton, 1982; Stott and Schnieders, 1983). In particular, Stott and Schwerdtner (1981) and Stott and Schnieders (1983) have proposed that the Shebandowan area (see Figure I-2 for the extent of the area they refer to) can be separated into zones where evidence of an earlier period of deformation is preserved and zones where evidence of a second later period of deformation is preserved (so called "D_1" & "D_2"). The location of these proposed zones is based primarily on the change in plunge of mineral lineations, from westerly in the "D_1" areas to easterly in the "D_2" areas. The eastern-most portion of Stott & Schwerdtner's area (see Figure I-2) encompasses the western part of the present study area (see Figure I-1).

An attempt will be made in this thesis to address each of the above problems and, if possible, to resolve them.

Location and Access

The study area lies between 35 and 100 kilometers west of Thunder Bay, Ontario, in the Shebandowan-Wawa sub-province of the Superior Province, Canadian Shield. As mapped by the Ontario Geological Survey on the Atikokan-Lakehead Sheet (see Figure I-1), the rocks concerned show up as roughly elliptical-shaped areas of predominantly metasedimentary rocks (so-called Timiskaming) surrounded by predominantly metavolcanic rocks (so-called Keewatin) from the Shebandowan Lakes (Upper, Middle and Lower) to Gorham Township. For the most part, access to the area is quite good. Highways 11, 17 and 11-17 transect the region as do several old logging roads, hydro-electric, gas and telephone lines. However, the portions studied were restricted to the better quality exposures along the Shebandowan Mine road and in the Shabaqua, Finmark and Strawberry Creek areas (see Figure (I-1).

Mapping of the area was carried out along roads, hydro-electrical, gas and telephone lines as well as along pace and compass traverse lines conducted between these engineered features. Outcrops were first located on 1:50,000 scale aerial photographs and later transferred to 1 inch to 1/4 mile base maps (Forest Resource Inventory maps). Two hundred and seventy-two hand samples were collected, from which sixty-three thin sections were cut. These formed the basis for the petrographic description of Chapter II. The structural elements of the rocks were measured in the field and later plotted on equal area stereonets. A discussion of the implications of these results is contained in Chapter III. Scanning electron microscope and magnetic susceptibility anisotropy studies constitute the submicroscopic investigations into the fabric of the rocks. Descriptions of the study procedures and the results form Chapter IV.

History of Research

The first major geological report and map of the Shebandowan Lakes area was produced in 1899 by W. McInnes for the Geological Survey of Canada. Typical for the geologists of that era, the area covered in his report was quite extensive; from Lake Shebandowan to

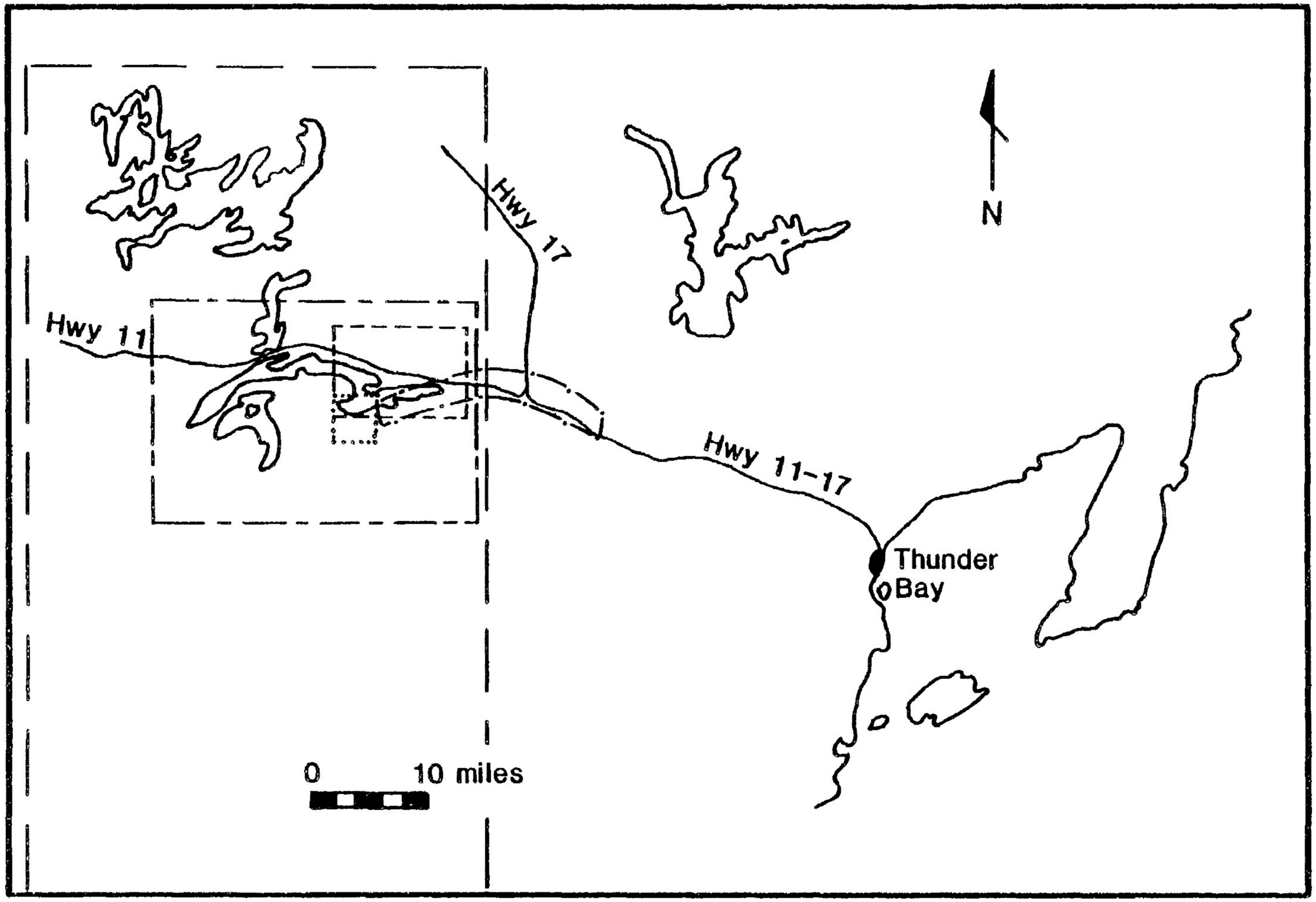

Figure I-2. General area of coverage by prominent previous authors.
—— —— ——Tanton (1938); – – – – – –Morin (1973); —·—·—Shegelski (1980);
—— – —– - Stott and Schwerdtner (1981); ············Morton (1982).

the Seine River, a distance of at least 100 kilometers. As a result, each map unit incorporated large segments of the Shield's stratigraphy and lithology. Outcrops of conglomerate, sandstone and argillaceous "shale" were included in the Keewatin unit because of their limited extent. However, McInnes noted the presence of clasts in the conglomerates which were similar in composition to the Keewatin volcanics themselves. It was concluded that the rocks in this unit varied greatly in relative age.

In 1928, R.J. Watson published a paper in the Ontario Department of Mines' annual report on a nickel-copper deposit on Lower Shebandowan lake (which later developed into the Inco-Shebandowan Mine). He classified the conglomerates, arkoses and greywackes of McInnes' Keewatin as "Timiskamian in age", and tentatively correlated them with T.L. Tanton's (1927) Windigokan Series of the Mine Centre area (to the west of the present study area), because of the similarity between all three. As well, he proposed that an unconformity separated these sediments from the Keewatin volcanics. The scientific basis for these proposals would not stand up to modern scrutiny.

In 1938, Tanton's own mapping of the Shebandowan Lakes area for the Geological Survey of Canada supported Watson's suggested correlation of the Timiskaming sediments with the Windigokan Series. Because of their less recrystallised appearance and relative lack of deformation, the unconformable relationship between these rocks and the underlying volcanics which Watson had proposed was upheld by Tanton. This relationship remained more-or-less undisputed up until more recent years.

In 1965, the Ontario Department of Mines published a map of the Atikokan-Lakehead area which constituted a compilation of information from previously-published government maps as well as mining companies' files. Rock unit names which implied ambiguous, blanketing correlations between wide-spread areas were dropped. "Timiskaming" and "Keewatin" became simply "predominantly metasedimentary" and "predominantly metavolcanic" lithological units. The former was placed stratigraphically above the latter solely on the basis of historical precedent, but no mention of any unconformable relationship between the two was made.

Detailed mapping of the Shebandowan Lakes area in 1973 by J. A. Morin for the Ontario Department of Mines confirmed the relative stratigraphic position of the two units, but resulted in a slight change in the extent of the former Timiskaming metasediments. Morin included in his conglomerate-arkose-argillite unit a rock that had been mapped as part of the older metavolcanic sequence since Watson (1928) first disputed its proposed sedimentary origin. It had been mapped as a volcanic rock rather than a conglomerate because, "... the similarity of the pebbles leads one to believe that this rock is a sheared acid volcanic agglomerate ..." (Watson, 1928). Morin mapped it as a conglomerate and included, in the same unit, a rock described as an oligomictic, orange-brown rock containing angular to subangular clasts of pink hornblende trachyte (Morin, 1973). Consistent top, or younging-of-bed, directions to the north (based on determinations from pillowed volcanics and graded beds) led Morin to propose that the structure of the area was a large isoclinal anticline, the hinge zone of which lay to the south of his map area. All the rocks, therefore, lie on the northern limb of this anticline.

In 1980, R. J. Shegelski worked in the area and he, too, placed the Timiskaming stratigraphically above the Keewatin, on the basis of the "truncation of structural trends in the Keewatin by structural trends in the Timiskaming". He also renewed the suggestion that a major unconformity exists between the two, pointing out the presence of pebbles of jaspilitic iron formation in the conglomerate of the younger rocks which is similar to the iron formation interbedded with the older rocks.

Shegelski's mapping led to the suggestion that, rather than a conglomerate, Morin's "orange-brown" rock was an unsorted volcanic breccia representing a phase of calc-alkalic volcanism in the Timiskaming which postdated the stabilization of a Keewatin "craton" and preceeded the deposition of the Timiskaming rudites, arenites and mudrocks. The reddish pigmentation of this rock (which is also seen in other outcrops of the Timiskaming further to the east of Lower Shebandowan Lake) was thought to be due to hematization of the rocks during red-bed development.

More recently, P. Morton (1979, 1982) studied the mafic and ultramafic rocks in the vicinity of the Inco-Shebandowan mine. As a result of very detailed mapping, she was able to propose a division of the Keewatin metavolcanics into an older and a younger sequence. She considered the sediments previously mapped as Windigokan/Timiskaming to be coeval with the older sequence of volcanics. Mortonalso proposed that the reddened unit at the east end of Shebandowan Mine road (referred to by Shegelski (1980) as a volcanic breccia and Morin (1973) as a conglomerate) was correlative with an unpigmented unit (mapped as a conglomerate by Morin (1973) and a felsic agglomerate by Watson (1928)) which cropped out closer to the mine. It was suggested that these rocks represented the north and south limbs, respectively, of a folded felsic pyroclastic breccia to lahar unit that occurred at the top of the older volcanic sequence. The folding in the area was considered to be isoclinal and Morton proposed that at least two periods of deformation had affected the rocks: an earlier event which produced isoclinal, vertical folds with easterly-trending fold axial traces; and a later event which resulted in a gentle warping, in a north-south direction, of the previous folds.

Structural mapping carried out around the same time by G.M. Stott and W.M. Schwerdtner (1981) also resulted in the suggestion that the rocks of the Shebandowan Lakes area have undergone at least two periods of deformation. Based on differing orientations of mineral lineations supported by magnetic susceptibility anisotropy determinations of the cryptic fabric, Stott and Schwerdtner delineated zones where only a single, earlier deformation was recorded by the rocks and zones where a second structural event had been superimposed on the first. (These "D_1" and "D_2" domains do not correspond simply to the areal distributions of the Shebandowan - type and Keewatin-type rocks.) Late asymmetric S and Z folds, and conjugate kink folds are cited as evidence of a possible third deformation. In a later paper with B.R. Schnieders (Stott and Schnieders, 1983), Stott supports Shegelski's suggestion that the Timiskaming rocks represent a very late-stage manifestation of crustal thickening and craton stabilization (Shegelski, 1980). They propose that this stabilization began either late in the history of the first deformation, or subsequent to it. As before, the lack of a well-developed fabric in the Shebandowan-type rocks, the fairly open nature of many of the folds in them, and the presence of clasts of jaspilitic iron formation in the conglomerates similar to that interbedded with the volcanics, are all cited as supportive evidence for these theories.

Petrology of the Rocks

The rock units of primary interest in the study area have been separated into a predominantly meta-volcanic sequence, which will be referred to as Keewatin-type, and a predominantly metasedimentary sequence, which will be referred to as the Shebandowan-type. The rocks are all Archean in age and have mineral assemblages typical of greenschist facies grade metamorphism. As metamorphism is ubiquitous in this area, the prefix "meta" will hereafter be dropped.

Keewatin-Type

The bulk of the Keewatin-type sequence consists of mafic to intermediate volcanic rocks. Both pillowed and massive flows are present and they vary in relative abundance throughout the area. In some of the larger outcrops where the exposure is better, a gradation from massive base, through pillowed flow, to flow top breccia is evident. Primary textures such as amygdules, hyaloclastite and spherulites have locally been preserved in these rocks. The grain-size is generally fine to medium, but coarser flows are present in small volumes. Phenocrysts of feldspar and horn-blende are common, the former being generally more abundant. Interflow sediments consisting mainly of banded iron formation made up of alternating laminae of magnetite and jasper, plus occasional tuffaceous horizons, only make up a small percentage of the total volume of mafic volcanic rock.

In a typical thin section, feldspar constitutes about 40% of the rock, as phenocrysts and in the matrix. The phenocrysts range in size from a few millimetres to half a centimetre in length. They have been subject to intense saussuritization, leaving very little of the original mineral visible (see Figure II-1, plate 4). Both plagioclase and alkali feldspars are present. Exact amounts of each cannot be determined due to the extent of alteration, however, in relative terms, plagioclase is much more abundant. Elongate, subhedral to ragged-edged crystal shapes predominate for this mineral.

Quartz usually constitutes up to 10% of the rock. It occurs both as a primary constituent in the matrix and phenocrysts, and as a secondary mineral introduced with carbonate into veinlets and fractures. The porphyritic crystals are generally anhedral to subhedral in shape. Some of the crystals appear to have broken edges, while other edges are distinctly rounded. Undulose extinction is common. Phenocrysts of quartz are generally a few millimetres smaller in size than the phenocrysts of feldspar, but in the matrix the fine-grained crystal size is common to both.

Amphibole and, less commonly, biotite, make up the remainder of the major primary minerals in the mafic to intermediate volcanics. They constitute from as little as 5% to as much as 40% of the rock. The amphibole occurs in euhedral to subhedral crystals, often zoned and twinned, (see Figure II-1, plate 6), ranging in size from two millimetres in length to seven millimetres. Very rarely do either of these minerals appear as matrix constituents.

The ratio of phenocrysts to matrix is quite variable in these rocks, but, in general, the phenocrysts constitute 25-35% of the total volume. The mineralogy of the matrix is typically quartz and feldspar with minor to subordinate chlorite, epidote and sericite.

Intermediate to felsic volcanics only make up a small percentage of the Keewatin-type succession. They are spatially restricted to the western-most portion of the study area, and to a small area near the Shebandowan Mine (see Plate A at back). They consist almost wholly of agglomeratic and brecciated deposits with only rare outcrops of massive or pillowed flows (see Figure II-1, plate 3).

The agglomerate is best exposed at the west end of the Shebandowan Mine road. Here, the felsic, feldspar-phyric to massive bombs are up to 30 centimetres in length and 12 centimetres in width. Generally, though, dimensions of four to eight centimetres by two centimetres are more common. In shape, they are angular to sub-rounded spindles. Compositionally, the bombs are predominantly felsic volcanic material but mafic volcanic bombs can locally constitute up to 2% of the rock. The interstitial material is simply a more pulverized version of the bombs themselves. The relative proportions of the bombs and the matrix is quite variable.

In a typical thin section of the bomb material, 50% of the volume is taken up by euhedral to subhedral phenocrysts of feldspar up to seven millimetres in length. The feldspar laths are almost completely altered to sericite and often they appear bent and broken. Quartz constitutes another 46% of the volume. Generally the quartz occurs in very small crystals, 0.5 millimetres in size, but some larger, sub-porphyritic crystals are also present. These are often recrystallized or severely strained and show subhedral to anhedral crystal shapes. The rest of the bomb is composed of carbonate and opaque minerals.

The matrix material in the agglomerate is composed primarily of quartz and feldspar. These occur in

Figure II-1. Features and textures of the Keewatin-type rocks.

Plate 1. An example of flow top breccia from the mafic volcanics along the Shebandowan Mine road. A large pillow fragment is visible in the central portion of the photograph.

Plate 2. The intermediate volcanics occur primarily in the form of brecciated deposits, as shown in this outcrop. Note the massive texture of the rock; no tectonic fabric is visible.

Plate 3. A typical outcrop of felsic volcanic agglomerate from the west end of the Shebandowan Mine road. This outcrop had previously been mapped as a conglomerate.

Plate 4. An example of the intensity of alteration typical of the rocks in the area. Both the feldspar phenocrysts (FP) and the feldspar crystals in the matrix are completely saussuritized. PPL.

Plate 5. Typical texture visible in the matrix of the felsic agglomerate. Note the thin, wispy cleavage (------) predominantly developed around the edges of the fragments. PPL.

Plate 6. Zoned hornblende phenocrysts (H) are fairly common in the mafic volcanic rocks. XPL.

Plate 7. A fragment of mafic volcanic rock from a brecciated outcrop, showing a spherulitic texture (S). PPL.

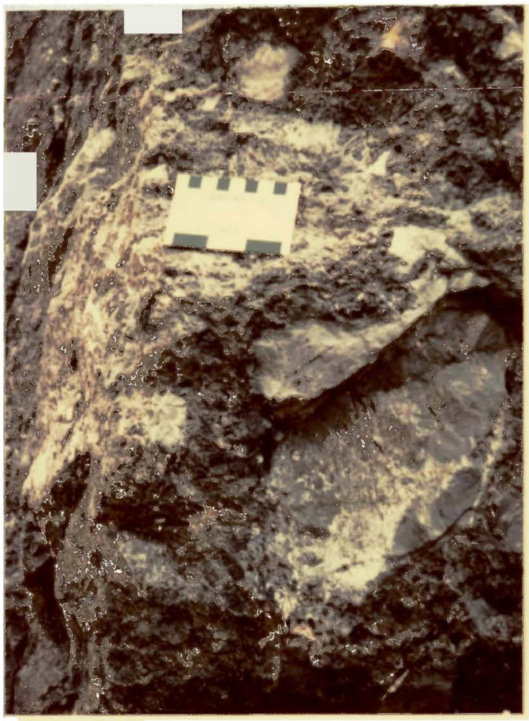

Plate 1

Plate 2

Plate 3

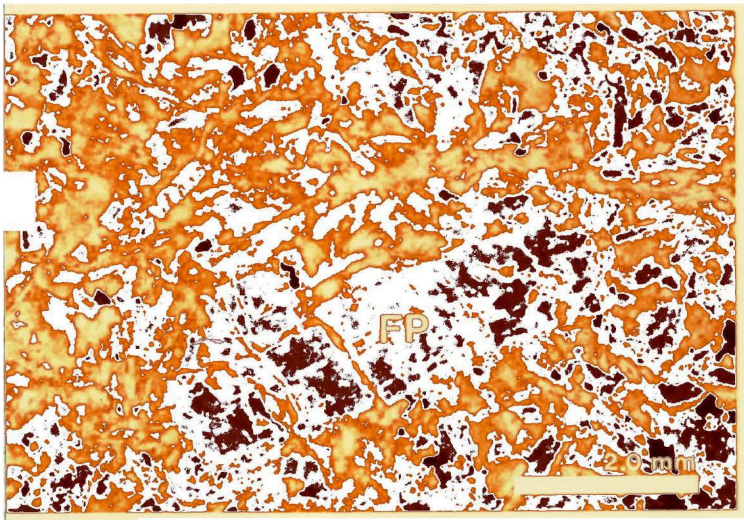

Plate 4

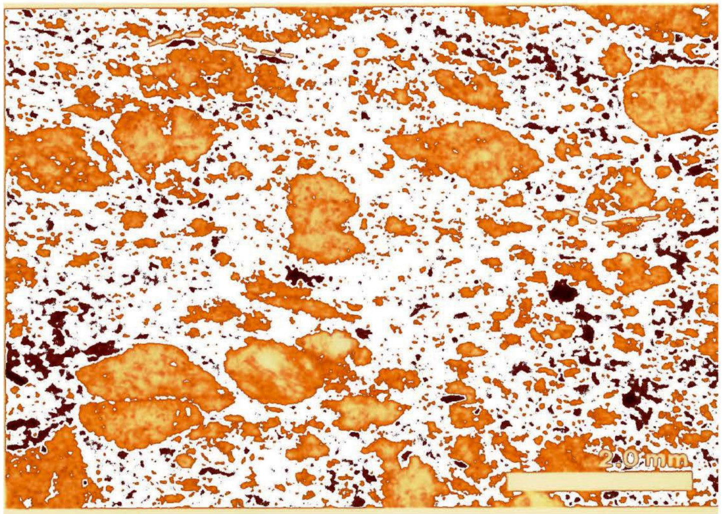

Plate 5

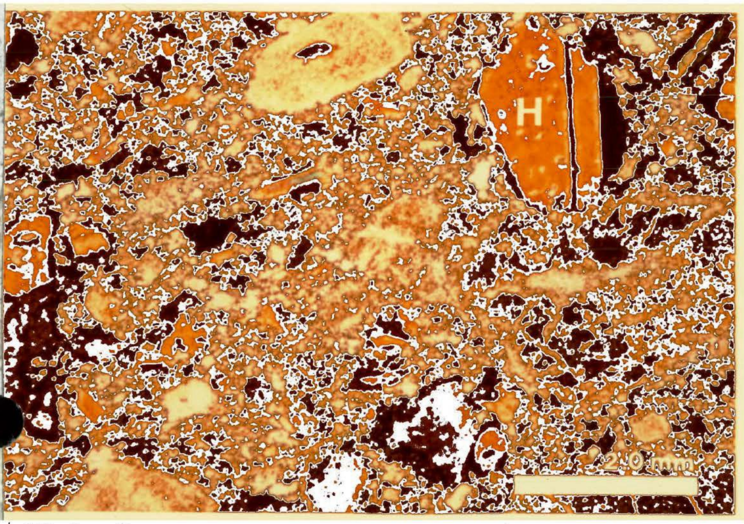

Plate 6

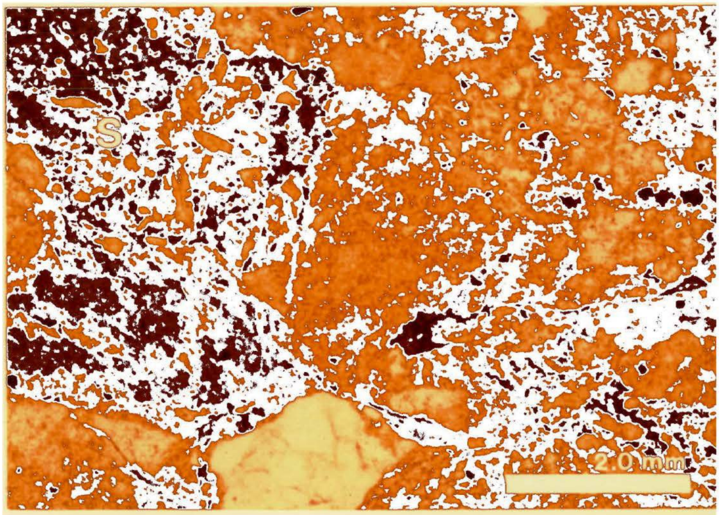

Plate 7

broken and squashed crystals ranging from 0.01 millimetres to 0.25 millimetres in size. Other constituents are carbonate, opaque minerals (pyrite and specular hematite), sericite and epidote.

This rock unit has been previously mapped as both a felsic agglomerate (Watson, 1928), and a conglomerate (Morin, 1973). The compositional similarity between the bombs, their shape, and the textures of the crystals in the matrix and the bombs preclude a sedimentary origin for this rock. The alignment of fragments and shape indicate some local ductile behaviour during subsequent tectonic deformation.

Shebandowan-Type

These rocks consist predominantly of arenaceous, rudaceous and argillaceous sediments with subordinate, but locally important, breccias and agglomerates which Shegelski (1980) has determined are calc-alkaline volcanics of shoshonitic affinity.

The arenaceous rocks consist of sandstone, arkose and greywacke. Primary features are well-preserved in these sediments (see Figures II-2 and II-3). The sandstone, in particular, exhibits planar and wavy bedding, ripple marks, sole marks, ball and pillow structures, channel scours and rip-up clasts. Cross-bedding and grain-size gradation is fairly common in all of the arenites, making top direction determinations possible at quite a few localities.

Individual beds vary from one millimetre to ten centimetres in thickness. None of these sediments appear to be very mature. The clasts are predominantly subangular to angular and poorly sorted. Argillaceous material composes up to 10% of the matrix in the sandstones; even more in the arkoses and greywackes. Both lithic clasts and crystals are present, but the lithic fragments predominate.

The rudaceous component of the Shebandowan-type rocks consists of conglomerates and breccias, with the former being by far the most abundant. As with the finer-grained sediments, clast size and degree of roundness is highly variable. Both matrix-supported and clast-supported units are present.

There appear to be two types of conglomerate (see Figure II-2, plates 1 and 2). In the outcrops where sandstone is the prevalent rock, the conglomerates are a polymictic collection of rounded quartz clasts, feldspar-phyric felsic clasts, granitic pebbles, pyrite nodules, layered sedimentary clasts, and jaspilitic clasts. A preferred orientation of the clast shape has generally been only weakly developed, and the degree of metamorphism of both the clasts and the matrix is low. Clast size varies from 5cm x 2cm to 15cm x 9cm in this rock, and only a moderate amount of argillaceous material is present in the matrix.

Figure II-2. Features and textures of the sedimentary rocks of the Shebandowan-type sequence.

Plate 1. A typical outcrop of conglomerate. Note the presence of bedded (B) and porphyritic (P) clasts. The competency difference between these and the granitic clasts (G) is readily visible. Also note the fairly massive texture of this rock.

Plate 2. This outcrop of conglomerate shows a much better-developed cleavage. The granitic clasts (G) have remained virtually undeformed in contrast to the volcanic clasts (V) which can be discerned only with difficulty.

Plate 3. An example of one of the larger clasts of jaspilitic iron formation seen in the Shebandowan-type conglomerates. More commonly, clasts of this rock type are only about one centimetre in length. Jaspilitic iron formation occurs interbedded with the Keewatin-type volcanics.

Plate 4. One of the rare breccias seen in the study area. Note the bedding visible in the large fragment in the upper portion of the photograph.

Plate 5. This photograph illustrates many of the primary sedimentary features preserved in the Shebandowan-type rocks. Graded bedding and load casts can be discerned in the upper portion of the photograph; lenticular and wavy bedding predominates in the central portion; and a few rip-up clasts can be seen in the lowermost section of the photograph.

Plate 6. Cross-bedding, as illustrated in this photograph, is quite common in the arenites of the study area.

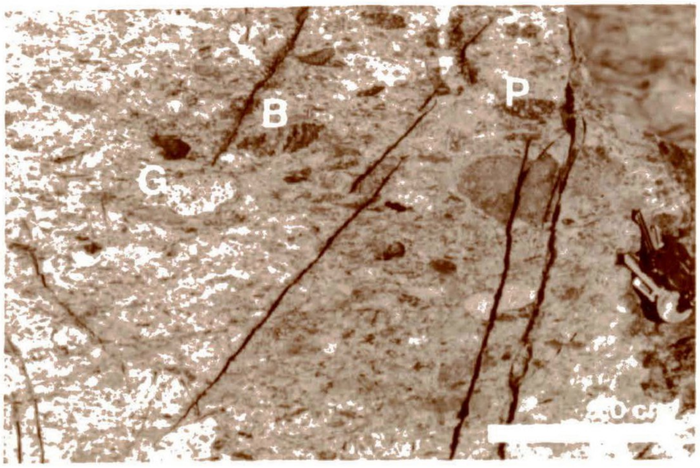

Plate 1

Plate 2

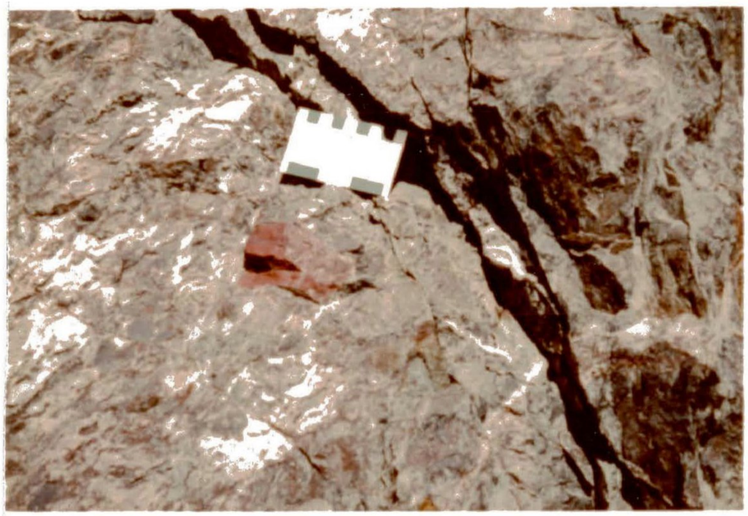

Plate 3

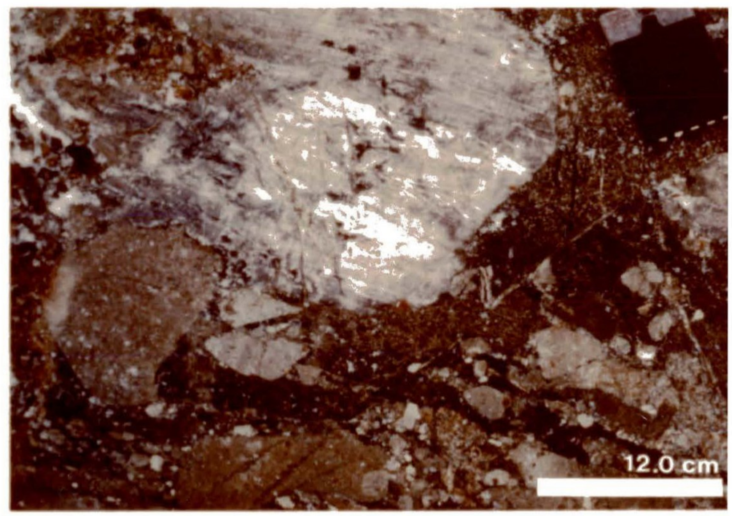

Plate 4

Plate 5

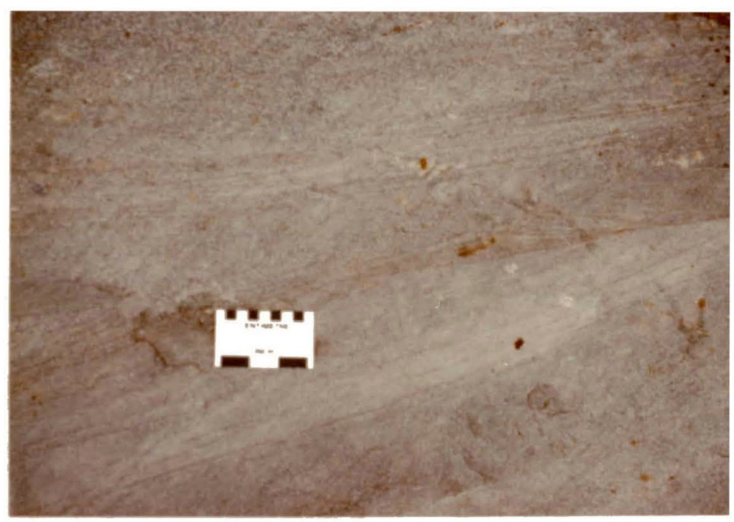

Plate 6

Figure II-3. Some larger-scale sedimentary features, typical of deposition by traction currents, preserved in the Shebandowan-type rocks.

Plate 1. Ripple marks, seen here in cross-section, occur frequently in the sedimentary rocks of the Finmark area.

Plate 2. Ripple marks seen in plan view.

Plate 3. Sole marks, such as those illustrated in this photograph, are more rarely-preserved than other features.

Plate 1

Plate 2

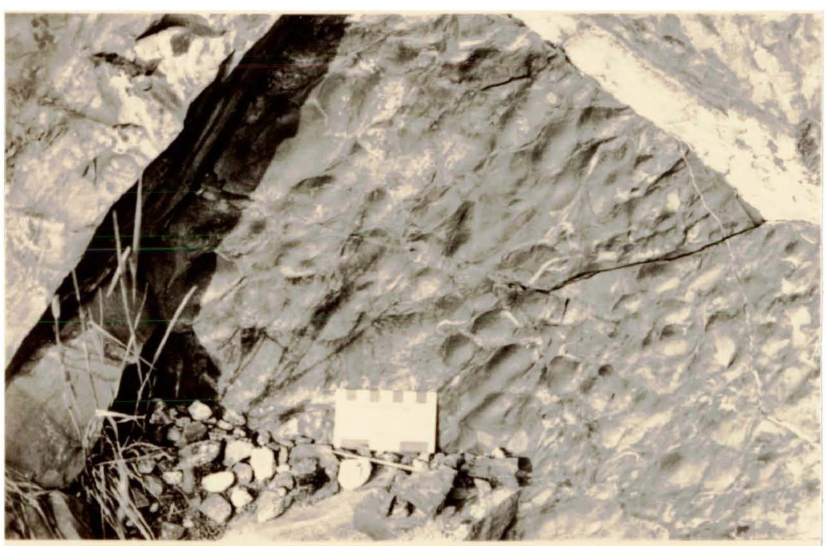

Plate 3

Figure II-4. Textures of the Shebandowan-type rocks visible in thin section.

Plate 1. One of the rare bedded clasts (lower portion of the photograph) seen in the arenites. S_0 represents the plane of bedding in the clast. XPL.

Plate 2. The textures in this photograph typify those of all the arenites studied. Note the wide range in clast size, as well as the variability in degree of roundness. Also note the lack of visible tectonic fabric in this rock. XPL.

Plate 3. The quartz grains developed in the pressure shadows of the pyrite crystals (Py) have a single, similar orientation; possibly indicative of a single growth period. XPL.

Plate 4. At this scale, a slight tectonic fabric is visible in the rock, oriented from the top left to the bottom right of the photograph. Note the high proportion of epidote (tiny, needle-like, yellowish crystals) in the matrix. XPL.

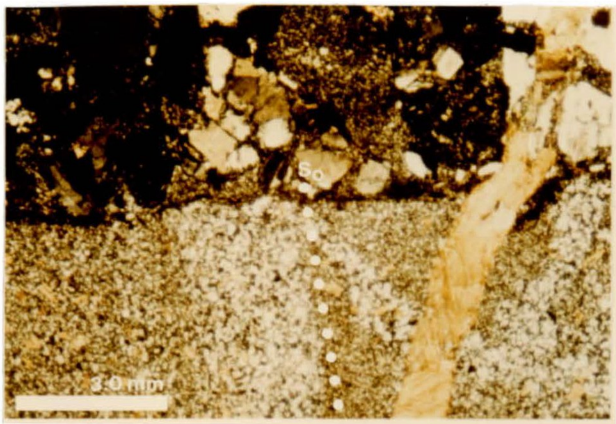

Plate 1

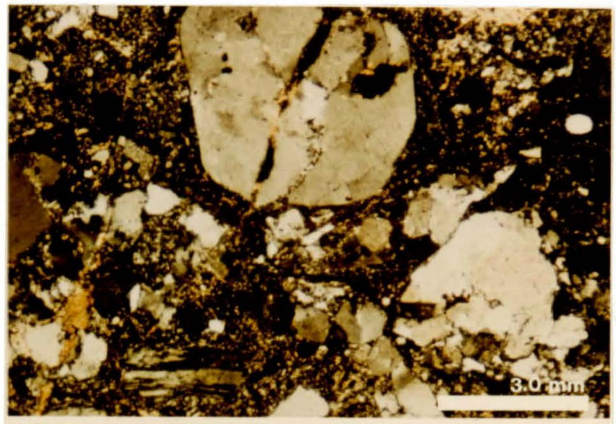

Plate 2

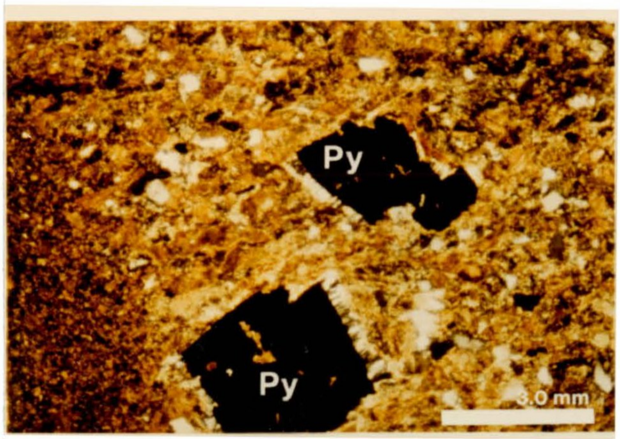

Plate 3

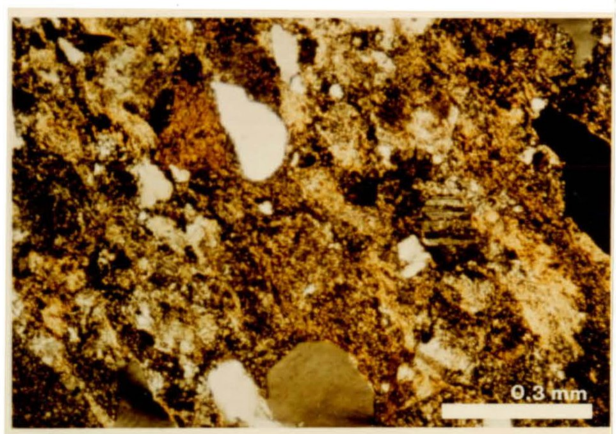

Plate 4

In areas where the arenites are arkose and greywacke, the conglomerate is composed mainly of clasts which are of mafic to intermediate volcanic composition. Sub-rounded granitic pebbles only constitute approximately 5% of this rock. Cleavage is well-developed in these rocks, and the volcanic clasts have become elongate parallel to this fabric. The matrix contains a higher proportion of argillaceous material than the previously described conglomerate, and the majority of it is now chlorite. The clasts themselves are highly chloritized as well.

As well as comprising a portion of the matrix of the coarser-grained sediments, the argillaceous component of the Shebandowan-type rocks occurs as inter-bedded slate. A scanning electron microscope study was carried out on samples of this rock type as part of the textural analysis of the fabric of the study area. The results are presented and discussed in a later chapter.

The volcanic component of the Shebandowan-type rocks consists primarily of a rock unit that has been called a volcanic agglomerate, a pillow breccia, an oligomictic conglomerate, and a lahar deposit. The uncertainty is due to its unusual appearance and texture (see Figures II-5 and II-6. It is a jumbled collection of angular to sub-rounded blocks and fragments of reddish and greenish rocks either fine-grained or hornblende- and feldspar-phyric. Large (up to 1cm long) crystals of amphibole are present in both the matrix and the clasts, rarely comprising as much as 5% of the whole rock. In most of the outcrops, these amphibole crystals have no preferred orientation; rarely, a weakly-defined fabric is developed. The fragments vary in size from one centimetre square to 60cm x 60cm, but the majority of them are 8-10cm x 4-5cm. Compositionally they can be fine-grained and reddish in colour (sometimes with the appearance of a chilled margin), fine-grained and greenish, feldspar-phyric and reddish, feldspar-phyric and greenish, and feldspar- and hornblende-phyric in both colours. The surrounding matrix is equally as variable. Sometimes the reddened clasts are in a greenish matrix, sometimes greenish clasts are in a reddened matrix, sometimes both reddish and greenish clasts occur in a variably reddened and green matrix.

In the present study, it is believed that this unit is a breccio-conglomerate whose source material was wholly volcanic, and which has been carbonatized and hematized to varying degrees subsequent to deposition. Although the clasts in this rock appear exotic, massive deposits of all the constituent rock types can be found in the

Figure II-5. Features of the pigmented, breccio-conglomerate unit of the Shebandowan-type sequence.

Plate 1. Numerous clast types are visible in this photograph: feldspar-phyric (top left); hornblende-phyric (left central); and massive clasts (right central).

Plate 2. This photograph illustrates well the textures which most likely resulted in this rock being mapped as a conglomerate.

Plate 3. The reddish pigmentation typical of these rocks is due to both hematization prior to brecciation and deposition, as well as later carbonatization. In this photograph, a late fracture filled with carbonate (denoted by the arrow), can be seen cutting through a clast of the breccio-conglomerate.

Plate 4. The variability of the pigmentation of these rocks is evident in this outcrop. The left-hand side of the photograph shows the whole rock to be reddened; only the clasts are reddened on the right-hand side.

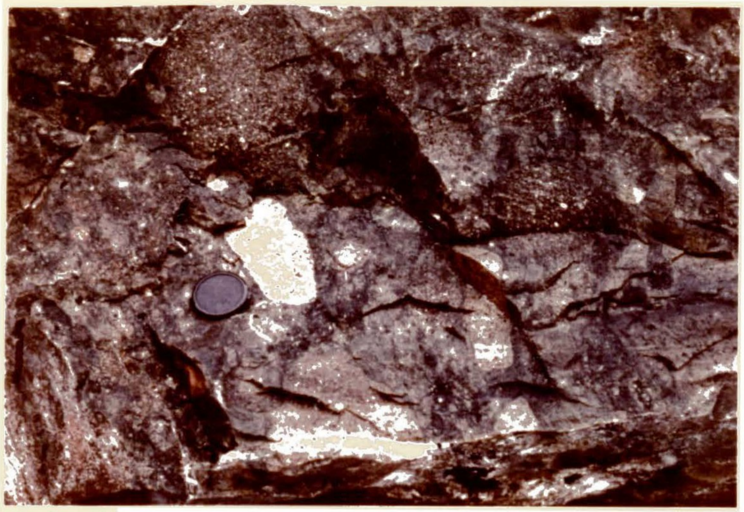

Plate 1

Plate 2

Plate 3

Plate 4

region, not necessarily within the boundaries of the study area, however. Recent mapping by Ontario Geological Survey geologists in Goldie and Horne Townships has located outcrops of massive reddish and greenish rocks very similar in composition to the majority of the clasts in this unit (Carter, personal communication, 1985).

Shegelski (1980) suggested that the reddening of these rocks, as well as in the other rocks of the Shebandowan-type, was due to hematization as a result of red-bed development. He found that there was a higher Fe_2O_3/FeO ratio in the pigmented outcrops of the Shebandowan-type rocks than in similar outcrops that lacked this reddish pigmentation. Other evidence for a subaerial depositional environment of these rocks include the presence of mud-cracks in the arenites.

Evidence that the Shebandowan-type rocks represent a proximal facies of alluvial-fluvial sedimentation is unequivocal (Shegelski, 1980), however, whether or not they exhibit evidence of red bed development will not be addressed in this thesis.

Figure II-6. Textures of the breccio-conglomerate visible in thin section.

Plate 1. In certain outcrops, particularly along the Shebandowan Mine road, the matrix of the breccio-conglomerate contains abundant hornblende (H) and feldspar (F) phenocrysts, as shown in this photograph. It is likely that these areas represent extremely proximal deposits of flow breccia. Note the intensity of the alteration of the feldspar crystals (F). PPL.

Plate 2. A clast (lower right-hand section of photograph) surrounded by hornblende- and feldspar-phyric matrix, exhibiting both hornblende (H) and feldspar (F) phenocrysts itself. Note that one hornblende phenocryst has been broken off at the edge of the clast, and therefore represents a mineral phase present prior to deposition. PPL.

Plate 3. Rounded quartz clasts (Q), such as the one shown in this photograph, are rarely seen. Note the reddish lithic clast (C) and the saussuritized feldspar crystal (F). PPL.

Plate 4. The textures visible in this thin section appear more typical of an agglomeratic rock. This sample most likely represents one of the more proximal deposits. PPL.

Plate 5. The reddened nature of the matrix (m) of many of the Shebandowan-type rocks in the area is readily visible in this photograph. PPL.

Plate 6. At very high magnifications, it can be seen that much of the reddish pigmentation is due to specular hematite (hem). PPL.

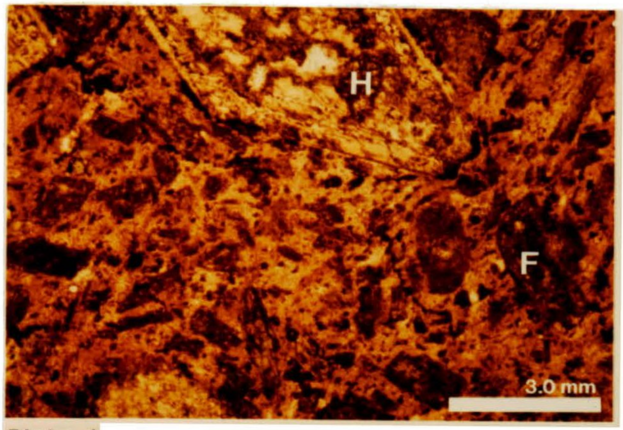

Plate 1

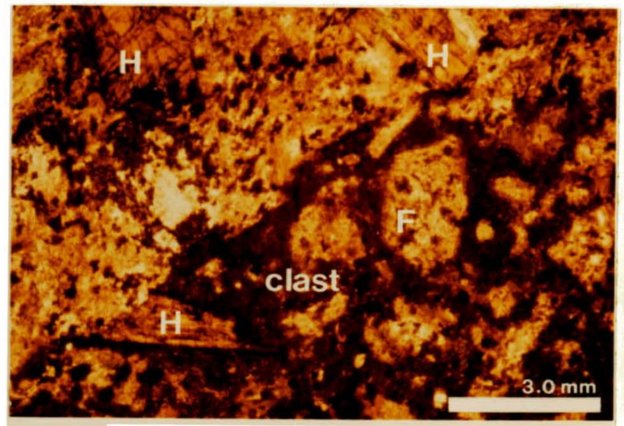

Plate 2

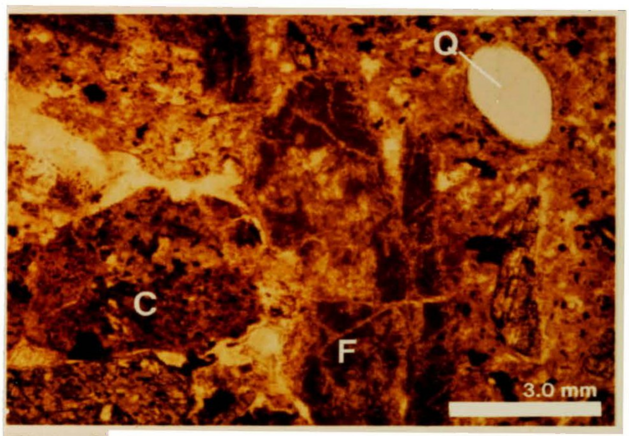

Plate 3

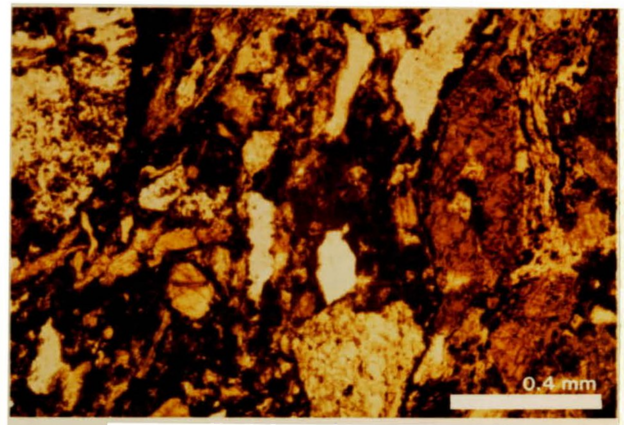

Plate 4

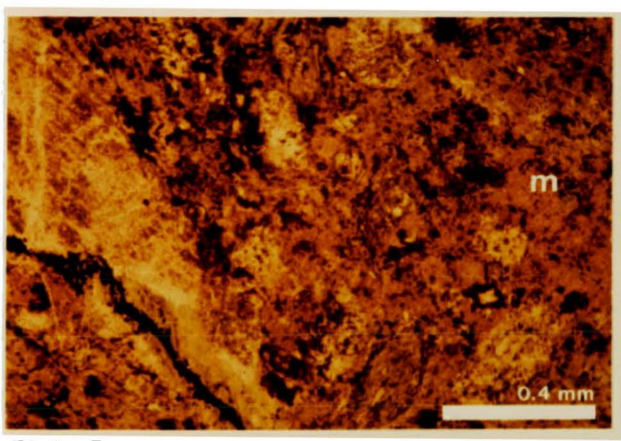

Plate 5

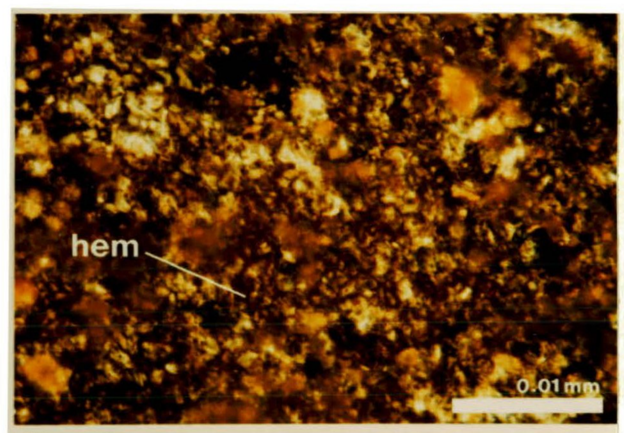

Plate 6

Macroscopic Fabric of the Rock

To address the questions of whether the rocks in the area are singly-folded or have undergone two or more periods of folding, and how much of that history has been experienced by the Shebandowan-type rocks, a detailed examination of the tectonic fabric of both groups of rocks was undertaken. The various structural elements measured in the field include: the strike and dip of cleavage and bedding; orientation of bedding-cleavage intersection lineations; and orientation of fold axes. Cleavage measurements were possible at nearly every outcrop; reliable bedding, however, was almost restricted to the metasedimentary rocks and, as a result, too few cleavage-bedding intersection lineations were measurable in the field. Visible folds, crucial to obtaining a clear picture of the regional structure, were scarce. However, their relative position could be predicted, outcrop by outcrop, by applying the cleavage-bedding relationship theory (Borradaile, 1980). (See Figure III-1). Caution was exercised when applying this theory because cleavage and bedding must be measured in the same spot on the outcrop, and the cleavage must be axial planar to the coeval folds. As the relationship between cleavage and the axial plane of folds is not a point on which many

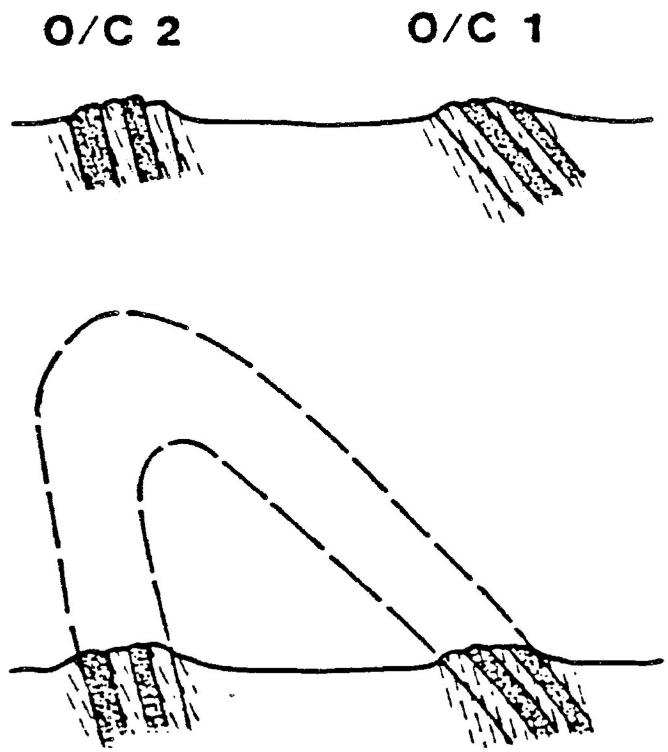

Figure III-1. The cleavage-bedding relationship rule: Where cleavage and bedding dip in the same direction, if the cleavage has a steeper dip than the bedding (for example, o/c 1), the outcrop is on the right limb of an anticline. (After Borradaile, 1980). This rule may equally be applied to steeply plunging folds, as in the present study area, by considering a sketch analagous to the above, as a plan view.

authors can agree, a brief discussion of the nature of cleavage and its orientation relative to fold axial surfaces may be necessary in order to vindicate some of the suppositions made in this regard.

Review of Cleavage Theory

Whether or not cleavage represents a true approximation of the orientation of the axial plane of a fold has been disputed often and by various authors (for example Bayly, 1974; Williams, 1976). These questions arise due to the uncertainties surrounding the formation of cleavage, and the nature of cleavage itself. Most of the early speculations about cleavage were concerned with slaty cleavage only. As originally described by such early workers as Sharpe and Harker (see discussions in Siddans, 1972, and Wood, 1974, for example) slaty cleavage referred specifically to phyllosilicate-rich rocks - slates - however this strict application of the term is frequently relaxed. Rocks such as marbles with a preferred orientation of carbonate grains have been described as having slaty cleavage (as discussed by Wood, 1974). It is more common now to use only the general term - cleavage. Theories and experiments pertaining to slaty cleavage implicitly include regular cleavage, or continuous cleavage, as well. ("Continuous cleavage" is used here to denote the exclusion of crenulation cleavages - usually the result of more than one period of deformation - and therefore spaced cleavages from the discussion, at the scale of observation).

Slaty cleavage is a penetrative, planar fabric in fine-grained, low-grade metamorphic rocks (Ramsay, 1967). It is defined by a preferred orientation of platy minerals, generally phyllosilicates, but also inequant quartz and feldspar crystals (Ramsay, 1967). Slaty cleavage is a fabric of incipient separation of the constituent minerals that grades into schistosity with an increase in grain size (Williams, 1977). It is generally restricted to the green-schist facies of metamorphism. Wood (1974) gave limits for a field of slaty cleavage deformation based on his contentions that a certain minimum amount of strain is required before cleavage will form, and that after a certain maximum amount of strain, a <u>cleavage</u> fabric will no longer be recognizable (see Figure III-2). Microscopically, slaty cleavage sometimes appears to have a domainal fabric as well as a simple mineral lineation (Hobbs et al., 1976). In such cases the rock will be separated into two domains: a lenticular one containing mainly non-phyllosilicate minerals, predominantly quartz; and

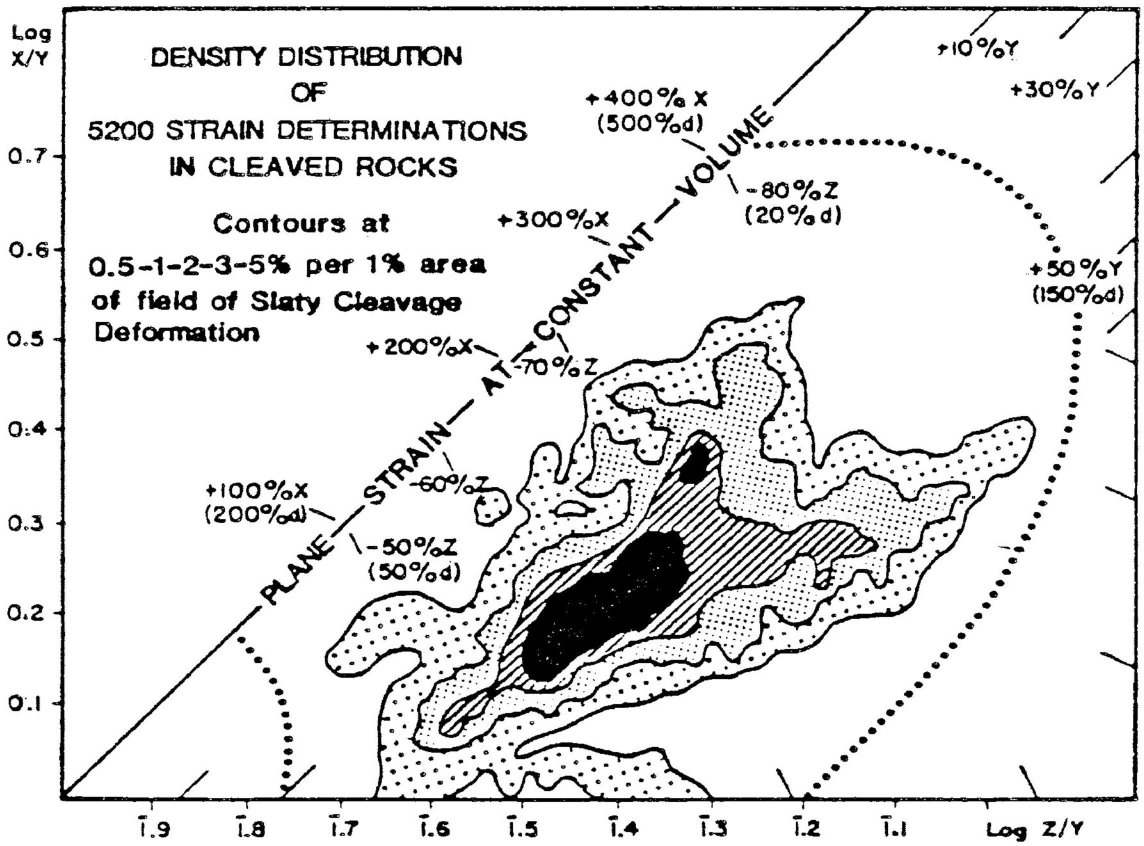

Figure III-2. Field of slaty cleavage deformation, marked by dotted lines. (From Wood, 1979, p. 378). X, Y and Z refer to the principal axes of the strain ellipsoid; X≥Y≥Z. The amount of strain is expressed as a percentage increase or decrease in the X, Y and Z axes relative to a sphere of unit diameter d (where d = 100% X, Y and Z).

a film-like one, dominated by phyllosilicates, which wraps around the lenticular one. Any phyllosilicates in the lenticular domain do not generally show any preferred orientation but the overall shape of the domain conforms to the orientation of the film domain (Hobbs et al, 1976). The domains vary in size and this fabric varies in predominance from rock-type to rock-type. There are three widely acknowledged theories for end members of the formation of a preferred orientation in a rock. They are 1) mechanical rotation, 2) the growth of new minerals under stress, and 3) pressure solution transfer.

1) Mechanical rotation by bulk finite strain involves the passive rotation of platy minerals such that they come to be in one plane of preferred orientation (Wood, 1974). A mathematical model devised by a crystallographer named March attempted to show theoretically how platy minerals could be rotated to a plane of preferred orientation when subjected to shortening. His paper, published in 1922, has been discussed and tested by various authors in order to determine how well it can be applied to the real situation in nature (for a discussion see Wood, 1974, or Williams, 1976). In his model, March assumes an initial random orientation of the platy minerals, rigid-body rotation, and

non-impingement of rotating flakes. It has been shown by various authors (O'Brian, 1970, and Moon, 1972) that the original fabric of the clay-rich sediments which produce slates is most often non-random (see Figure III-3). The same is true for the original fabric of most other rocks. Whether the platy minerals would behave passively or not has also been questioned. An experiment by Tullis, which supported March's model and changed his original equation only by a factor added to account for grain shape, relied on a "rigid body in a viscous fluid" model. This interpretation is also regarded as being an oversimplification of the problem (Williams, 1976).

2) The proposed theory of recrystallization and new mineral growth under stress as a cleavage-forming process appears to be generally more accepted than the above mechanism. This theory states that, when grown under conditions of stress, minerals with anisotropic growth properties will grow with their long axes (direction of fastest growth) perpendicular to the direction of maximum compression for the stress being applied (Wood, 1974). In this configuration, the crystals will be in their most thermodynamically stable position (Wood, 1974). Obviously, how well the cleavage develops depends on the amount of new crystal

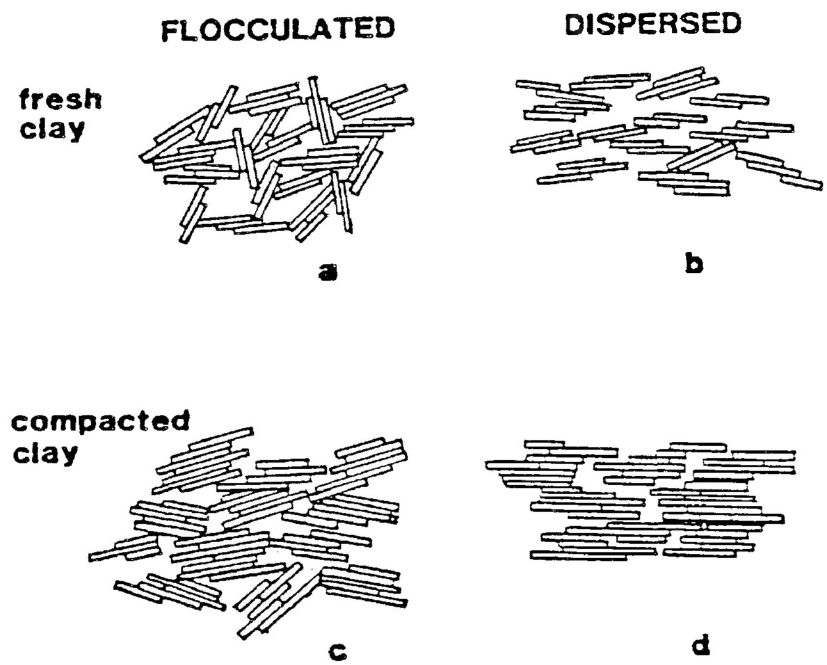

Figure III-3. A suggested scheme of particle arrangement in clay sediments. a) Open, random arrangement of domains of 2-3 particles per packet. b) Parallel or sub-parallel arrangement of domains of 2-3 particles per packet. c) Increased parallelism and more particles incorporated into each domain than in a), i.e., mudstone. d) Complete parallelism and more particles per packet than in b), i.e., shale. (From Moon, 1972, p.318).

growth. However, it should be pointed out that it is generally accepted that more than one mechansim can operate during the deformational history. As a result, there will most likely be no simple relationship between the degree of preferred orientation and the amount of recrystallization (Wood, 1974; Williams, 1976).

Other authors (notably Powell, 1974) believe mimetic growth to be an important factor in the formation of cleavage. Mimetic growth occurs by newly formed crystals mimicking a pre-existent fabric of the rock in which they grow (Whitten and Brooks, 1972). Powell contends that this mimetic growth will not necessarily show the same relationship to the applied stress as the syntectonic growth described above, depending on the orientation of the fabric being mimicked (Powell, 1974).

3) Pressure solution transfer is another means of cleavage formation which is not purely mechanical. Some authors (for instance Ramsay, 1967) are of the opinion that the first-described mechanism may be predominant at low temperatures (generally very early in the deformation), while the latter two would predominate at higher temperatures. An experiment by Etheridge et al (1974) backs up Ramsay's ideas. They

found that with higher temperatures, a better preferred orientation was produced with increased strain. At lower temperatures the amount of strain did not have a visible effect on the preferred orientation. Etheridge et al concluded that this was due to the growth of new minerals at higher temperatures.

Pressure solution transfer involves the dissolution (under non-hydrostatic stress) of readily soluble minerals in areas of high average mean stress; that is a crystal face statistically perpendicular to an axis of gravitational load or an axis of tectonic compression (Durney, 1972). The solute is then transported out of the area either by intracrystalline diffusion or in an aqueous, dispersed phase along the grain boundary. Precipitation from the solute occurs in an area of low average mean stress (Durney, 1972). Readily soluble minerals include quartz and feldspar. In a rock of the composition typical of slates, therefore, the insoluble minerals left would be the phyllosilicates. Once this insoluble residue loses the mechanical support afforded by the soluble minerals, the structure tends to collapse resulting in a plane of preferred orientation parallel to the pressure solution surface (Durney, 1972). Some authors believe that intracrystalline diffusion is much less dominant than diffusion along grain boundaries, under diagenetic or low grade metamorphic conditions (Durney, 1972).

Early evidence provided by deformed fossils led to the suggestion that slaty cleavage was produced by flattening and that the cleavage plane was perpendicular to the maximum compression direction of the finite strain ellipsoid (Wood, 1974). It was also very commonly found that, in a folded area, the plane of the slaty cleavage was a closer approximation to the axial surface than the limbs of the fold were, even in the case of fanning cleavage (Borradaile, 1978). So many examples of these special relationships were found that they became almost inviolable laws. Even in the absence of deformed fossils or other comparative indicators of the strain, slaty cleavage was used as a measure of the orientation of the axial surfaces of regional folds and, in strain studies, of the orientation of the XY plane of the finite strain ellipsoid that characterized the deformation of a region. Shear displacements parallel to the cleavage found in some localities have been used as evidence that the plane of cleavage is a plane of high shearing stress and therefore must be at some angle to the XY plane (Becker as well as other, more recent, authors, as discussed in Williams, 1976). It has been pointed out, however (Williams, 1976), that some shear displacements may be only apparent. (See Figure III-4). Dieterich (1969) proposed that shear displacements along the cleavage

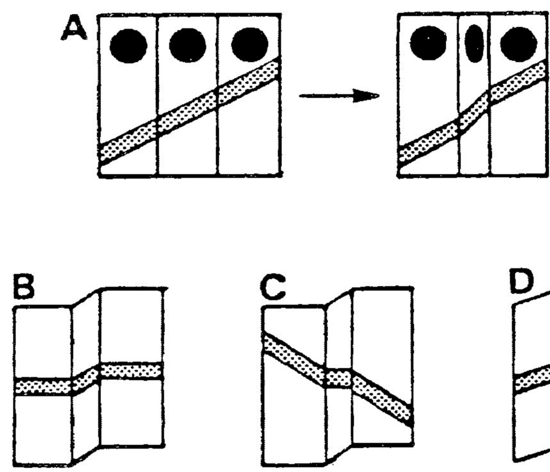

Figure III-4. Apparent (a) and real (b-d) shear displacements. Apparent shear displacement (a) by domainal volume change. True shear (b) the marker is perpendicular to the foliation, (c) the marker has the wrong sense of displacement to be volume change, and (d) the sense of displacement differs in adjacent domains. (From Williams, 1976, p.186).

plane may have formed later than the cleavage, as a result of shear stress.

Whether slaty cleavage has any particular relationship to the finite strain ellipsoid at all has been brought up by numerous authors (for example Bayly, 1974; Williams, 1976). Most tend to agree that parallelism with the XY plane of the finite strain ellipsoid is a theoretically special, although seemingly commonly occuring state. Williams (1976) believes that any foliation, regardless of its origin, will tend to rotate towards the XY plane of the incremental strain ellipsoids as stress is applied. However, it is only in very special cases that the cleavage will be parallel to the XY plane of the finite strain ellipsoid (Williams, 1976). He proposed that, in slaty cleavage, which is defined by a mineral lineation alone, the cleavage will develop parallel to the XY principal plane of strain and will follow it throughout the deformation only if the strain is coaxial, and if that cleavage had developed by rotation of particles which had initially been randomly oriented (Williams, 1976). For cleavages which have a domainal fabric (a "planar discontinuity") as well as a mineral lineation, the strain history must have been coaxial for the cleavage to be parallel to the finite XY plane, as long as the cleavage was initiated at the same time as the folding (Williams, 1976).

Powell (1974) and Borradaile (1978) have shown that cleavage is not necessarily initiated synchronous with folding. Borradaile (1978) demonstrated how cleavage development may be suppressed in the early stages of deformation if the strain is preferentially accommodated by grain-boundary sliding and other processes, together termed "particulate flow", rather than the other mechanisms described above. Grain-boundary sliding, rolling, etc., may not leave a visible fabric, but the other mechanisms do (Borradaile, 1981). Particulate flow has been used to explain non-axial planar cleavages such as are found in transected folds. Transected folds have cleavages which cut the axial surface and both limbs, with the same sense (Borradaile, 1978). Examples of transected folds are rare and, in general, the plane of cleavage is more closely approximate to the orientation of the axial plane of a fold than the limbs are (Borradaile, 1978).

It would appear from the evidence that cleavage can form by a variety of mechanisms. Not all cleavages have to have formed in exactly the same manner.

There are very strong feelings for and against the theory that cleavage is parallel to the XY plane of the finite strain ellipsoid. Those who argue in favour of the theory cite the evidence provided by deformed fossils and reduction spots, as well as the anisotropic nature of the growth of the minerals which define the cleavage and their tendency to align themselves in the most thermodynamically stable position when subjected to stress. Other authors point to the fact that shear displacements parallel to the cleavage have been documented in some outcrops (as discussed in Williams, 1976). This would seem to imply that the cleavage formed initially at some angle to the finite XY plane, probably 45° as is commonly seen in sheared rocks (eg. with C/S fabrics). Williams (1976) makes the point, however, that shear displacements may be apparent. It has also been noted that they may have formed later than the cleavage (Dieterich, 1969).

It is apparent that many factors need to be taken into account before deciding if the cleavage does represent a close approximation to the XY plane of the finite strain ellipsoid and to the axial plane of folds or not. The mode of cleavage formation is an important factor. Powell (1974) proposes that mimetic growth can occur along a former bedding plane. This may be inclined to the finite strain ellipsoid, although sufficiently close that the mineral growth would be stable. In the absence of any other markers in such a rock, the assumption of the orientation of the strain ellipsoid based on the cleavage would be erroneous. Also if the cleavage formed by mechanical rotation there is no way of determining if the deformation continued long enough for precise parallelism of the crystals to occur. The time of cleavage formation also appears to be an important factor, relative to folding of beds.

With regard to the axial planar nature of slaty cleavage (the cleavage gives a closer approximation to the axial surface of a fold than the limbs do), it is a very commonly seen relationship, but examples of a non-axial planar relationship have also been documented (Powell, 1974; Borradaile, 1978; and references therein). Examples of transected, coeval folds are rare, as are examples of first phase tectonic cleavages at an angle to the XY plane of the total strain ellipse, but they are in existence and cannot be disregarded (Borradaile, 1981).

In conclusion, cleavage is not always axial planar and it is not necessarily <u>precisely</u> parallel to the XY plane of the finite strain ellipsoid, although both appear to be common relationships. In the majority of cases, slaty cleavage is sufficiently parallel to the axial plane of folds for the cleavage-bedding relationship rule (Figure III-1) to be correct.

Obviously, then, the first objective of practical importance was to establish whether the slaty cleavage in the study area represents a good approximation of the axial plane of the regional folds. Of the limited number of folds seen in the Shebandowan area, all of them displayed axial planar slaty cleavage. Figure III-5 illustrates the best example of this relationship. The regional picture of the structure of the study area, drawn from the visible folds and the cleavage-bedding relationships, will be presented in a later chapter.

Fabric of the Keewatin-Type Rocks

As mentioned previously, cleavage is the most widespread of the various structural elements visible in the rocks. It is developed to varying degrees in all the rocks, but, as a whole, the Keewatin-type rocks have the best-developed cleavage. Only a small area of intermediate volcanics had no visible fabric. In outcrop, the cleavage is most often a fine, closely-spaced, continuous cleavage. No crenulations were seen in the study area, and kink zones were rarely observed. In thin section the cleavage is seen as an alignment of phyllosilicate minerals in the matrix and by faint trails of opaque minerals undulating between the crystals along films and wisps. (See Figure III-6).

Figure III-5. One of the rare folds seen in the study area. The cleavage in this outcrop, as in all the outcrops with visible folds, is axial planar. S_o = Plane of bedding; S_1 = Plane of cleavage.

Figure III-6. Typical texture in thin section of the Keewatin-type volcanics. Note the weakly-developed cleavage evidenced by the preferred orientation of some of the elongate crystals and the sinuous, wispy trails of opaque minerals. The section is from an outcrop of volcanic agglomerate. The darker portion in the centre of the drawing is the matrix, now mostly epidote, sericite and opaque minerals. S_1 represents the orientation of the weak cleavage.

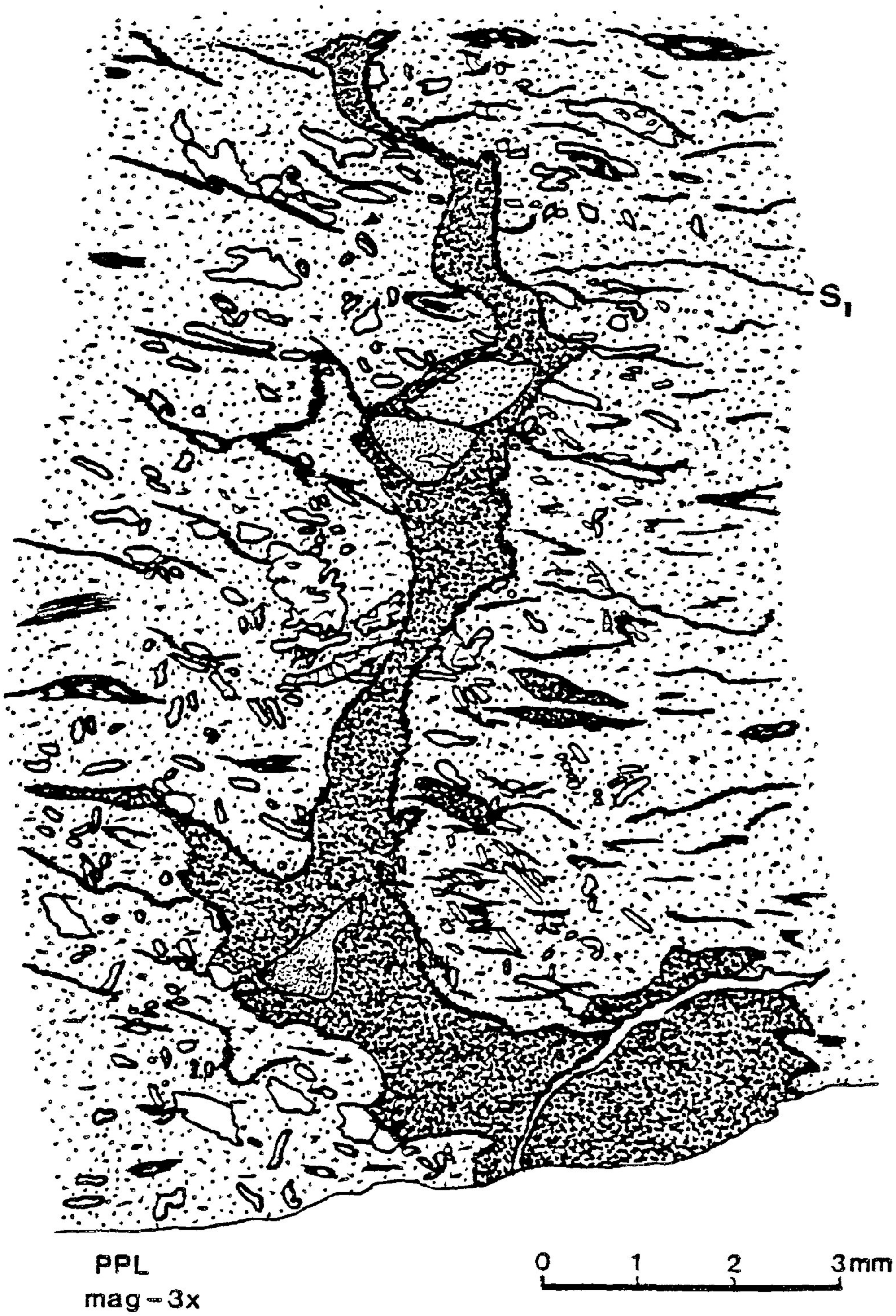
S1
PPL
mag - 3x
0 1 2 3mm

Fabric of the Shebandowan-Type Rocks

Conversely, the Shebandowan-type rocks generally have a more weakly-defined cleavage, with the exception of a few areas where the fabric is very pronounced (as noted in Chapter II). In these areas, dominated by deposits of arkose and greywacke, the rocks display few primary features, and the interbedded conglomerates are quite deformed. In general, though, the cleavage in these rocks is very similar to that in the Keewatin-type; fine, pervasive and defined by an alignment of phyllosilicate minerals. Again, it appears to be a first phase, continuous cleavage and no crenulation cleavages were seen.

Comparison of Fabric

Regardless of the degree to which it has been developed, the orientation of the cleavage varies little throughout the area. The mean strike of the cleavage is around 100°, and the dip is always very steep to the north, south, or vertical.

Figures III-7a and -7b show equal area stereonet plots of the poles to the cleavage in the rocks of the study area. In Figure III-7a, the data have been separated according to rock type. The X's represent the poles to cleavage measured in the Shebandowan-type

Figure III-7a. Poles to the cleavage measured in outcrop, plotted on equal area stereonet diagram. The cleavage in the Keewatin-type rocks is indistinguishable from that of the Shebandowan-type rocks.

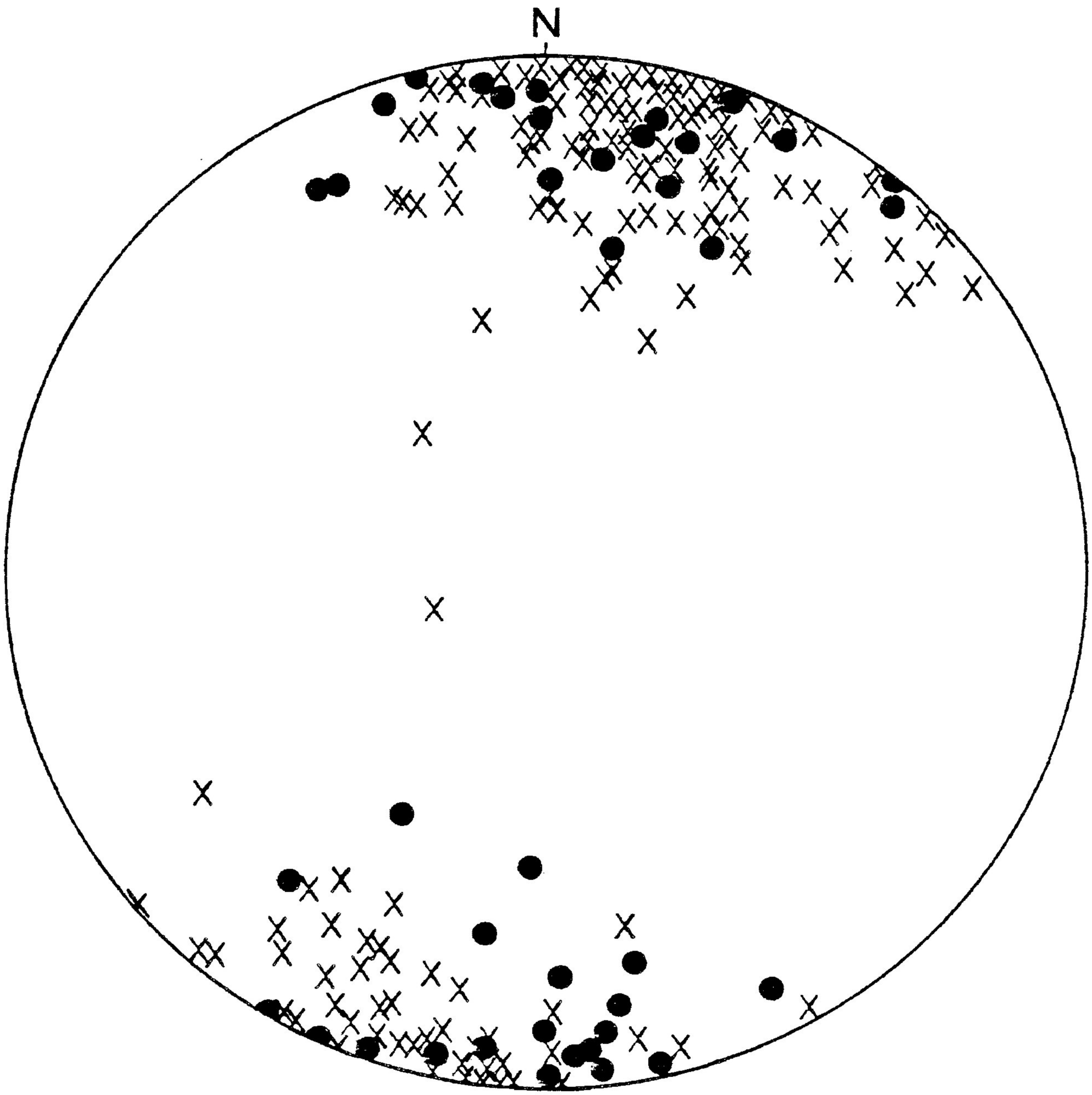

POLES TO CLEAVAGE

X = SHEBANDOWAN-TYPE

● = KEEWATIN-TYPE

200 measurements

Figure III-7b. Poles to cleavage in both rock types contoured at 1 - 8 - 15 - 22 - and 29 poles per 1% area. The centre of the maxima is the pole to the average plane of cleavage, oriented 98-80.

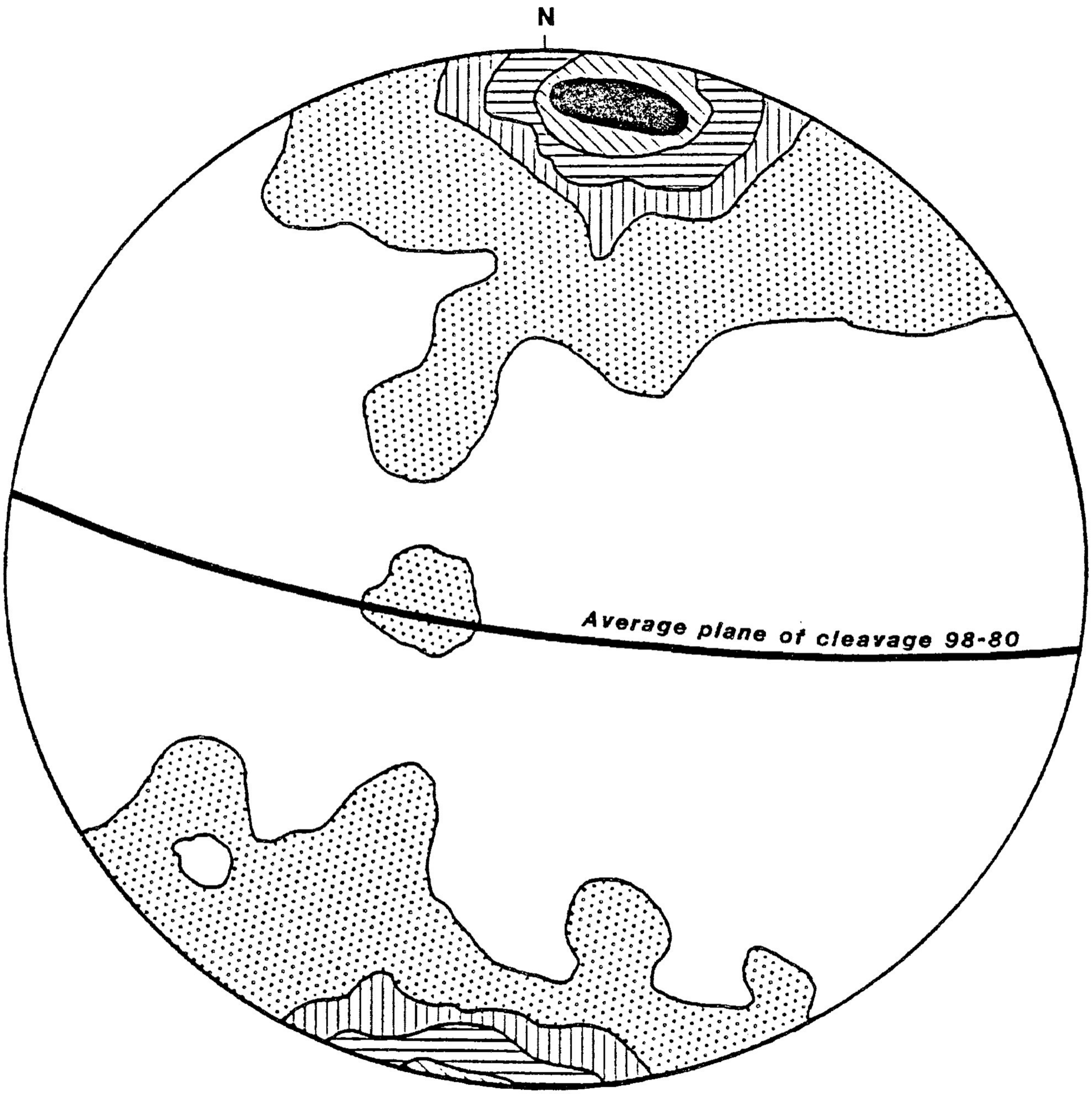

POLES TO CLEAVAGE
Contoured at 1-8-15-22-29 poles per 1% area

rocks, the circles represent poles to cleavage measured in the Keewatin-type rocks. The distribution of the data points indicates that the cleavage in both groups is virtually identical. The cleavage measured in the Shebandowan-type rocks and the Keewatin-type rocks is the same cleavage in terms of orientation, and since both are primary it is suggested they are correlative. In Figure III-7b, the data have been contoured at 1-8-15-22 and 29 poles per 1% area. They show an obvious clustering around a single maximum, the centre of which represents the pole to a plane of average cleavage, oriented 98-80°.

These results would appear to indicate that both groups of rocks have only a single visible tectonic fabric. However, that this means they have undergone a single episode of deformation cannot be immediately assumed. Although the development of a later tectonic fabric in other cases can be sufficiently strong to completely overprint an earlier one, that is unlikely here in view of the low grade and fine texture of the continuous cleavage, and low degree of recrystallization.

While, in outcrop, the rocks have only a single fabric, microscopic examination in some cases reveals evidence of more than one period of deformation.

Figure III-8 is an illustration of a previous fabric which may only be evident in thin section. It can be seen that the larger, more eroded crystals of biotite retain an orientation representative of an earlier-developed fabric while the smaller, fresher crystals define a later fabric oriented at an angle to the first one.

No evidence of a previous fabric was visible in any of the sixty-three thin sections examined.

Another possible explanation for the appearance of the singletectonic fabric in the rocks is that successive periods of deformation may have been coaxial or nearly so, again resulting in a single visible cleavage. This latter possibility generates more complications and will be discussed in a later chapter.

Figure III-8. A sketch from a teaching slide, illustrating the appearance in thin section of two rock cleavages. The more recent fabric would not be visible in outcrop. S_1 = the older cleavage; S_2 = the younger cleavage.

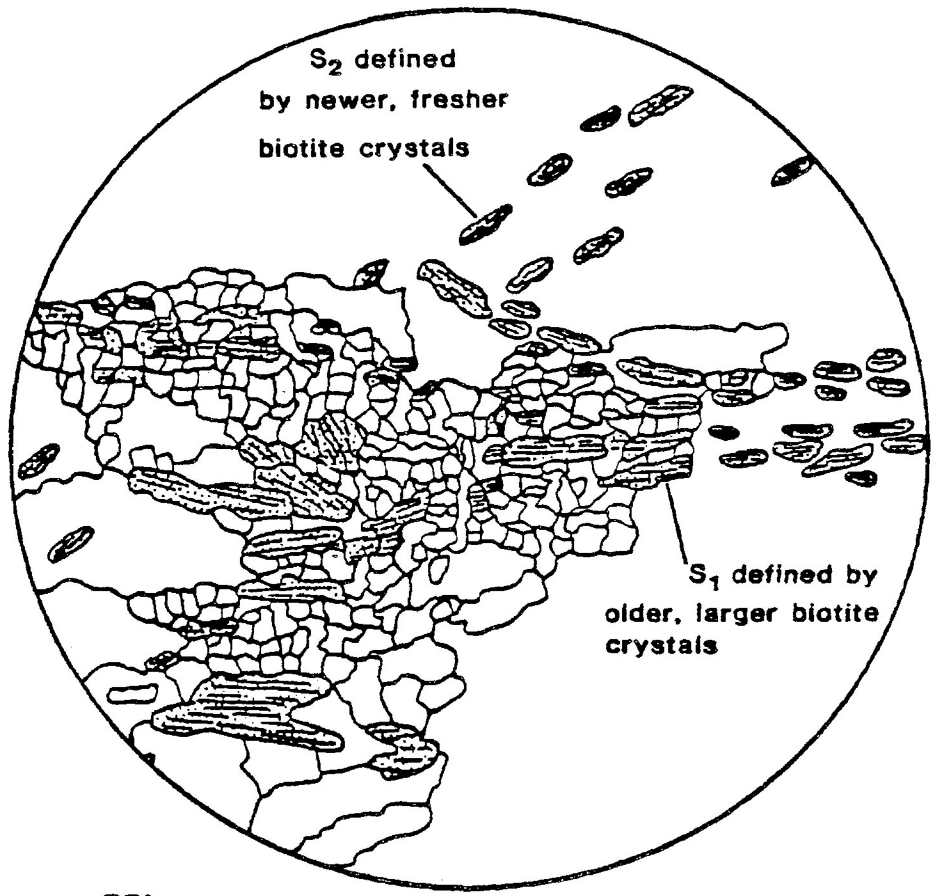

PPL

Diameter of circle = 0.5cm

Cryptic Fabric

On the basis of the readily visible fabric in the rocks, the conclusion would be reached that both the Shebandowan-type and the Keewatin-type groups of rocks have undergone a single period of deformation. This would agree with the findings of Morin (1973), and of Beakhouse (1974; for an area just west of the present study area). However, evidence of structural deformation in rocks can be present in more imperceptible ways. The scanning electron microscope has been used with much success (Weber, 1982) to reveal fabrics undetectable under normal magnifications, and the characteristics of the anisotropy of magnetic susceptibility of a rock can give an indication of the hidden tectonic fabric of the rock as well.

A scanning electron microscope (SEM) study was carried out on selected samples from the study area in an attempt to detect any evidence of previous fabrics (cf. K. Weber, 1982). Magnetic susceptibility anisotropy (MSA) determinations were also carried out on samples from rocks of the study area in order to supplement the information on the tectonic history obtained from the macroscopic fabric of the rocks.

SEM Study

In Weber's work (1982) the scanning electron microscope was used to examine the internal structure of samples of slate from the Rheinische Schiefergebirge. He found that, even though these rocks can readily accommodate successive periods of deformation through a re-orientation of their fabric into a direction which is relatively stable under each new set of stress conditions, some earlier fabrics may be retained, visible only on a sub-microscopic scale. These earlier fabrics are preserved as a preferred orientation of minerals within the microlithons of the more recent fabric.

In the present study, three samples of slate: from the Shebandowan Mine Road; Shabaqua Corners; and Finmark, were examined under the scanning electron microscope. Mineralogical determinations by X-ray diffractometry were also carried out on the samples to ascertain whether they represent typical pelitic slates or not. Figure IV-1 is a graphical representation of the results of the scan done on the sample from Shebandowan Mine Road. It can be seen that the mineralogy is predominantly quartz and clay minerals with subordinate chlorite, feldspar and micas. This typifies the mineralogy of all the samples.

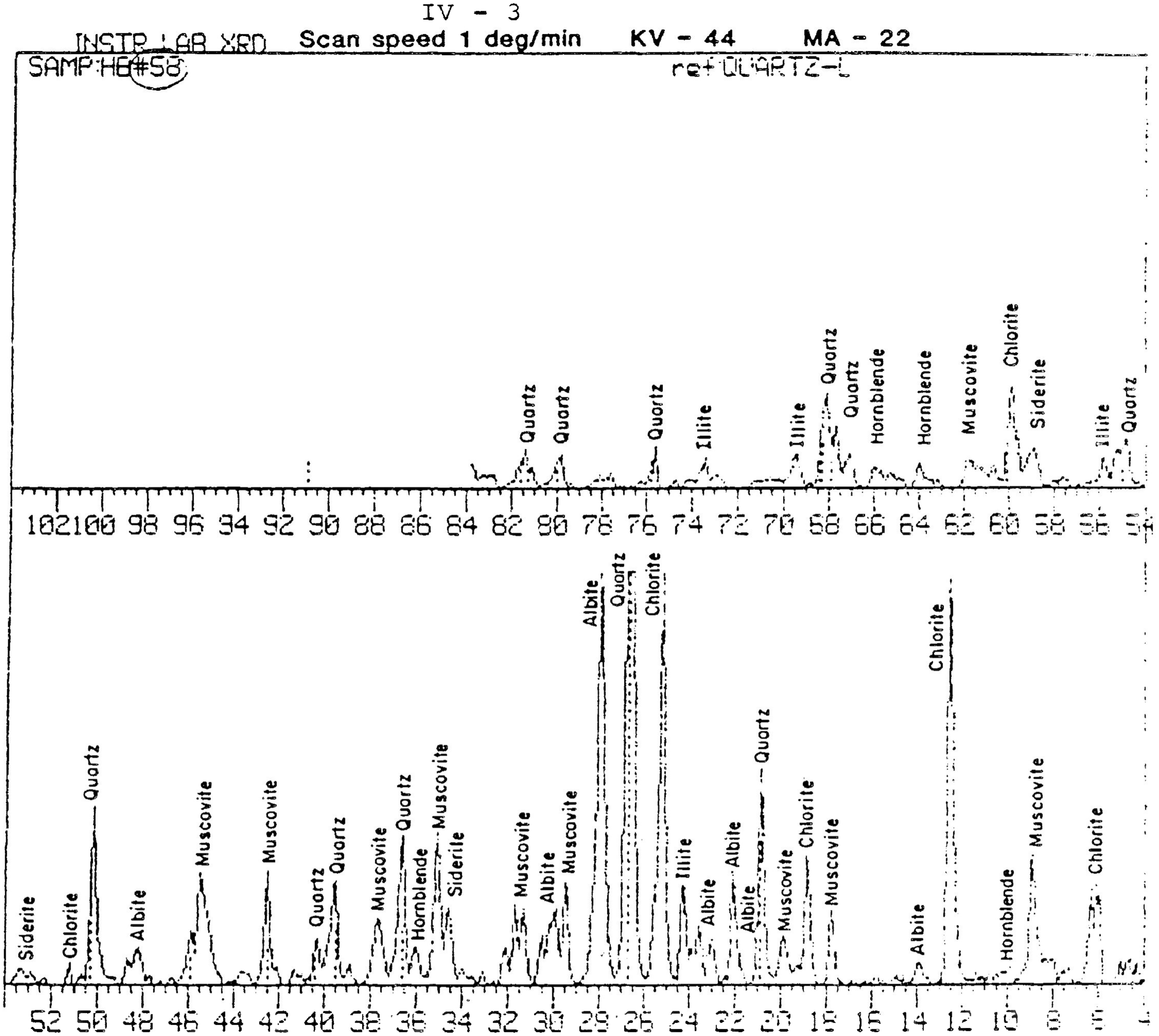

Figure IV-1. X-ray diffractometry analysis of a sample of slate from the study area. The mineralogy is typical of true pelitic slate; predominantly quartz and clay minerals. This example is representative of all the samples from the study area which were used in the SEM work.

Under the SEM, it was clear that, as in the coarser-grained rocks, the cleavage in the slates has been developed to varying degrees. Figures IV-2a and -2b are fairly representative illustrations of the cleavage in the samples studied. The preferred orientation of the components of the cleavage is readily visible. A slight preference of orientation of the platy minerals is discernible within the microlithons, but it is not well-developed enough to represent an earlier tectonic fabric (c.f.Weber,1982). Rather, it may indicate a syndepositional fabric developed by settling through water. Figure IV-3 illustrates various aspects of the cleavage in the rocks, and demonstrates the variability in the degree of development of their fabric. Figure IV-4 exemplifies the mineralogy and fabric typical of the slates studied. It can readily be seen that the preferred orientation of the platy minerals has been fairly well-developed. No previous tectonic fabric is visible in the microlithons, however.

Magnetic Susceptibility Anisotropy (MSA) Study

In recent papers by G. M. Stott and W. M. Schwerdtner (1981) and Stott and B. R. Schnieders (1983) a suggestion is put forward that the Shebandowan

Figure IV-2a. Slaty cleavage under the scanning electron microscope (white bar indicates the mean orientation of cleavage (S_1)): The overall preferred orientation of the shapes and, to some extent, the crystal alignment, of the platy minerals defines a single orientation of cleavage. At this scale (3 cm = 40μ) this is a good representation of a continuous fine cleavage (sense 1; Borradaile, Bayly and Powell, 1982) in which no discrete surfaces determine the cleavage.

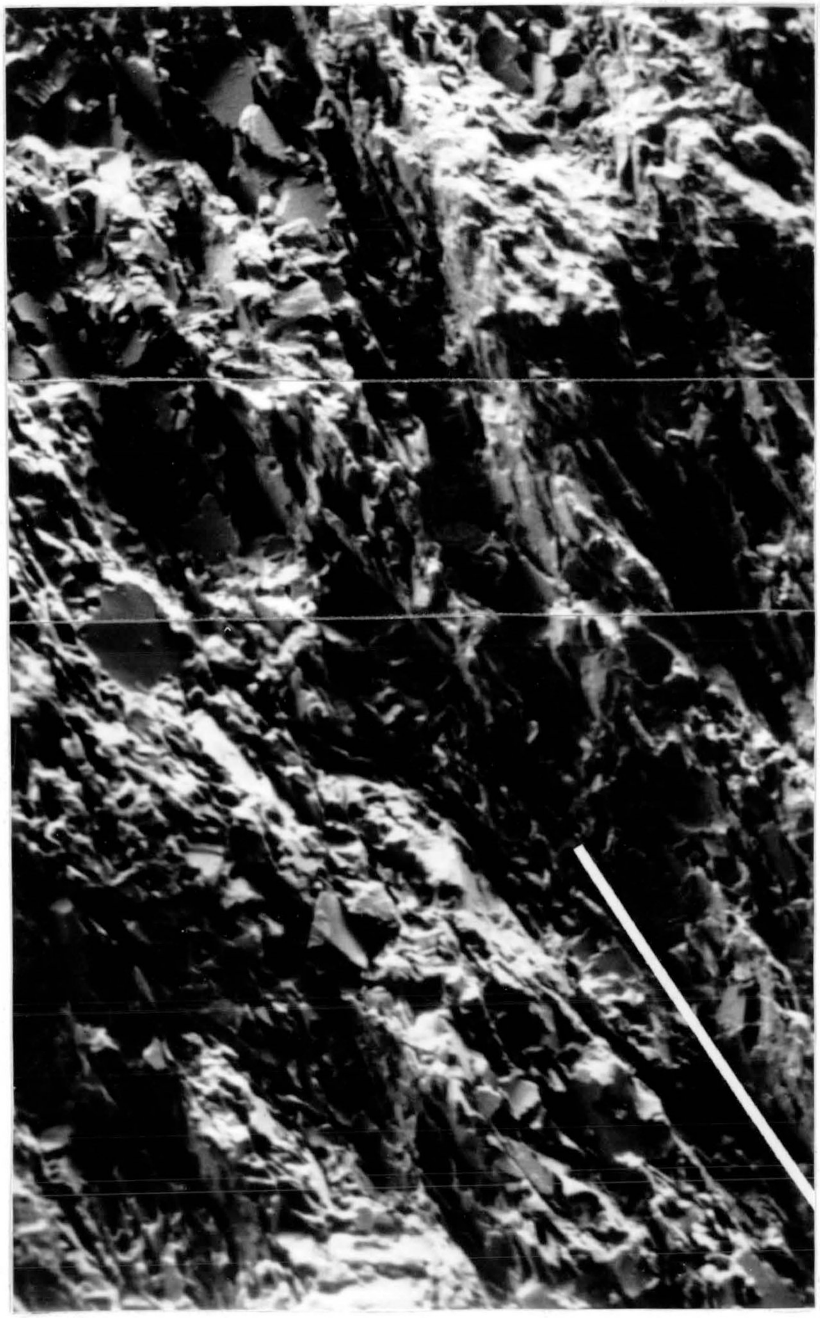

3 cm = 40 μ

Figure IV-2b. The same area as in the previous figure, under higher magnification. The regular nature of the slaty cleavage is still obvious, but at this scale a few discrete surfaces are now noticeable, for instance the microlithon (M) outlined by the dashed white lines. Note the weaker preferred orientation of platy minerals in the microlithons - possibly indicating some component of their original fabric. Also note the lack of evidence of an earlier tectonic fabric in the microlithons (cf K. Weber, 1982). Q = quartz, M = microlithon, S_1 = rock cleavage.

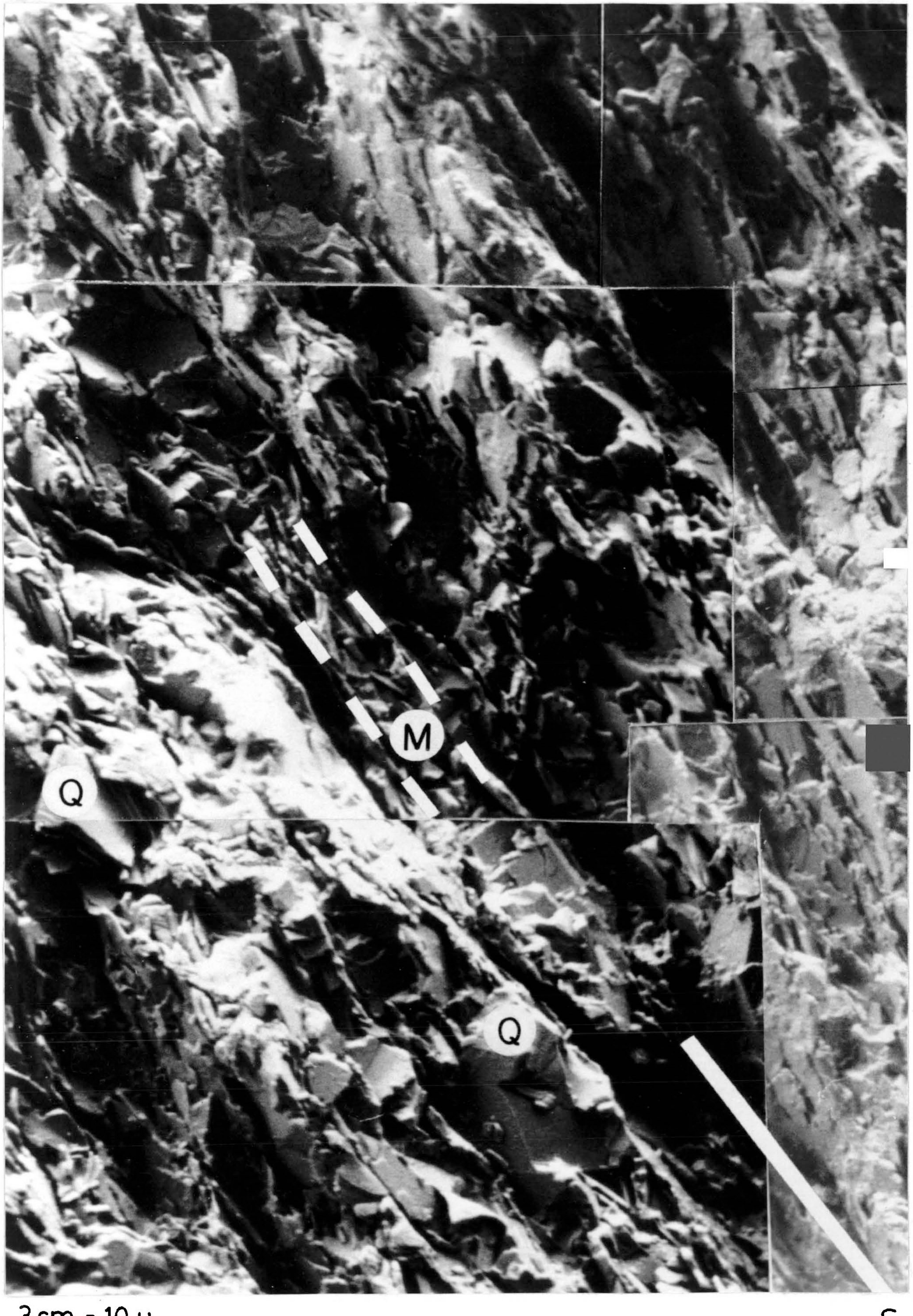

3 cm = 10 μ

S_1

Figure IV-3.

Plate A. A more poorly-defined rock cleavage than that illustrated in the preceeding figures. However, one can still pick out a subhorizontal cleavage indicated by the preferred orientation of platy minerals. The large, fresh-looking crystals in the central portion of the photograph are probably syntectonic blasts. (3 cm = 40μ).

Plate B. Detailed photograph of a slate, illustrating the small-scale variations in orientation of the platy minerals, particularly in the shadow of the quartz crystal (Q). The slaty cleavage, oriented from the top left to the bottom right of the photograph, is still discernable however. (3 cm = 20μ).

Plate C. Slaty cleavage (dashed white line) defined by thin, delicate platy minerals, wrapping around more rigid quartz and feldspar crystals, illustrating the presence of "pressure" shadow structures even in this fine-grained slate. Q = quartz, S_1 = rock cleavage. (3 cm = 20μ).


Q


Q
S_1

Figure IV-4. A detailed, composite photograph showing the textures and mineralogy typical of the slates from the Shebandowan-type rocks. The mineralogy is predominantly platy clay minerals and quartz, both original crystals and probable syntectonic blasts (the relatively larger, fresher crystals). At this scale, the fine, continuous slaty cleavage shows a more discrete nature and domains of weaker preferred orientation of platy minerals (for example domain "b" in sketch below) can be distinguished from domains of well-developed preferred orientation (for example domain "a" in sketch below). Note the lack of an earlier tectonic fabric (cf K. Weber, 1982) in the domains of weaker preferred orientation. Q = quartz, F = feldspar, U = grain of unknown composition with possible mineral overgrowth, S_1 = rock cleavage; white bar represents mean orientation of slaty cleavage.

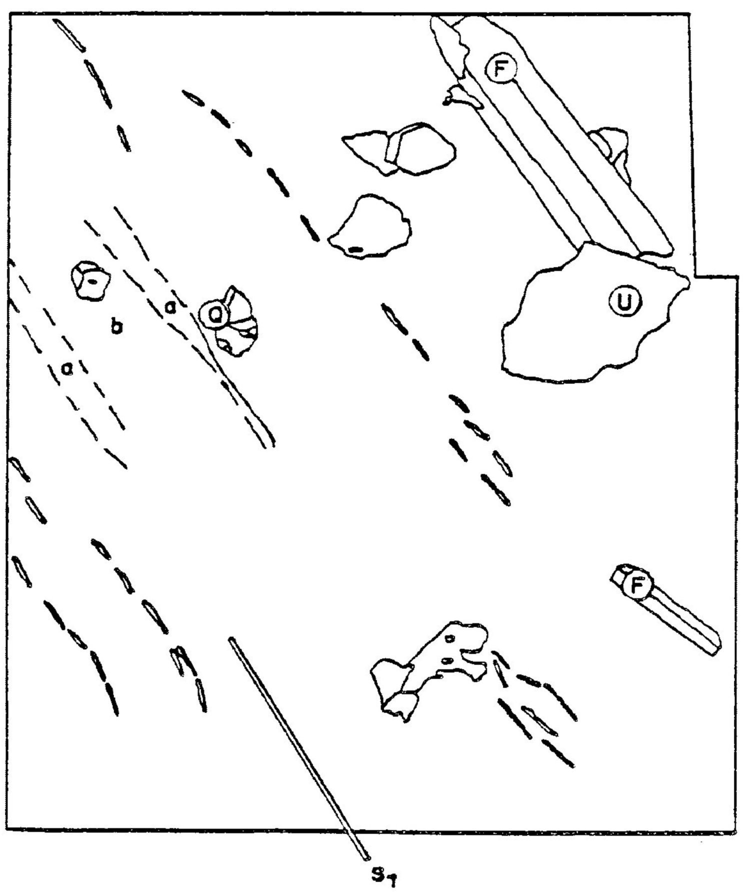

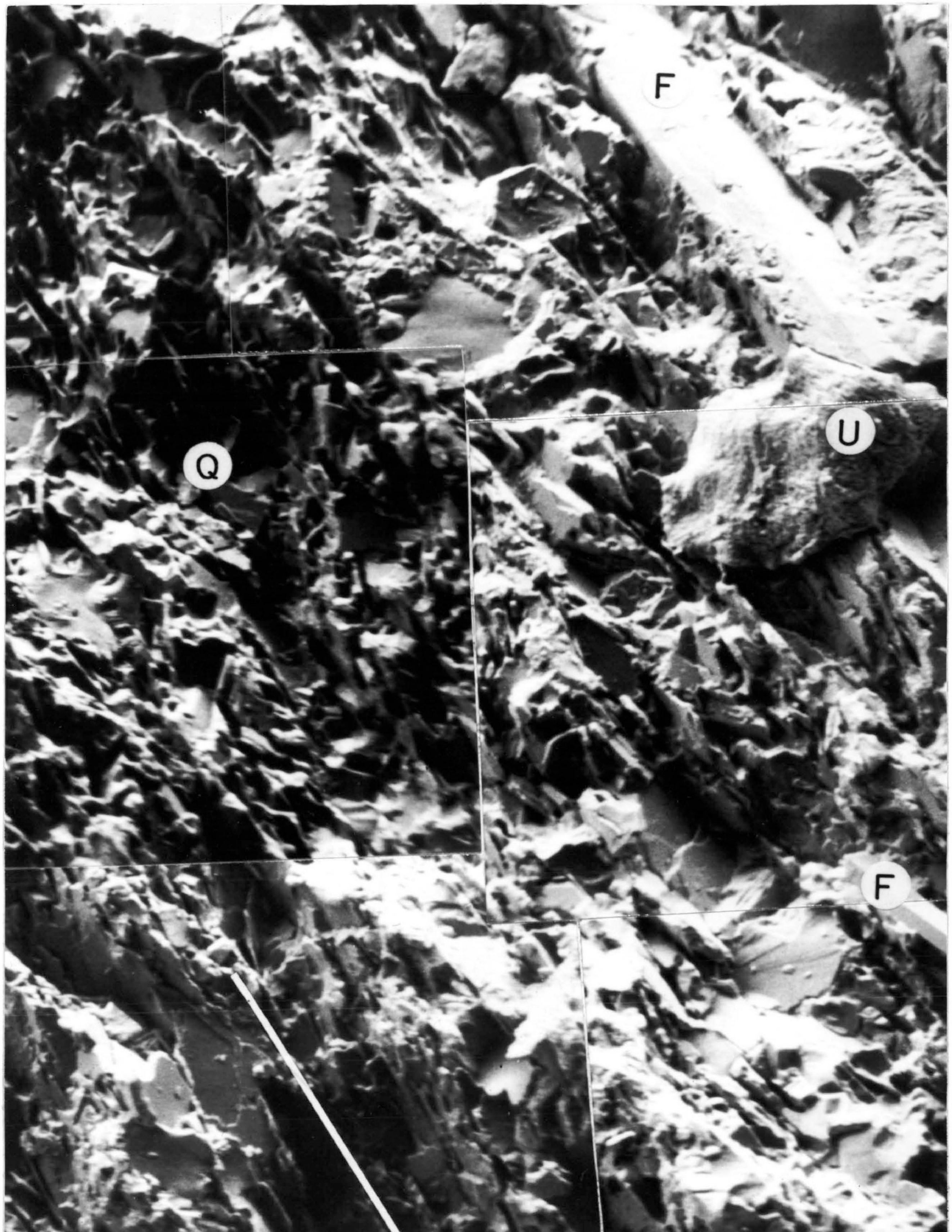

S_1

3 cm = 10 μ

metavolcanic-metasedimentary belt has undergone at least two periods of deformation: 1) An earlier, regional, D_1 event which produced a weak cleavage, mineral lineations plunging to the west and southwest, and upright folds, also plunging west to southwest generally parallel to the mineral lineations; 2) A later, localized, D_2 event characterized by a well-developed cleavage, mineral lineations plunging to the east and northeast, and generally tight isoclinal folds, with more open folds locally, that plunge parallel to the mineral lineations. The main manifestation of the separate deformation regions is the mineral lineation produced on the cleavage surfaces (G. M. Stott, personal communication, 1985). In the D_1 areas (see Figure IV-5) this lineation is fairly well-developed, but in the D_2 areas it has been less well-developed (Stott and Schnieders, 1983). Magnetic susceptibility anisotropy determinations were carried out on samples collected by Stott and Schwerdtner (1981) from both domains, to attempt to corroborate the sometimes uncertain lineation measurements. The results very strongly indicated a definite difference in orientation of the fabric in the two domains (see Figure IV-6).

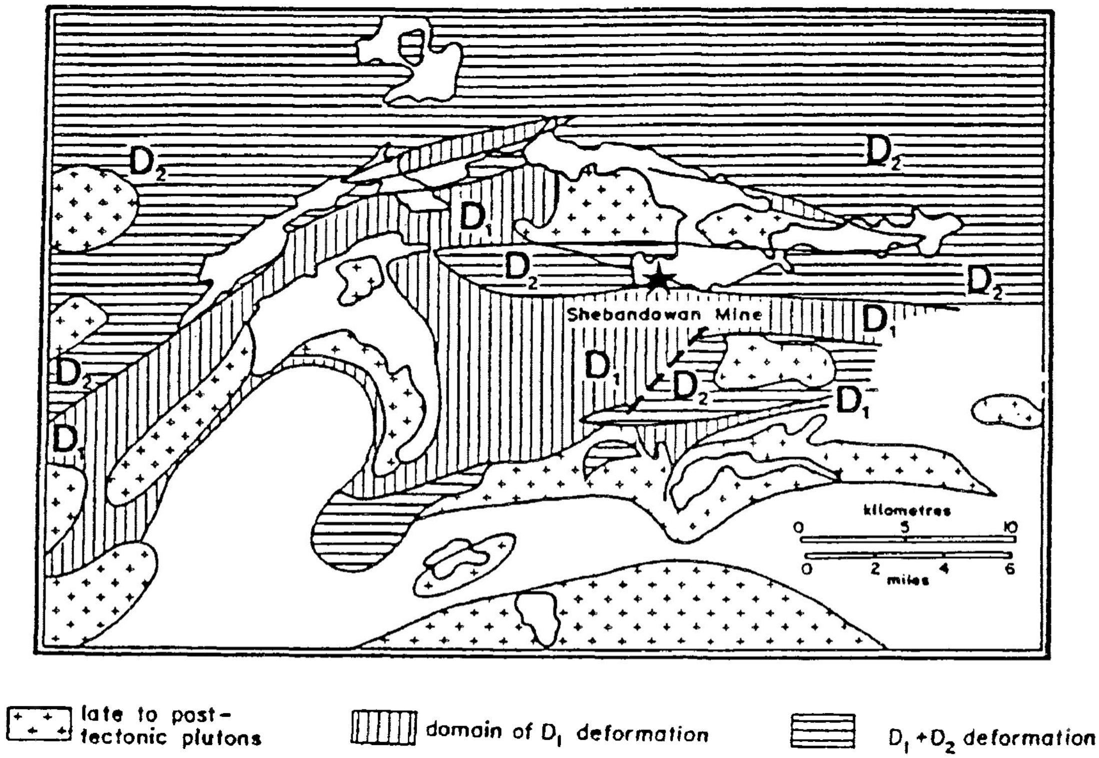

Figure IV-5. Simplified map of the distribution of Stott and Schnieders' D_1 and D_2 domains of total deformation. D_2 domains comprise a composite of D_1 + D_2 deformations. (From Stott and Schnieders, 1983, p.184).

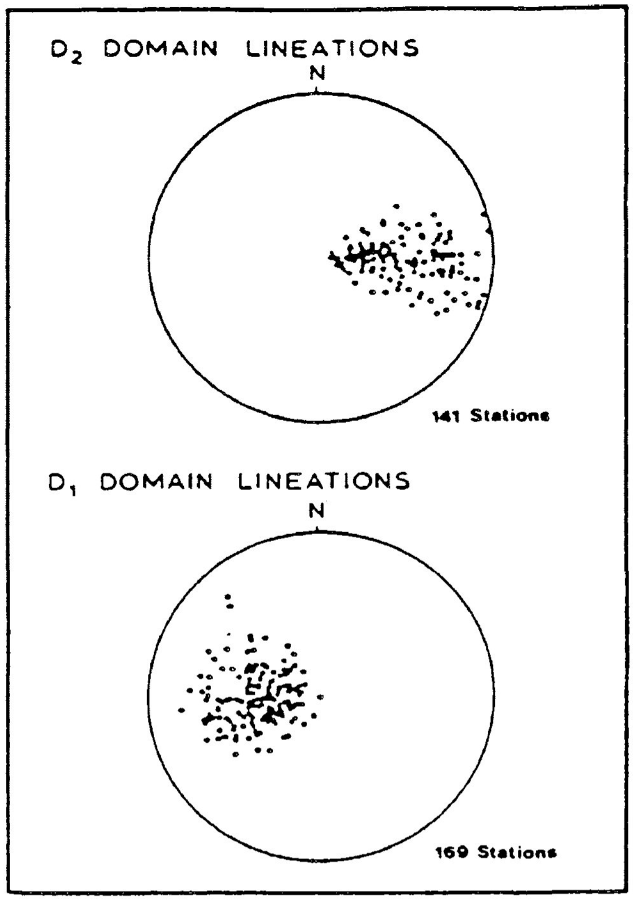

Figure IV-6. Equal area stereograms: top, D_2 domain; bottom, D_1 domain (from area in Figure IV-5). (From Stott and Schnieders, 1983, p.185).

The Shebandowan-type sedimentary rocks and their related volcanics along the Shebandowan Mine road lie in a D_2 domain, as determined by Stott and Schnieders (see Figure IV-5). The remainder of the rocks on the Mine road are included in an area which they designated as D_1.

Magnetic susceptibility anisotropy determinations were carried out on a number of oriented samples collected from the present study area, as well as from locations west of the study area but within Stott and Schwerdtner's (1981) area (see Figure I-2), to characterize the magnetic fabric of the rocks and to assess the reproducibility of Stott and Schnieders' results.

Magnetic Susceptibility Anisotropy: Background

It has long been recognized that the preferred orientation of inequant magnetic minerals influences the anisotropy of susceptibility (Graham, 1954). Thus the orientations of original bedding planes, of directions of paleomagmatic flow, and of orientation of the tectonic fabric of rocks is accurately reflected in the susceptibility fabric. Two characteristics of magnetic minerals make them useful:

1) They generally have an elongate crystal habit and, in the case of magnetite, they are relatively rigid so that, when in a non-static environment such as

a flowing stream or magmatic body, or a rock undergoing deformation, they respond for the most part as rigid bodies. This means that, in a flowing stream or intruding body of magma, the crystals of magnetic minerals tend to become aligned parallel to the direction of flow. In a rock undergoing deformation, these crystals tend to respond to instantaneous stress by mechanical rotation into the direction of instantaneous maximum elongation. Ultimately, it appears that the principal susceptibility directions are parallel to the axes of the finite strain ellipsoid (Hrouda, 1976a) with only certain special exceptions (Borradaile and Tarling, 1981).

2) The magnetic susceptibility of a rock is now a parameter easily measured with considerable precision, and the ratios of principal susceptibilities can be accurately fixed.

The primary mineral of use in MSA studies is magnetite, mainly due to its nearly ubiquitous presence in rocks, and high intrinsic susceptibility. Hematite and pyrrhotite are also useful, however (Hrouda, 1982). One property of magnetic minerals is that they exhibit a directional control of their ease of magnetization. Usually the magnetic domains magnetize most easily in their longest dimension, especially where magnetocrystalline anisotropy is low, so that the overall shape anisotropy of the grains controls the anisotropy of susceptibility (Irving, 1964; Hrouda, 1982).

The bulk anisotropy of the magnetic fabric in a rock can be produced by various means: shape alignment of ferromagnetic grains; lattice alignment of crystals with a magnetocrystalline anisotropy; alignment of magnetic domains by mechanical means or recrystallization; and inequant clustering together of magnetic grains by grain growth (Hrouda, 1982). In rocks where magnetite is the main magnetic constituent, the anisotropy will be controlled by both the grain anisotropy and the degree of preferred orientation of the long axes of the crystals. Where hematite and pyrrhotite are the primary magnetic minerals, the anisotropy will be determined solely by the preferred orientation of the long axes of the crystals (Hrouda, 1982). Studies by various authors have shown that hydrodynamic forces produce a strong preferred orientation of ferromagnetic minerals, resulting in a depositional magnetic fabric parallel to the plane of bedding, but the orienting forces of a flowing magma are not as effective (Hrouda, 1982). Penetrative, tectonic deformation, however, is highly effective as an orienting mechanism (Ibid).

In studies conducted by Hrouda (1976 a, 1976 b) it was concluded that, during deformational processes, magnetite grains in slate respond as rigid particles in a ductile matrix resulting in a change of orientation of the magnetic fabric (generated by the shape alignment of elongate crystals of magnetite). From being parallel to the original bedding plane, the rotation of the magnetite grains in response to the imposed stress produces a magnetic fabric parallel, or very nearly so, to the cleavage formed during deformation. As such, the magnetic fabric of a deformed rock will correspond very closely in orientation to the tectonic fabric of that rock. The directions of maximum and intermediate susceptibility will lie in the plane of cleavage, the direction of minimum susceptibility will be perpendicular to this plane (Rathore, 1979). Multiple fabrics or fabrics arising through pressure solution give characteristic susceptibility orientation fabrics (Borradaile and Tarling, 1981).

Figure IV-7 shows the results of three MSA determinations carried out on rocks from the study area plotted on equal area steronet diagrams. In the two lower diagrams, the great circle represents the average plane of cleavage for the outcrop from which each sample was collected. The upper-most diagram, however, illustrates data from a sample of the matrix of a Shebandowan-type breccio-conglomerate which showed no tectonic fabric. The magnetic fabric also has not been developed to any degree; the maximum, intermediate and minimum susceptibility directions have a completely random distribution. The rock from which the data for the middle diagram were obtained, an outcrop of Keewatin-type mafic volcanic, showed a weakly-developed tectonic fabric. It can be seen that the magnetic fabric has also begun to develop a more measureably consistent orientation. In the lower-most diagram, representing data from another outcrop of Keewatin-type mafic volcanic, the well-developed tectonic fabric is reflected by the well-developed magnetic fabric. The directions of maximum and intermediate susceptibility lie in, or close to, the plane of cleavage. The directions of minimum susceptibility cluster around a point which is the pole to this plane. The tectonic fabric is coaxial with the magnetic fabric so that the minimum susceptibility is perpendicular to cleavage.

Figure IV-7. The magnetic fabric of a deformed rock corresponds well with its tectonic fabric. a) This sample of Shebandowan-type breccio-conglomerate showed no tectonic fabric; no magnetic fabric is evident either. b) A slight tectonic fabric in this sample of Keewatin-type mafic volcanic coincides with a slight magnetic fabric. c) When the tectonic fabric of a rock is well developed, as in this sample of Keewatin-type mafic volcanic, the magnetic fabric is also well developed. ● - Maximum susceptibility; ▲ - Intermediate susceptibility; ■ - Minimum susceptibility.

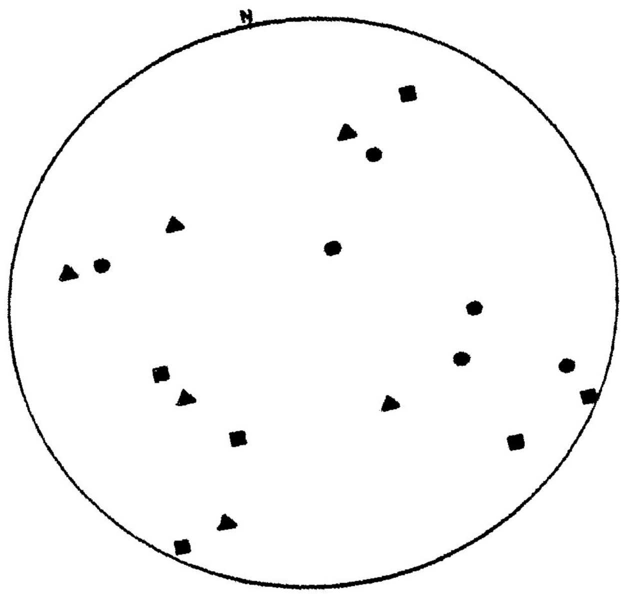

a)

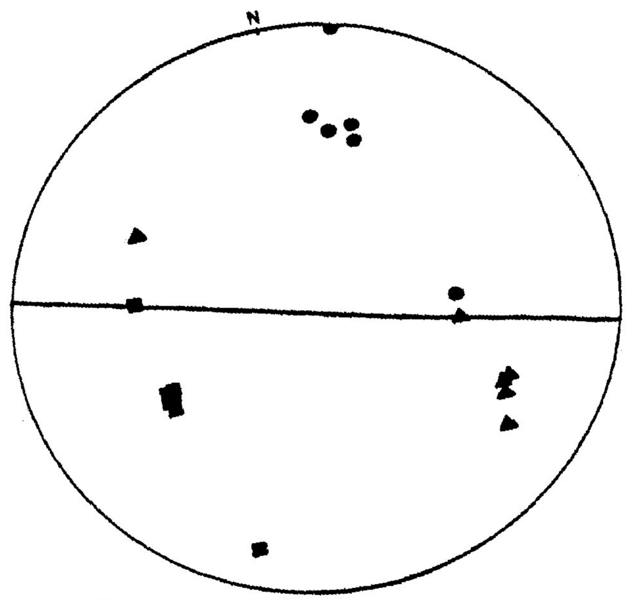

b)

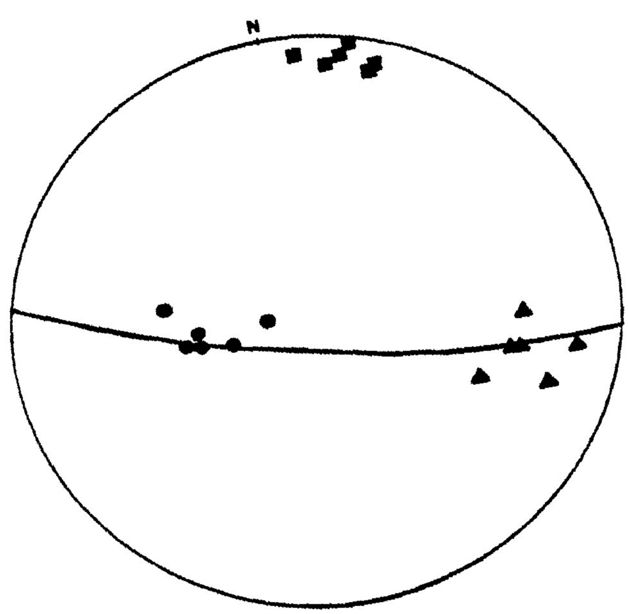

c)

Magnetic Susceptibility: Laboratory

The instrument used was an SI-1 Magnetic Susceptibility and Anisotropy Instrument which consists of a sensing coil operating at about 800Hz attached to a modified Hewlett Packard HP-41CV microcomputer. This instrument measures the inductance in the sensing coil produced when a sample is placed inside. The inductance in the coil is also measured in the absence of a sample to ensure that the measured values relate only to the magnetic susceptibility of the sample. Magnetic susceptibility and anisotropy of magnetic susceptibility programs have been built into the HP-41CV. The MSA program calculates values for the magnitude, inclination and declination of the maximum, intermediate and minimum susceptibility directions. The inductance in the coil is measured for a pre-determined length of time, and each sample is rotated through a set number of orientations so that values can be determined for all three major axes of the sample core (see Figure IV-8). In order to achieve the maximum precision when measuring samples with low susceptibility, such as those in the study area, the sample measuring time must be as long as possible, and the sample should be measured in many orientations. In the present case, the sample measuring time was four seconds, and each

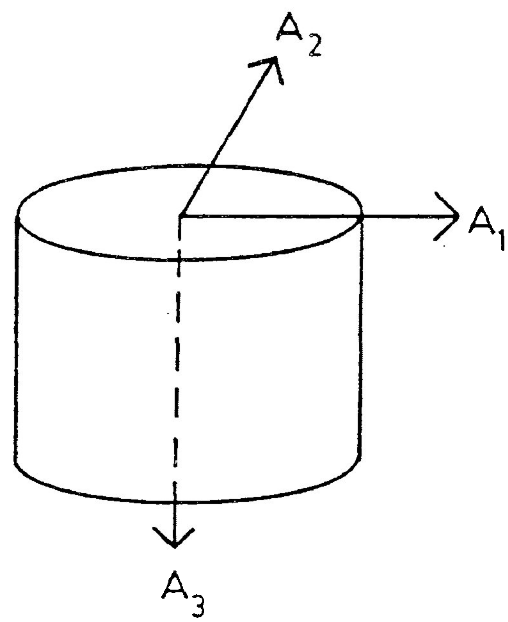

Figure IV-8. The orientation of the three orthogonal MSA axes measured, in relation to the sample core.

sample was rotated through twenty-four orientations, eight for each axis. The entire procedure was repeated six times for every sample. (The data are included in Appendix I).

The MSA study indicates the same results as the other work encompassed in this thesis: a single fabric is present in both the Keewatin-type and Shebandowan-type rocks of the study area. In Figures IV-9 to IV-16, the good correlation between tectonic fabric and magnetic fabric in the majority of the rocks is immediately evident. In each figure, the directions of maximum (●) and intermediate (▲) susceptibility lie very near to the plane of cleavage (denoted by the great circle) measured in each sample. The minimum susceptibility direction (■) is always close to the pole to this plane. The tectonic and magnetic fabrics, therefore, represent the same, single planar fabric element in the rocks.

Because of the correlation with tectonic fabrics, the magnetic fabric of a rock lends itself well to analysis using traditional structural techniques. The magnitude and orientation of the maximum, intermediate and minimum susceptibility directions can be used to define a susceptibility ellipsoid, as the maximum, intermediate and minimum strain directions define the

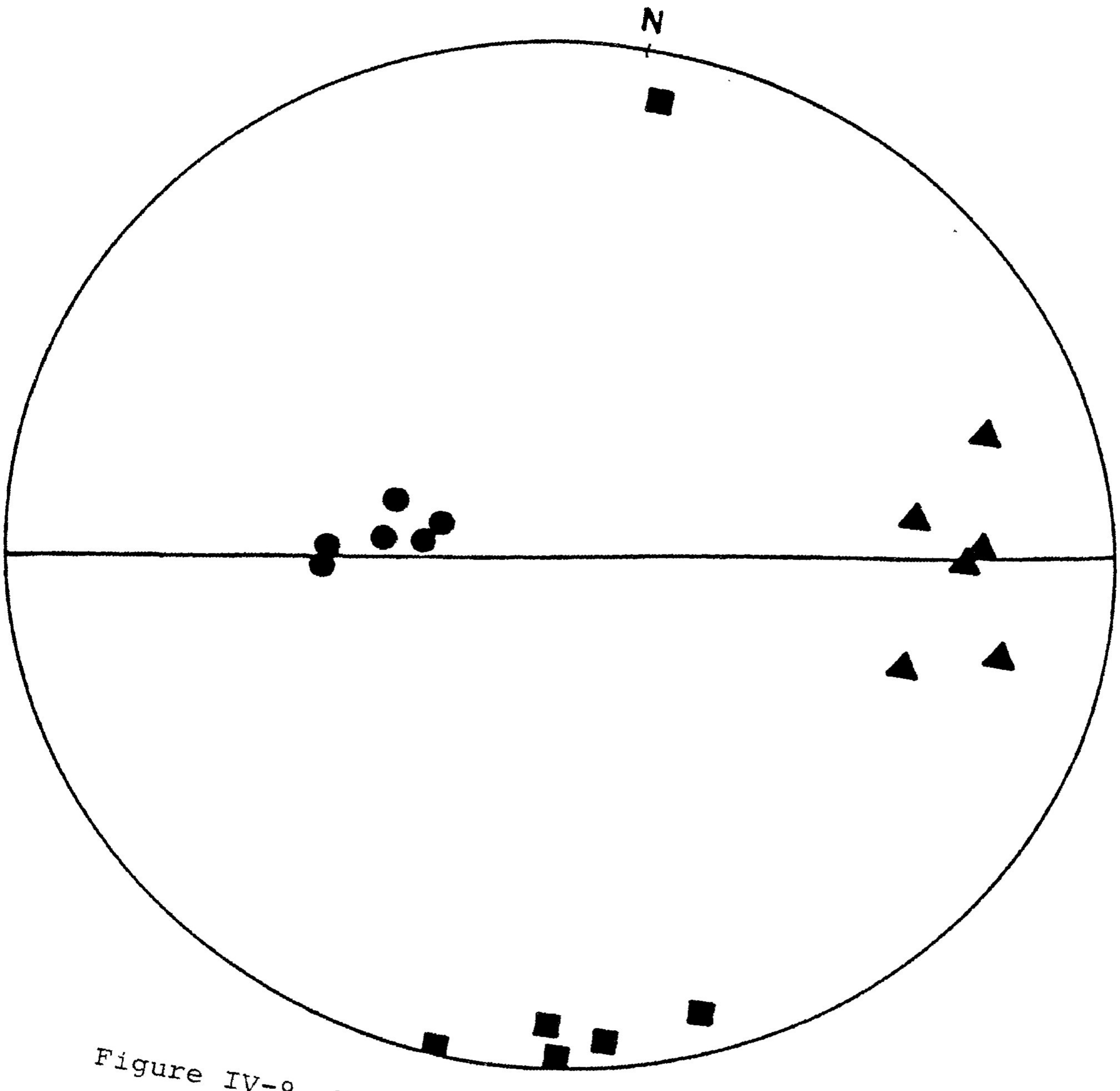

Figure IV-9. Keewatin-type mafic volcanic.

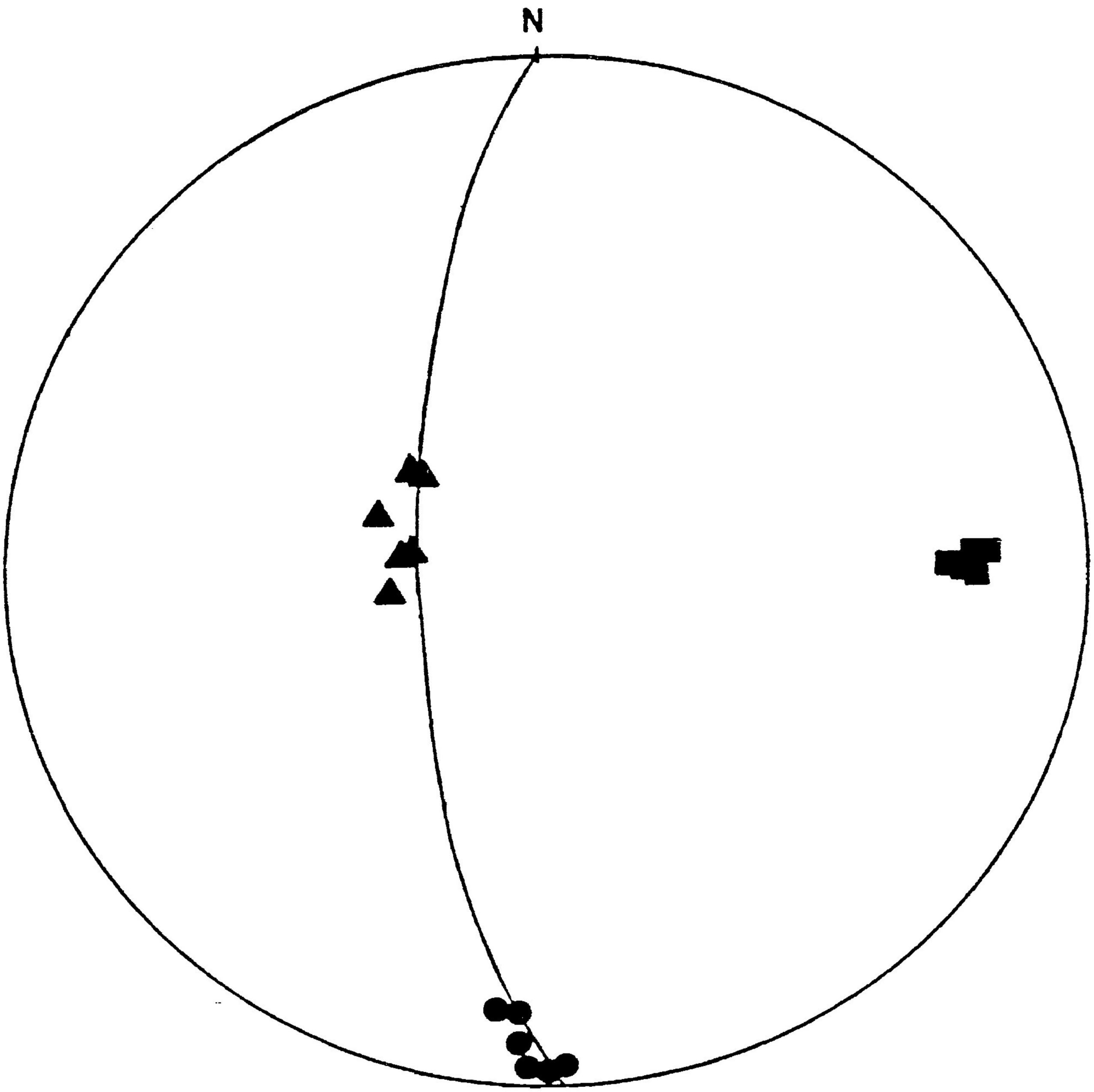

Figure IV-10. From west of present study area. Gabbro from the Kashabowie area.

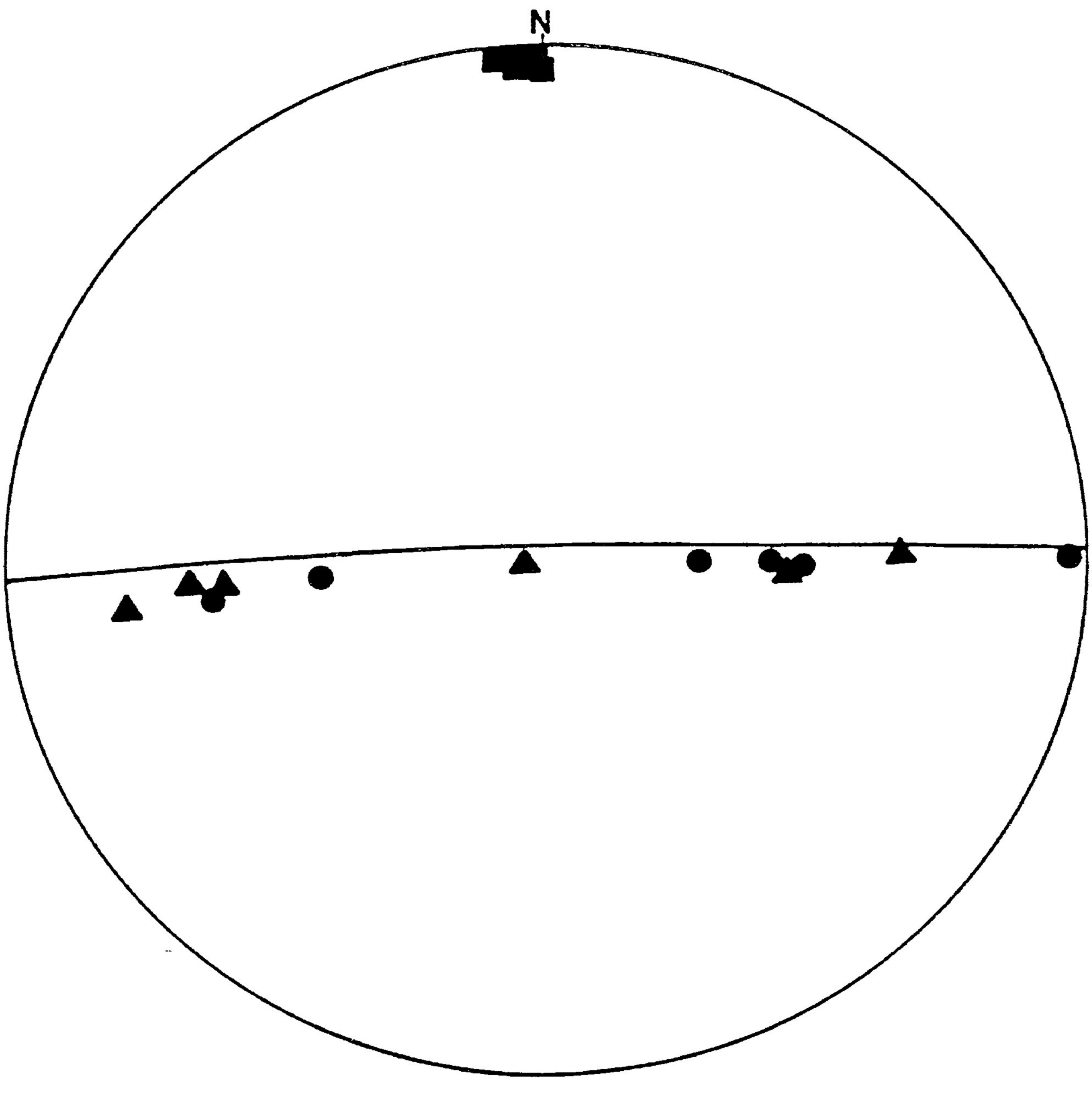

Figure IV-11. From west of present study area.
Gabbro from the Kashabowie area.

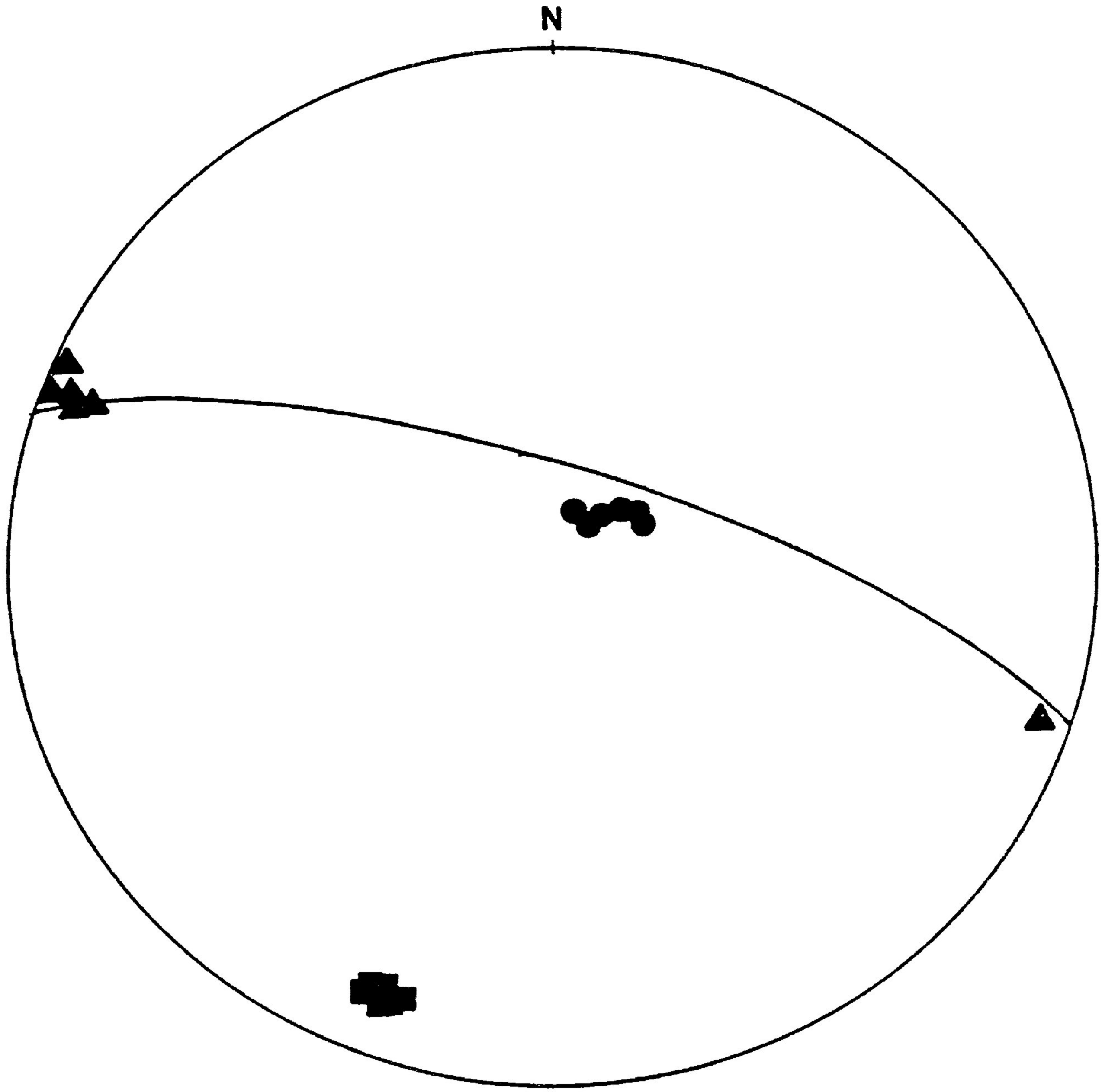

Figure IV-12. Shebandowan-type slate.

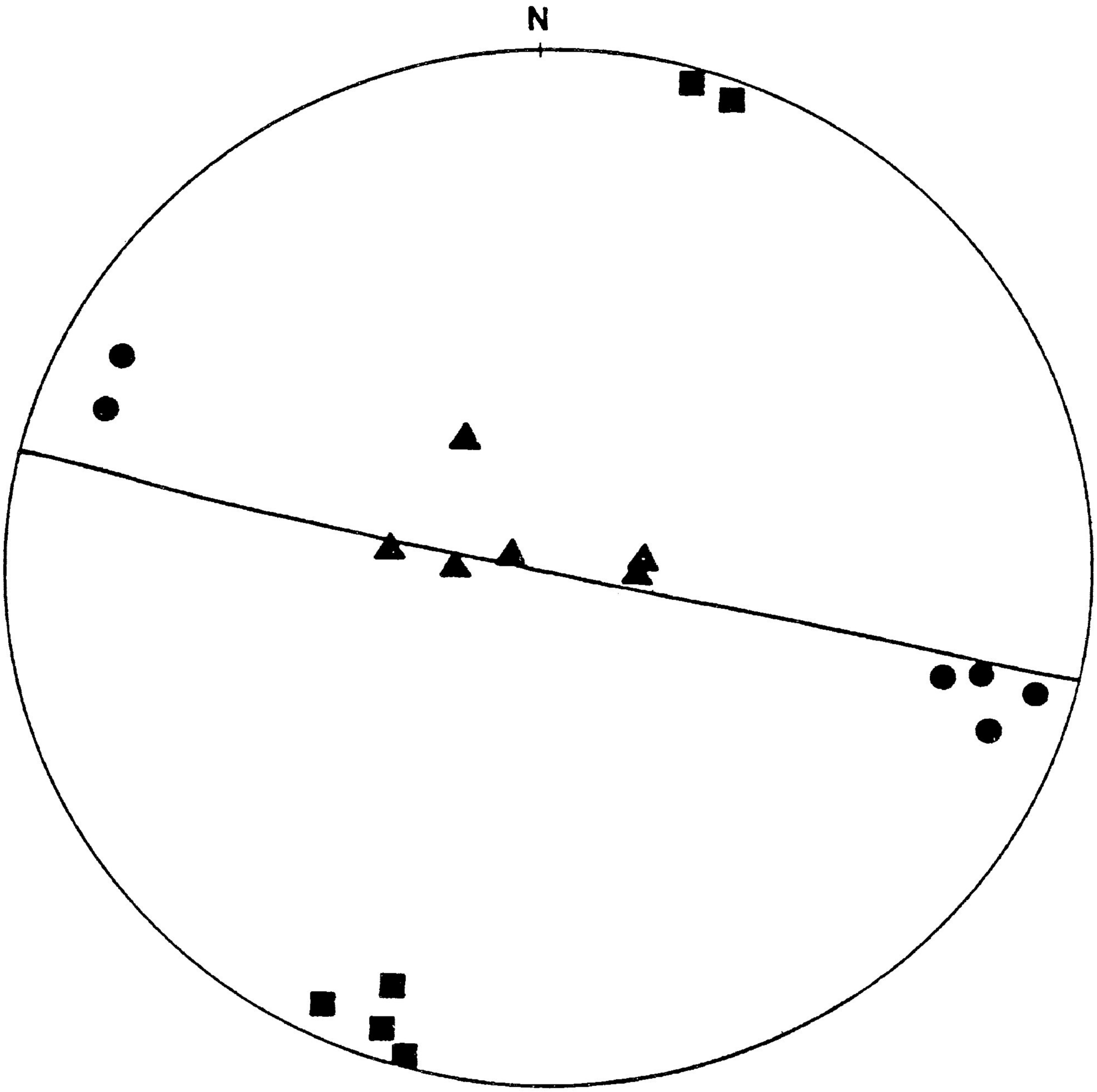

Figure IV-13. Shebandowan-type breccio-conglomerate.

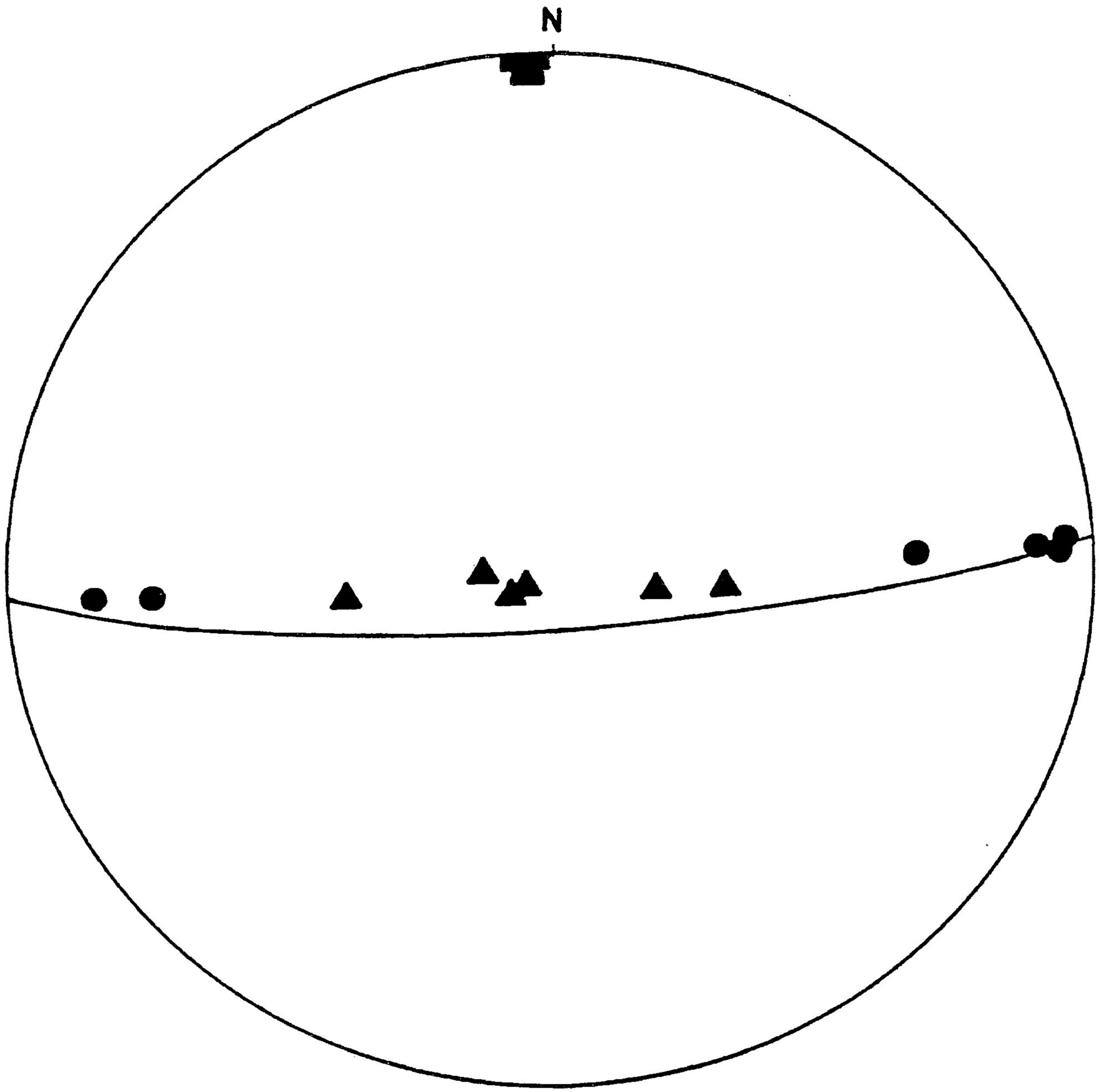

Figure IV-14. Shebandowan-type arkose from the Shabaqua area.

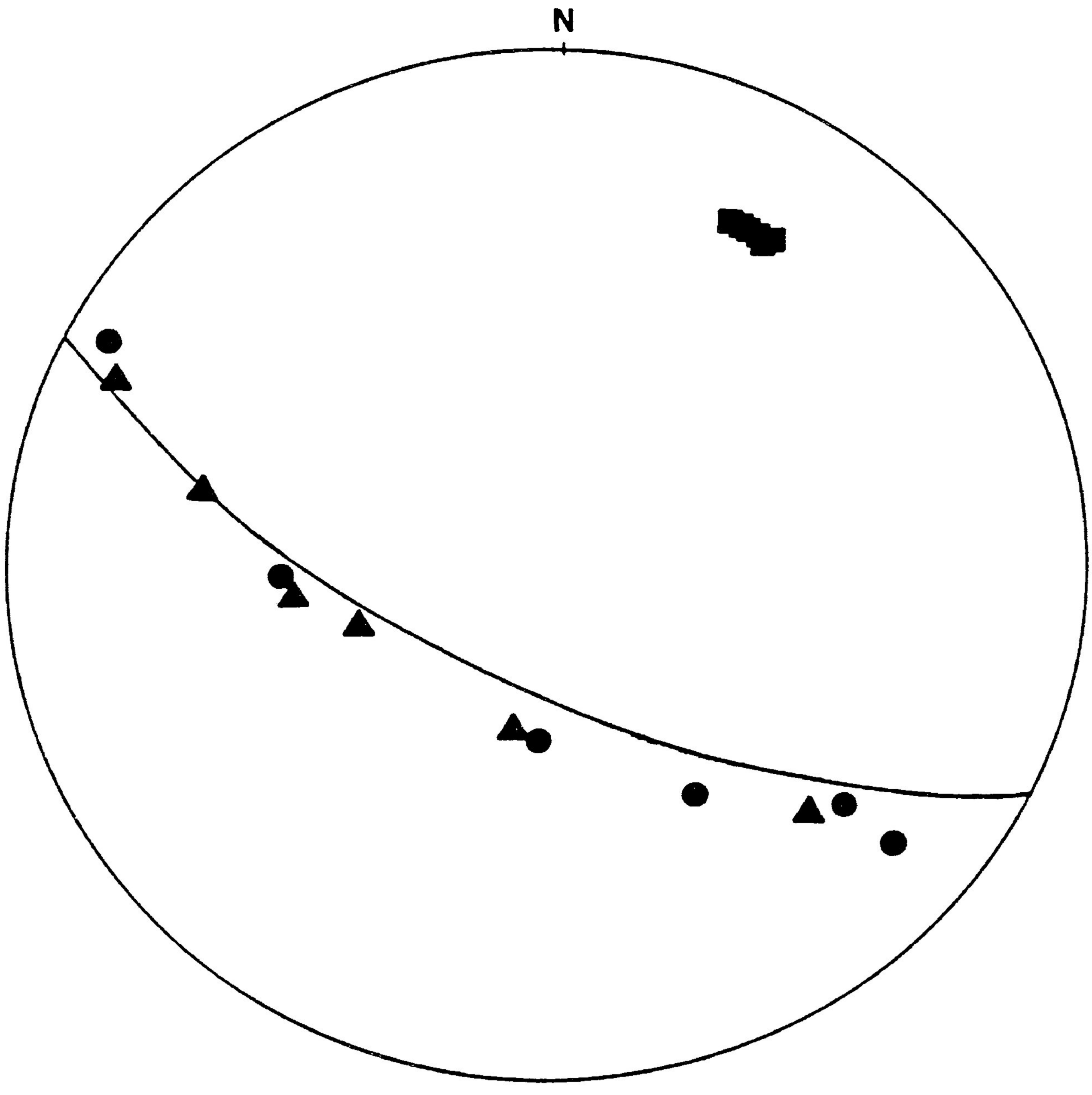

Figure IV-15. Shebandowan-type sandstone from the Finmark area.

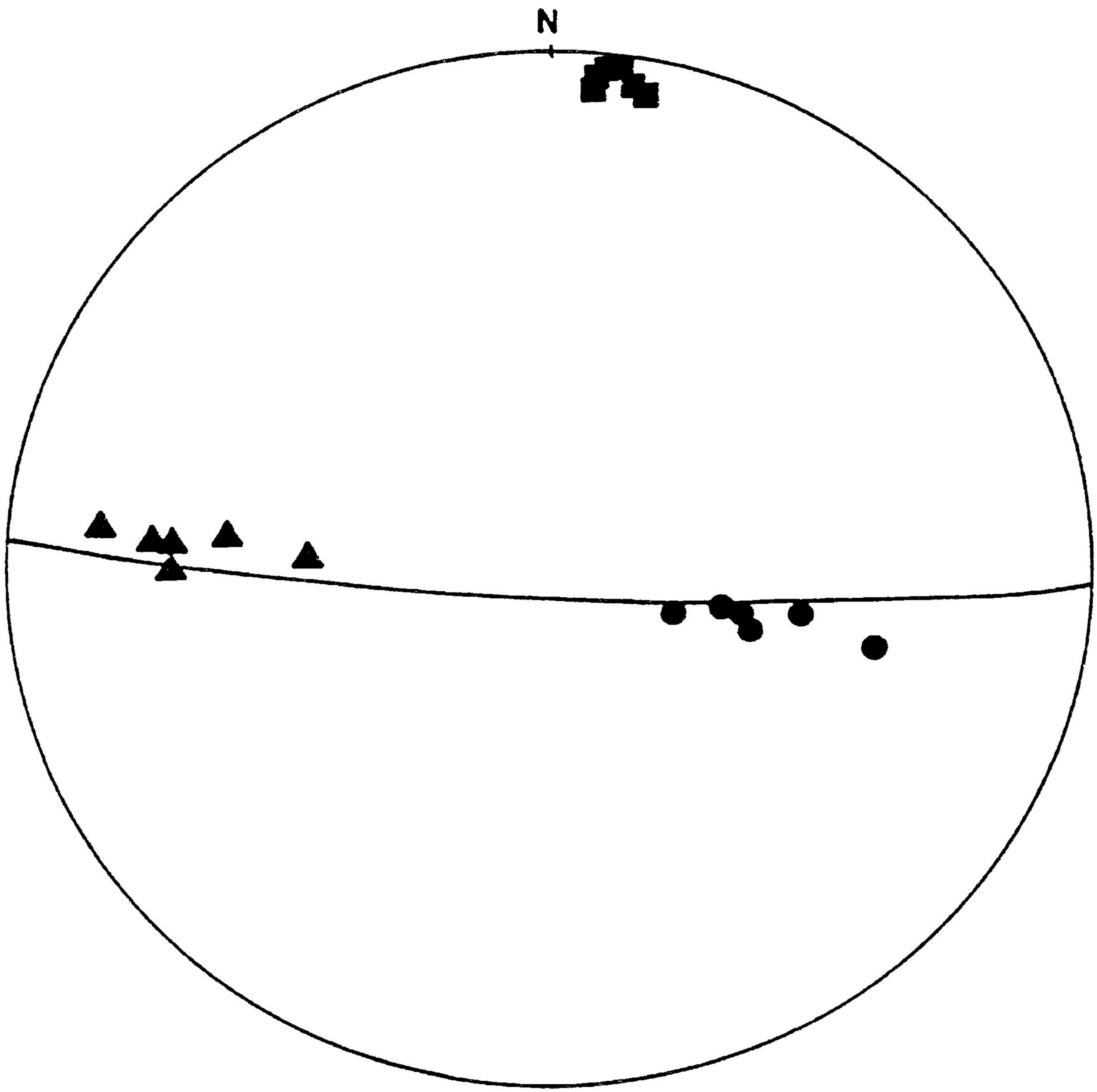

Figure IV-16. Shebandowan-type sandstone from the Finmark area.

strain ellipsoid of a deformed rock (Hrouda et al, 1971). In the absence of strain markers, the susceptibility ellipsoid might be used to characterize the deformation of an area (Kligfield et al, 1977).

The shape of susceptibility ellipsoids can be determined using either of two equations: 1) $E=(k_2)^2/k_1k_3$ (used in this study); 2) $P=(k_2-k_3)/(k_1-k_2)$ (where $k_1 > k_2 > k_3$) (Hrouda, 1982). Both equations represent modifications of traditional structural equations. Predominantly prolate ellipsoids are characterized by $E>1$ and relatively high values of P. Predominantly oblate ellipsoids are characterized by $E<1$ and relatively low values of P.

The values of E calculated for the samples of the present study are all very close to 1 (see data sheets in Appendix I) and, as such, were not taken as definitive characterizations of the shape of the susceptibility ellipsoids. Instead, the magnetic lineation ($L=k_1/k_2$) and magnetic foliation ($F=k_2/k_3$) (Hrouda, 1982) of each sample was calculated and the results were plotted on a modified Flinn diagram, similar to deformation plots. (Values of k_1, k_2 and k_3 are averaged from the results of the six determinations per sample). Figure IV-17 illustrates, more clearly than the calculated E values, the shape of the magnetic

Figure IV-17. k_n (n = 1, 2, 3) represents a measure of the ease of magnetization along the three orthogonal axes of the magnetic susceptiblitiy anistotropy ellipsoid. When the axial ratios are plotted on a modified Flinn diagram (cf Hrouda, 1982) a qualitative estimation of the degree of prolateness (constriction) or oblateness (flattening) of the MSA ellipsoid is possible.

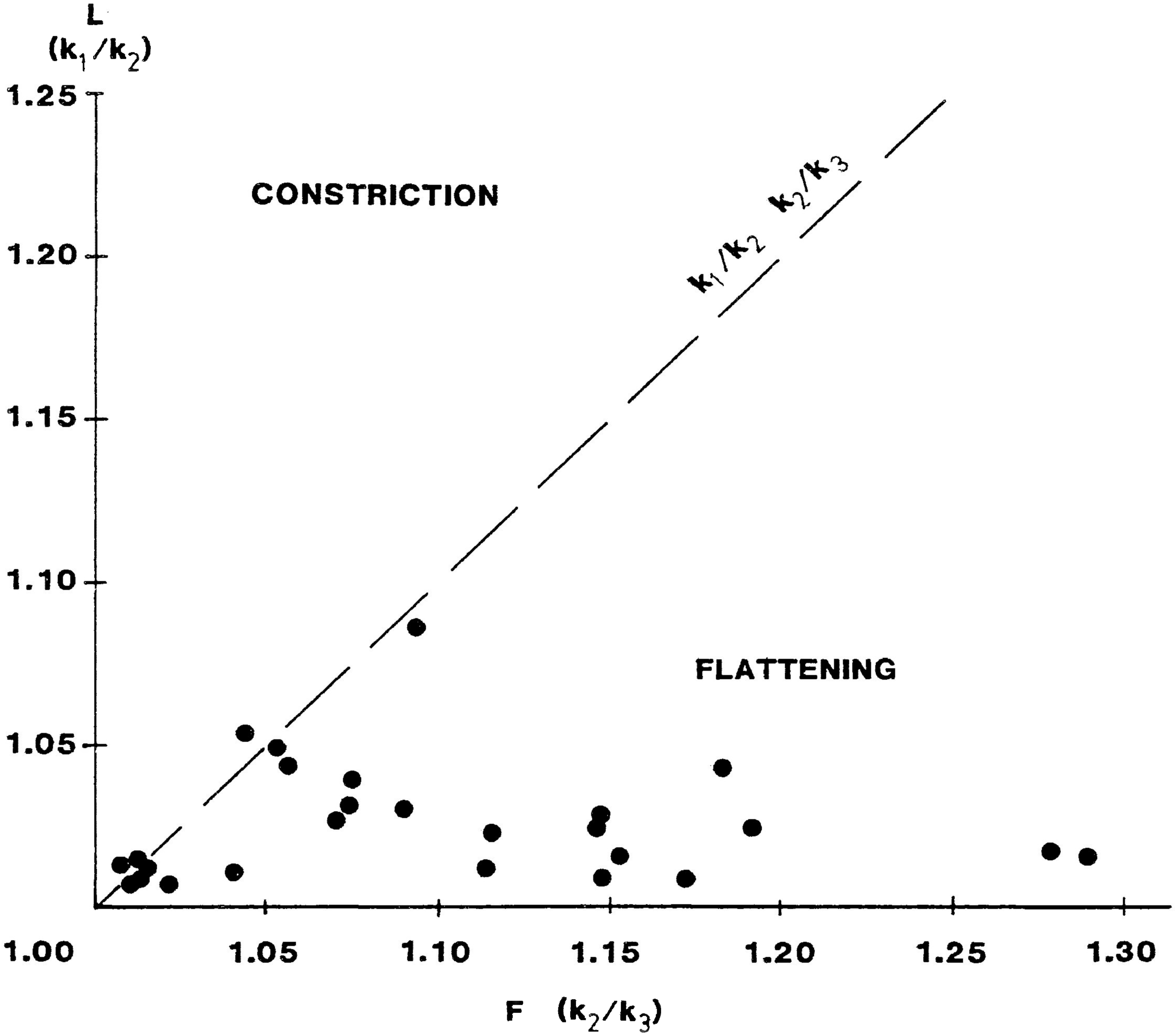
L
(k_1/k_2)
1.25
1.20
1.15
1.10
1.05
CONSTRICTION
k_1/k_2 k_2/k_3
FLATTENING
1.00
1.05
1.10
1.15
1.20
1.25
1.30
F (k_2/k_3)

susceptibility ellipsoids of the rocks in the study area. The majority of the samples plot in the field of flattening, characterized by pancake-shaped, or oblate, ellipsoids. The remainder of the samples lie in the field of constriction, but very close to the boundary of the field of flattening. None of the samples show a significant difference in magnitude between the maximum and intermediate susceptibilities, however, there is a great range in the ratio of the intermediate to minimum susceptibilities among the samples. This is most likely a reflection of the variability in the degree of development of the cleavage in the rocks.

To assess the reproducibility of Stott and Schwerdtner (1981) and Stott and Schnieders' (1983) results, oriented samples were collected from areas which had been specifically designated by them as being characterized by westerly-plunging or easterly-plunging mineral and magnetic lineations. The directions and magnitudes of the principal susceptibility directions of the samples were determined following the procedure outlined previously in this chapter. Figure IV-18a shows the directions of maximum susceptibility of the samples considered in this study plotted on an equal area stereonet. Their distribution shows a similar character to that found by Stott and Schwerdtner (1981)

(Figure IV-18b). In both figures, there appears to be a predominant westerly plunge to the maximum susceptibility of samples collected from some areas, and a predominant easterly plunge to the maximum susceptibility measured in samples collected from other areas. It would seem, therefore, that the rocks in the Shebandowan area can be differentiated based on the direction of plunge of their magnetic fabric. However, that this is an indication of polyphase deformation can not be concluded from the data presented herein. In other words, the single tectonic fabric can be reconciled with the changes in plunge of the magnetic lineation if we consider those changes in plunge to be gradual and transitional.

Figure IV-18a. Orientation of maximum magnetic susceptibility of samples collected from areas designated as "D_1" and "D_2" by Stott and Schwerdtner (1981), plotted on equal area stereonets. Each point is based on an average of six separate determinations.

Figure IV-18b. From Stott and Schwerdtner (1981, p.36). Equal area stereograms showing the westerly and easterly concentrations of MSA lineations. Steep north- and south-plunging lineations tend to occur close to strain domain boundaries. Those authors considered the westerly-plunging lineations to belong to a D_1 episode, and the easterly-plunging lineations to belong to a D_2 episode as indicated.

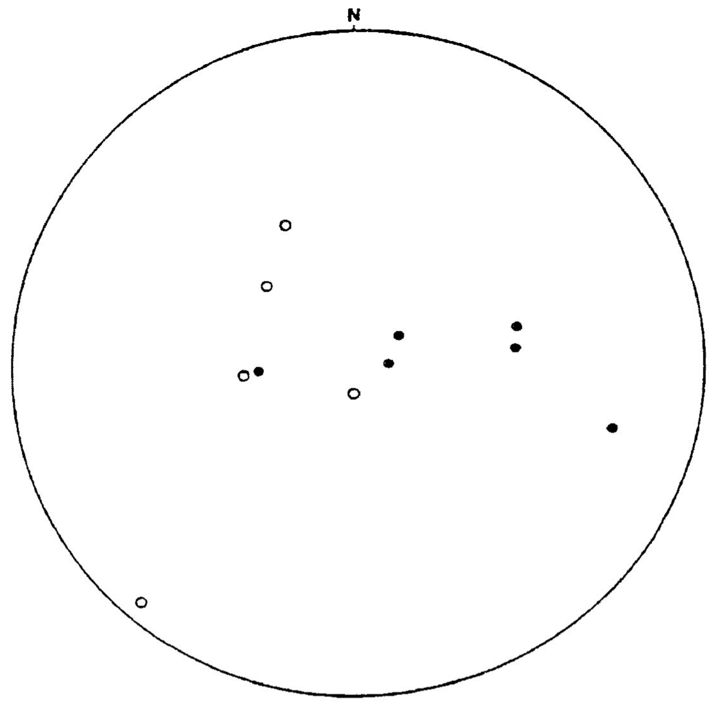

a) O Designated "D_1" area

● Designated "D_2" area

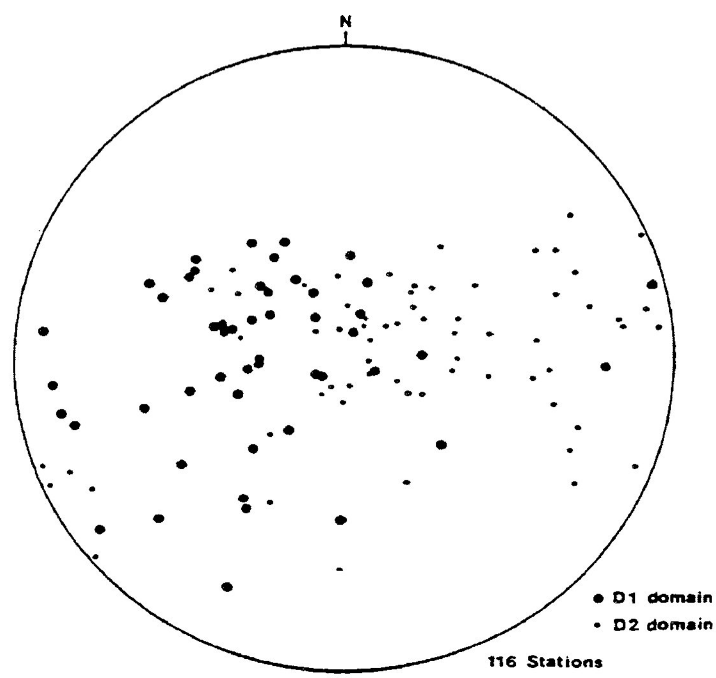

b)

Regional Structure and Stratigraphy

Although measurable key features such as minor folds are not particularly widespread in the rocks of the study area, the overall structure can still be deduced from the available cleavage, bedding and younging data. The orientation of major fold axes can be interpreted from the cleavage-bedding intersection relationships in the outcrops displaying reliable bedding and adds to the information which can be acquired from the few folds which are present in the outcrops of the Shebandowan-type rocks. The relative positions of major antiforms and synforms can be fixed by the sense with which cleavage cuts bedding, assuming that cleavage is axial planar.

Unfortunately, the majority of the structural data can only be obtained from the Shebandowan-type rocks. Even though pillowed volcanic flows are present in some outcrops of the Keewatin-type rocks, these were not used for cleavage-bedding interpretations of local major fold axes because the bedding was not considered to be reliable from pillow shape. As noted by Borradaile (1982) there are many variables which have an effect on the final shape of a deformed pillow. These include the initial shape of the pillow, its original position relative to the strain ellipsoid of the imposed deformation, the nature of the history of deformation (coaxial or non-coaxial) and the duration of the deformation. A simple measurement of the long axis of a deformed pillow is not necessarily an accurate indication of the orientation of original bedding. Where pillowed flows were present in the Keewatin-type rocks, therefore, they were only used as an indication of the approximate local younging or way-up direction, and not to determine structural facing.

From the data available in the Keewatin-type rocks, the structure appears simple. As an example, in the outcrops along the Shebandowan Mine road (see Figure V-1) where the exposure is best, only a single, primary cleavage is present, oriented at approximately 90° and dipping steeply to north or south, or vertical. The available younging data in these rocks indicate that the beds young consistently to the north. When projected on to the cleavage, the younging shows that structural facing is to the east. Apart from one or two very minor, localized kink zones, none of the evidence suggests more than one phase of penetrative deformation. (Note, however, that in similar volcanic rocks to the west of the study area, outcrops of schistose rocks with later folds have been noted by the author during separate field work, carried out for another purpose for the Ontario Geological Survey.)

The structural information in the Shebandowan-type

Figure V-1: Structure and stratigraphy along the Shebandwoan Mine road. (See Map 1, in pocket, for location).

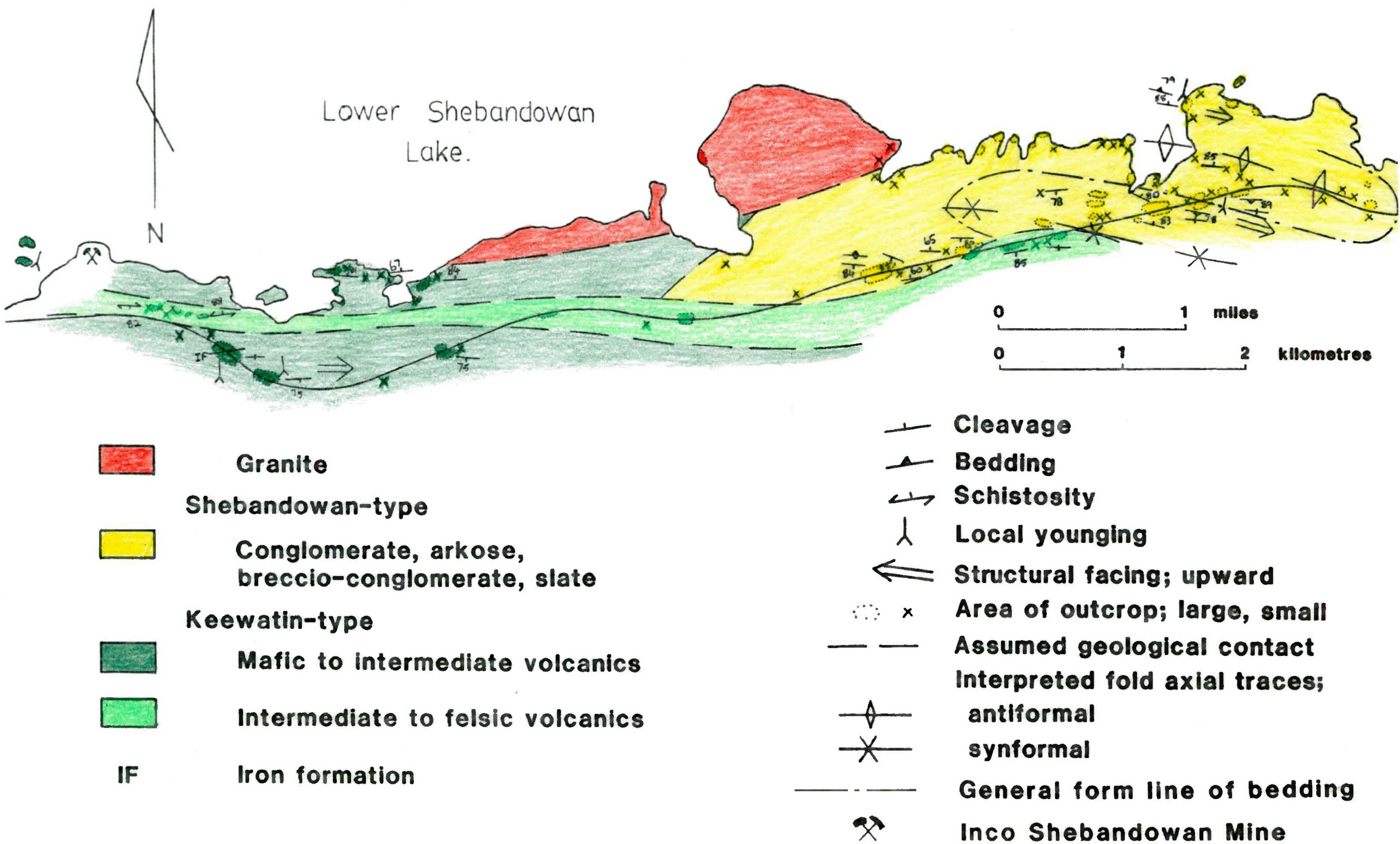

Lower Shebandowan Lake.
N
IF
0
1
miles
0
1
2
kilometres
Granite
Shebandowan-type
Conglomerate, arkose, breccio-conglomerate, slate
Keewatin-type
Mafic to intermediate volcanics
Intermediate to felsic volcanics
IF
Iron formation
Cleavage
Bedding
Schistosity
Local younging
Structural facing; upward
Area of outcrop; large, small
Assumed geological contact
Interpreted fold axial traces;
antiformal
synformal
General form line of bedding
Inco Shebandowan Mine

rocks is much more complete. Plane-bedded arkoses and sandstones are quite common, as are such younging indicators as cross-bedding, graded bedding and sand dykes, permitting reliable cleavage-bedding intersection and structural facing interpretations, respectively. The typical structure of these rocks is again best illustrated in outcrops along the Shebandowan Mine road. (See Figure V-1). The single cleavage in these rocks is oriented at approximately 90-100° with a variable steep or vertical dip. The cleavage-bedding relationships, however, indicate the presence of several major folds in this area. These folds are isoclinal, with steeply-dipping axial surfaces parallel to the cleavage. Local younging directions, when projected on to the cleavage, indicate that the folds close sideways and are structurally upward facing to the east. This typical regional structure still prevails in the Shabaqua area, approximately twenty kilometres to the east of the Shebandowan Mine road (see Figure V-2), possibly suggesting a very thick sequence of sedimentary rocks.

The regional structure as shown in Figure V-I also illustrates the nature of the boundary between the Keewatin-type and the Shebandowan-type rocks. The axial traces of folds in the Shebandowan-type rocks appear to be truncated by the contact with the Keewatin-type rocks. The boundary also cuts across the general trends of bedding and

Figure V-2: Structure in the Shabaqua area shows typically close-spaced, isoclinal folding. (See Plate C, at back, for location).

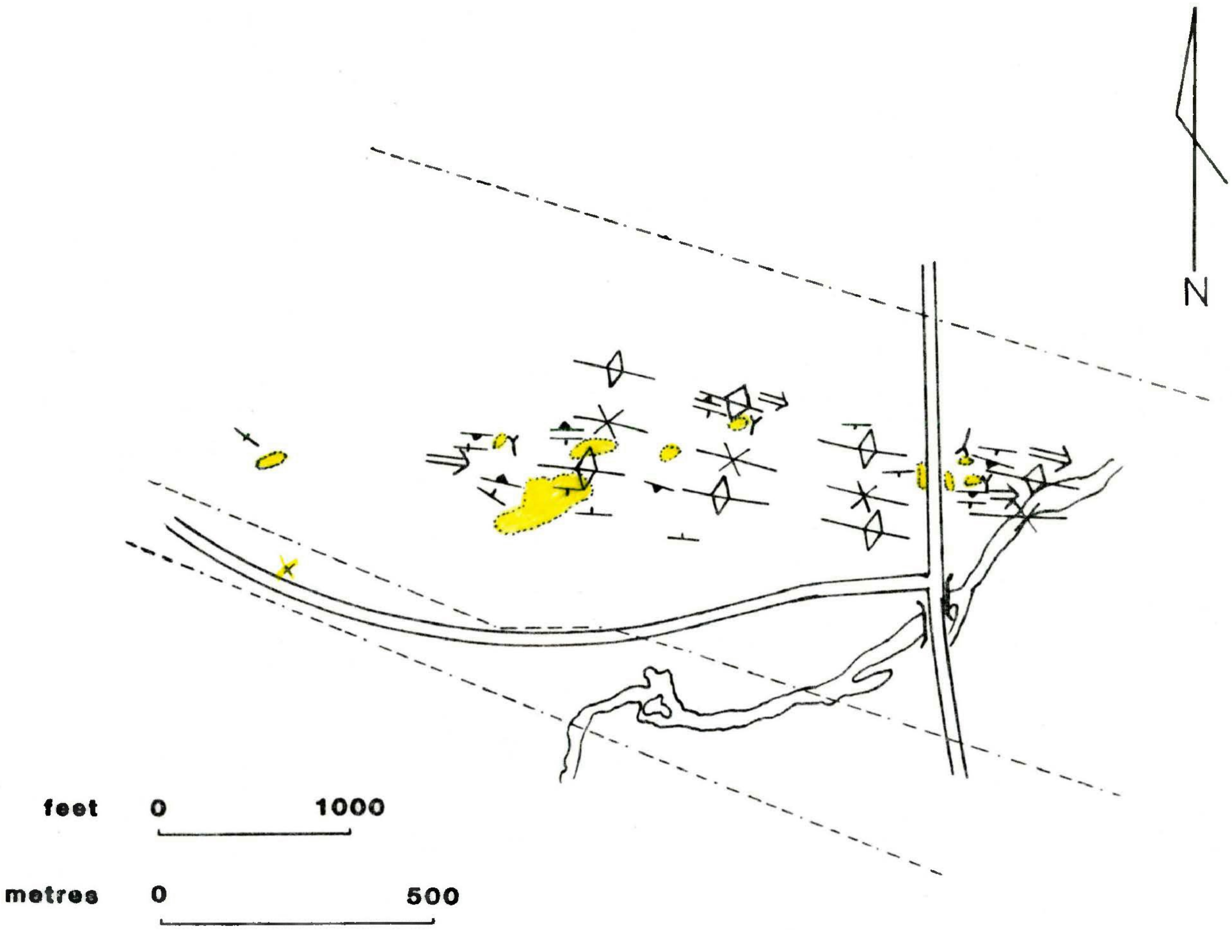

Conglomerate, arkose

Cleavage

Bedding

Local younging

Area of outcrop; large, small

Structural facing; upward

Interpreted fold axial traces;

antiformal

synformal

Hydroelectrical and telephone lines

cleavage in the Shebandowan-type rocks. This pattern is inconsistent with there being a conformable post-tectonic (let alone pre-tectonic) relationship between the two groups of rocks, and leads to the conclusion that the Shebandowan-type rocks are fault-bounded.

Although the typical structure of the Shebandowan-type rocks is that of isoclinally-folded, structurally upward and easterly facing, exceptions to this do occur. The prevalent structural style of the sedimentary rocks in the Finmark area is one of more open folding, although still with steeply-dipping axial planes, as illustrated in Figure V-3a. Plate 1 shows an outcrop of gently folded strata (S_0) cut by a steeply-dipping cleavage (S_1) which is axial planar. (The parallelism of S_1 cleavage with axial planes is shown by individual minor folds, as mentioned in Chapter III, but also by the clustering of S_1-S_0 (cleavage-bedding) intersection lineations, as shown in Figure V-3b). In this photograph, the fold axis down-plunges to the east (in the direction of the head of the hammer) at an angle of 70°. Although the lamprophyre dykes which intrude this outcrop disrupt the bedding, as shown in Plate 3, this effect does not extend to any great length into the host rock. Late fracturing and minor faulting in this area generally produce

Figure V-3a

Plate 1 - A more gentle fold than the typically isoclinal regional folds, in an outcrop of bedded Shebandowan-type sandstone and arkosic sandstone from the Finmark area. The hammer is oriented parallel to the fold axis. The head of the hammer indicates the direction of plunge of the fold axis. S_0 = bedding, S_1 = rock cleavage.

Plate 2 - The same outcrop as in plate 1. The seemingly incompatible strike of bedding on either side of the dashed white line represents a small fold, parasitic to the major fold, which has been cut by later fracturing parallel to the lamprophyre dike (top left-hand corner of photo).

Plate 3 - The same outcrop as in plate 1. The effects of the intrusion of the lamprophyre dike (LD) on the bedding only extend for a short distance from the contact.

Plate 4 - The same outcrop as in plate 1. Later faulting has also affected these rocks, but typically the offsets are only minor. The dashed white line in the top central portion of the photograph shows the offset of bedding along one such fault.

Plate 1

Plate 2

Plate 3

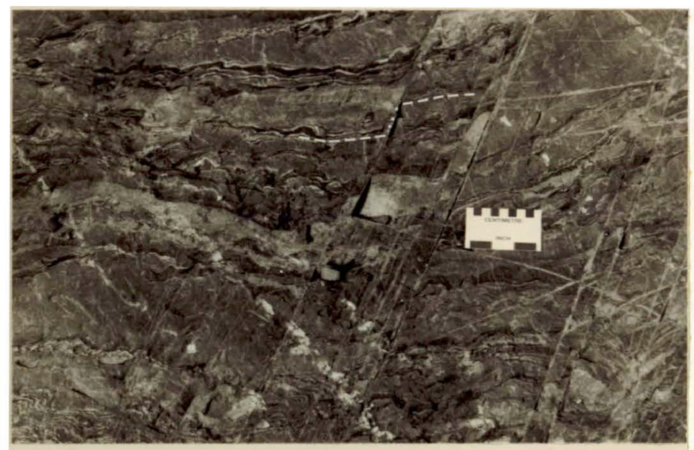

Plate 4

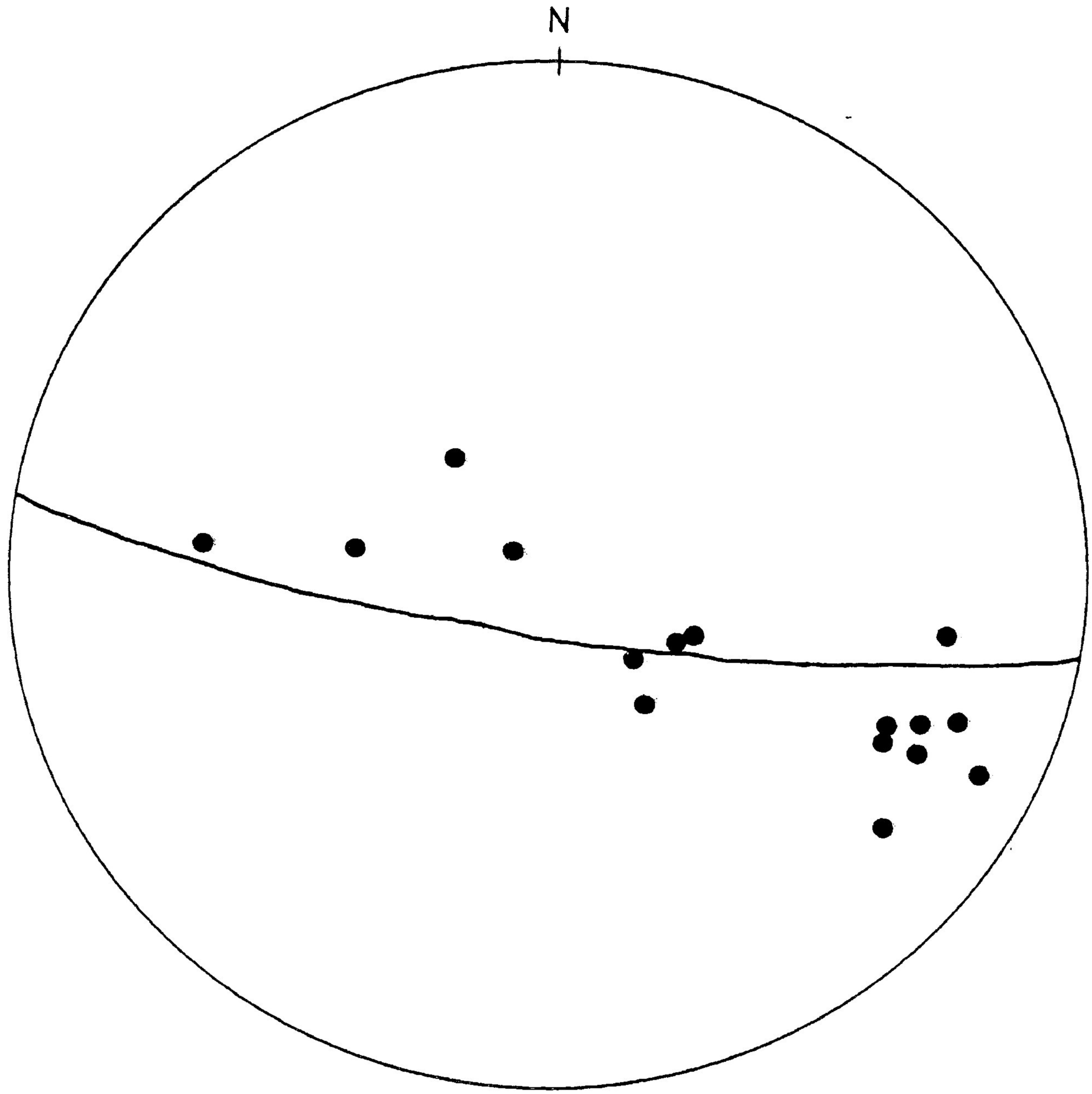

Figure V-3b: Measured S_1/S_0 intersection lineations and the mean S_1 cleavage orientation (mean of 200 measurements).

only slight offsets, as shown in plate 4.

This particular outcrop also exhibits downward structural facing, another feature not common in the study area. Figure V-4 illustrates that, although the fold axis plunges to the east, the way-up indicators show that the sequence of planar and wavy-bedded arenites youngs to the west. When projected on the the cleavage, the structure is downwards facing to the west; the bedding is slightly overturned. This relationship is rare and very localized, however. A series of outcrops of the same rock type approximately 1000 feet to the east of the outcrop illustrated in Figure V-4 shows a normal upward facing structure. (See Figure V-5.) The direction of younging is to the northwest, as is the dip of bedding. When projected on to the cleavage, the younging direction results in a westerly structural facing, which is consistent with the local, but not the regional structure. Although this appears to be the predominant direction of structural facing for all the Shebandowan-type rocks in the area of Fourway School (see Figure V-6), the strike of the cleavage in the area is still correlative with the regional strike of cleavage. In both folds which are present in

Figure V-4: Downwards structural facing in a folded outcrop in the Fourway School area. The direction of younging (indicated by graded bedding and load casts) is to the west and southwest, but the strata and fold axis have an easterly dip. Cleavage is axial planar. A small fault has offset some of the layers by up to 8 inches. (See Plate D, at back, for location).

Cleavage
Bedding
Younging
Downward structural facing
Fold axis
LD Lamprophyre dyke

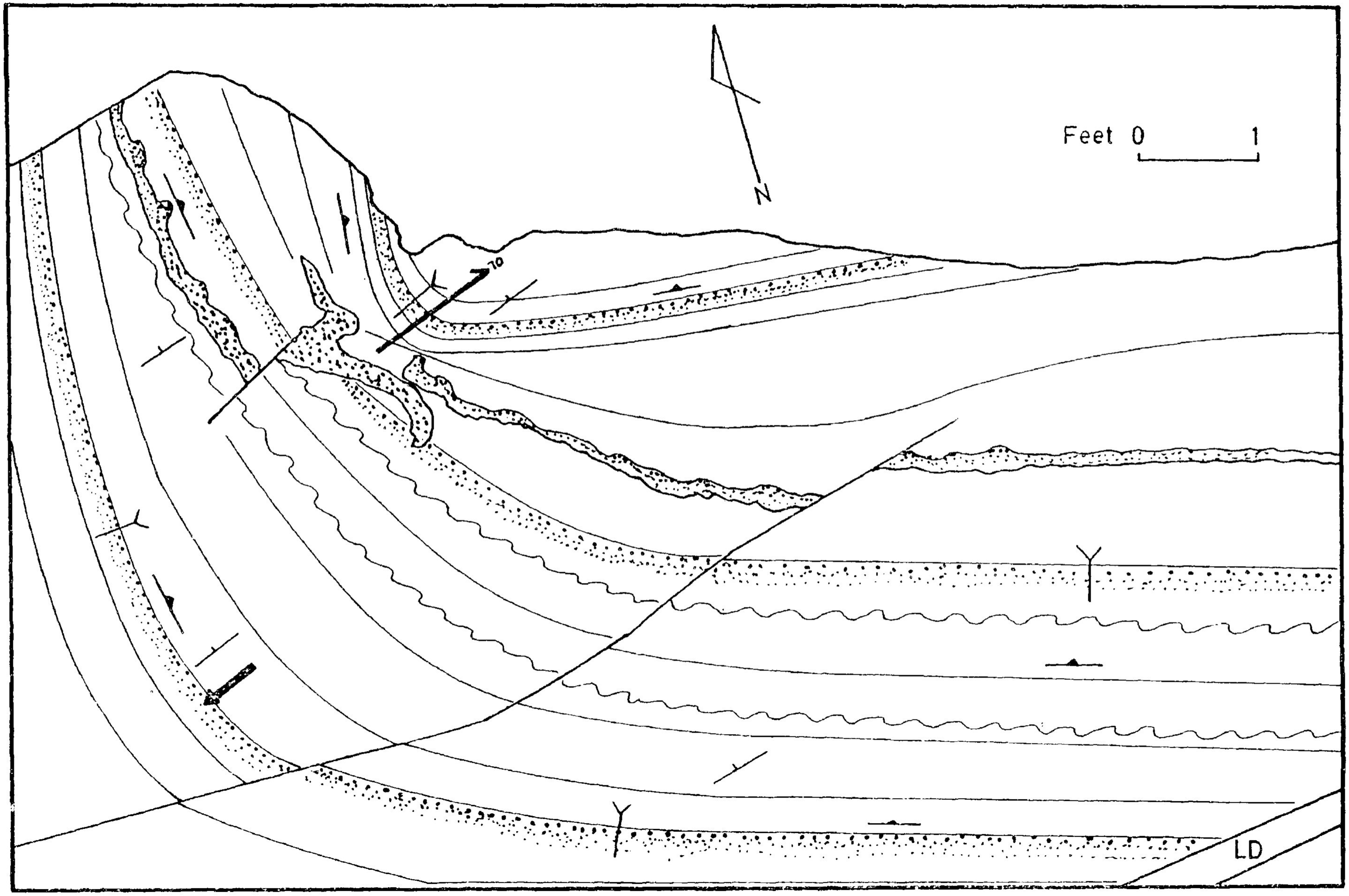
N
Feet 0 1
70
LD

Figure V-5: In this sketch of an outcrop in the Four-way School area the strata show more typical upward structural facing. The direction of younging (indicated by cross-beds and graded beds) is to the northwest, as is the dip of the bedding. Note the rip-up clasts and mud chips in the southeastern part of the outcrop, and the mud cracks, seen in plan view on the scoured-out surface at the eastern edge of the outcrop.

(See Plate D, at back, for location).

Cleavage
Bedding
Younging
Upward-facing structure

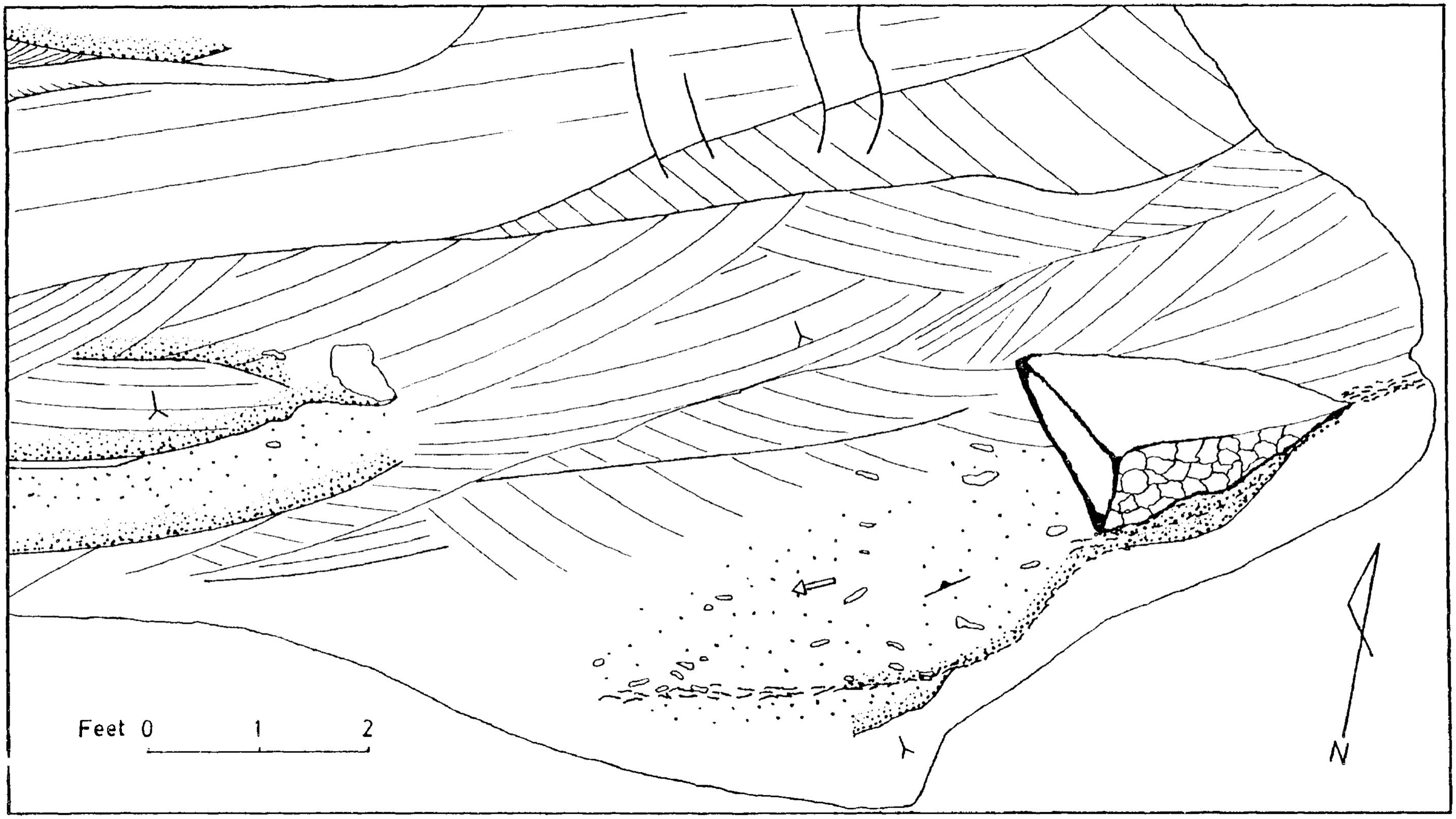
N
Feet 0 1 2

the area (see Figure V-6) the cleavage shows an axial planar relationship with fold axis.

This consistent strike of the single, penetrative cleavage, the relatively undeformed, fresh appearance of the rocks, and the fairly open folds present would not lead one to conclude that the downward and otherwise inconsistent structural facing is the result of tectonic refolding. If tectonic refolding of previously folded strata was proposed as the mechanism for producing the present structure in the area, one would have to assume that the sediments were laid down co-planar to those in the Finmark area, folded initially about the roughly east-west regional fold axis, then subsequently refolded, presumably about a northeast-southwest axis (judging from the geometry of the folds in the Fourway School area relative to the interpreted folds in the Finmark area, as shown in Figure V-7) to produce their slightly overturned structure. None of the evidence seen so far supports this theory, however: there is no evidence of a second cleavage in the rocks, which would have formed during a second deformation event, the single cleavage present has a much too consistent strike across the whole study area to

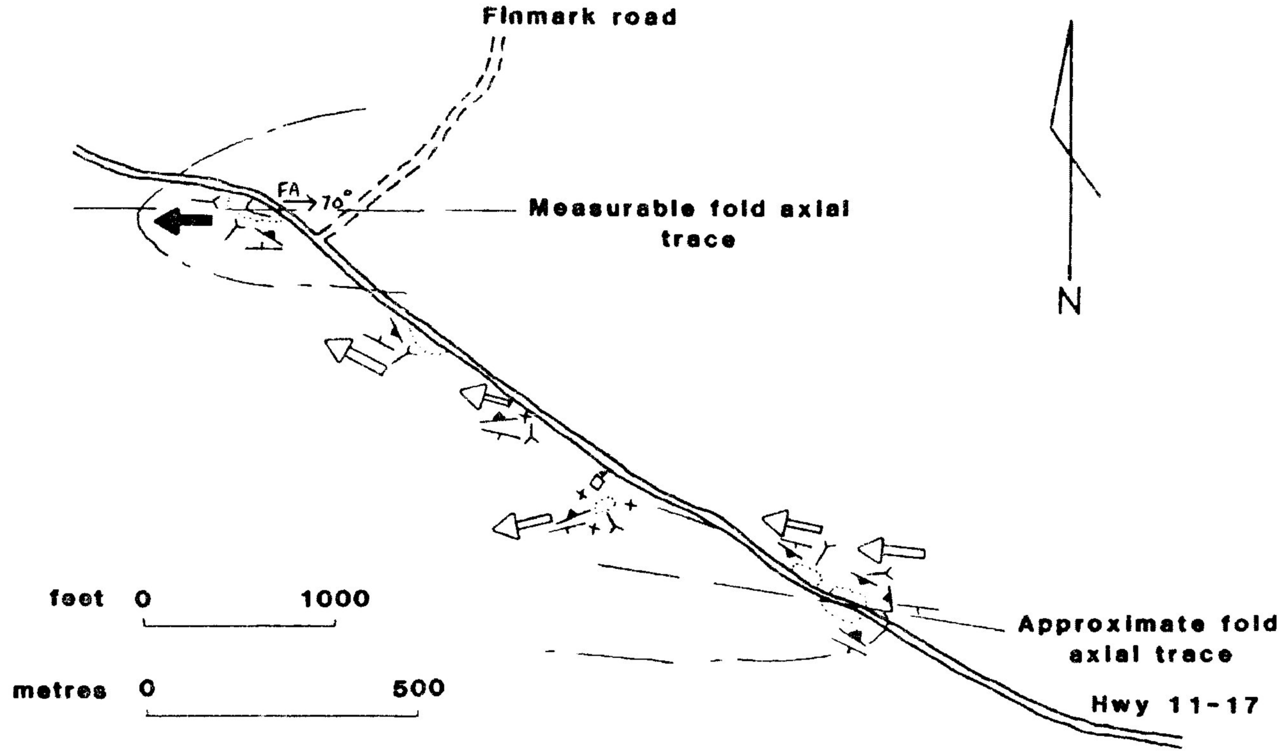

Figure V-6: Structural facing in the Shebandowan-type rocks in the Fourway School area is upwards to the west with only local downwards structural facing. (See Plate D, at back, for location).

X Area of outcrop; large,small

Cleavage

Bedding

Local younging

Structural facing; upward,downward

Fold axial trace

FA 70° Fold axis, with direction and amount of plunge

General form of bedding

Figure V-7: Fold axes and regional cleavage are correlative from the structurally upward-facing to the structurally downward-facing strata of the Shebandowan-type rocks in the Finmark and Fourway School areas. (See Map 1, in pocket, for location). (Generalized form line of bedding __________ ___ __________).

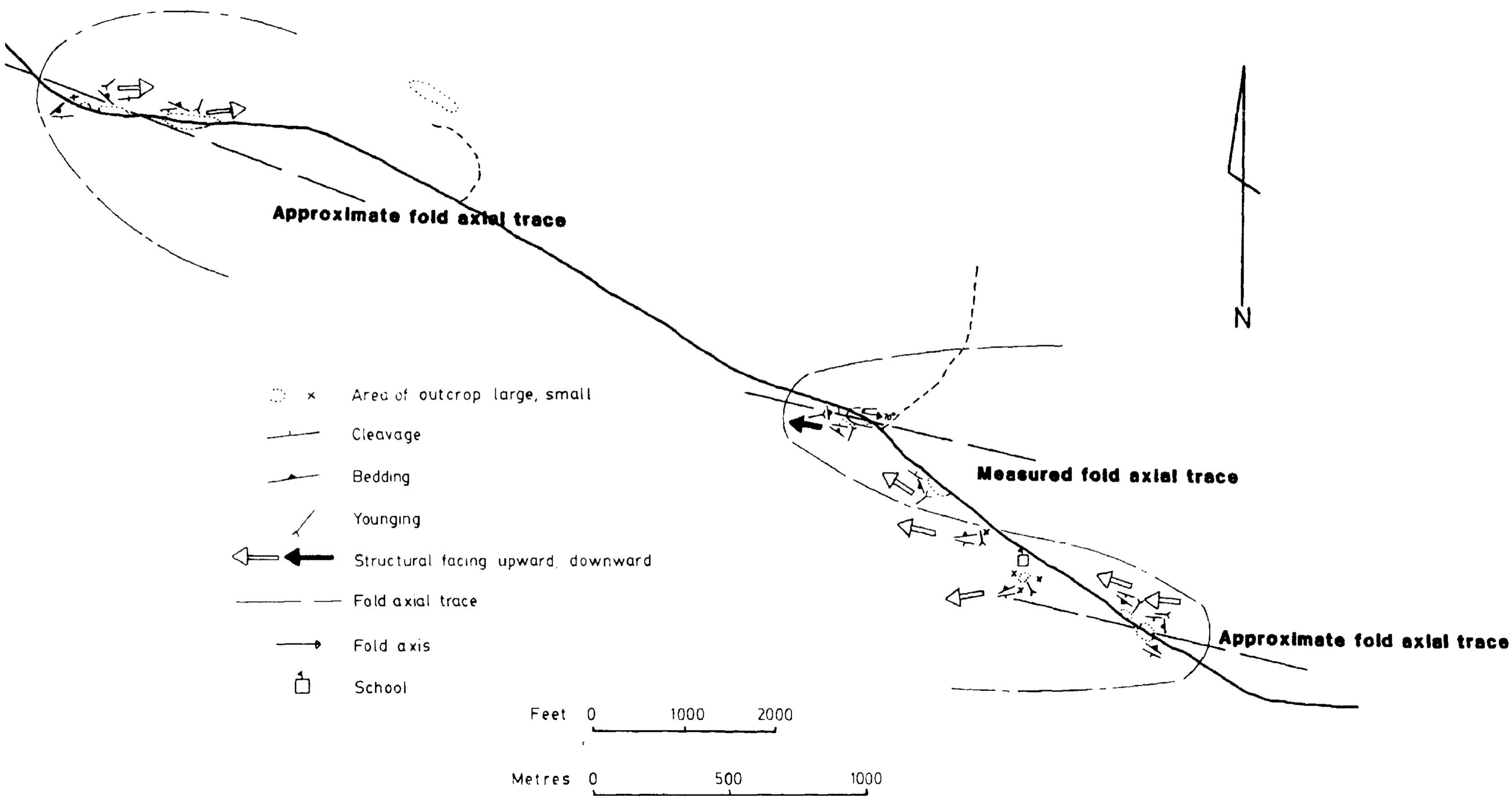

Approximate fold axial trace
N
Measured fold axial trace
Approximate fold axial trace
Area of outcrop large, small
Cleavage
Bedding
Younging
Structural facing upward, downward
Fold axial trace
Fold axis
School
Feet 0 1000 2000
Metres 0 500 1000

have been refolded (see Figure V-8); and some very delicate primary sedimentary structures have been excellently preserved (as shown previously in Chapter II). Also, if there had been a period of refolding, one would expect to find more examples of downward-facing structure or reversals of structural facing in an area the size of that encompassed in the present study. In a structural study by Kehlenbeck (1983), which resulted in the delineation of refolded folds in the Hazelwood Lake area (northeast of the present study area), there was also only a single, consistent cleavage present in outcrop and in thin section, and only one generation of folds was visible in outcrop. However, numerous examples of reversals of structural facing were found which led to the conclusion that there might have been two periods of folding in that area.

From the available evidence in the present area, it is more likely that the overturned strata and inconsistent structural facing of the rocks in the Fourway School area is a pre-deformational feature. "Nappe-like" inversion structures with undisturbed original bedding and sedimentary structures can be produced by syndepositional slumps or gravity sliding (Pettijohn, 1975). The actual variation in fold plunge may be attributed to primary sheath-fold geometry (Henderson, 1981).

Figure V-8: Poles to cleavage, plotted by locality on equal area stereonet. Both Shebandowan-type and Keewatin-type rocks are represented. The fine, continuous, penetrative cleavage is correlative in strike across the entire study area.

■ Shebandowan

▲ Shabaqua

● Finmark

X Kaministiquia

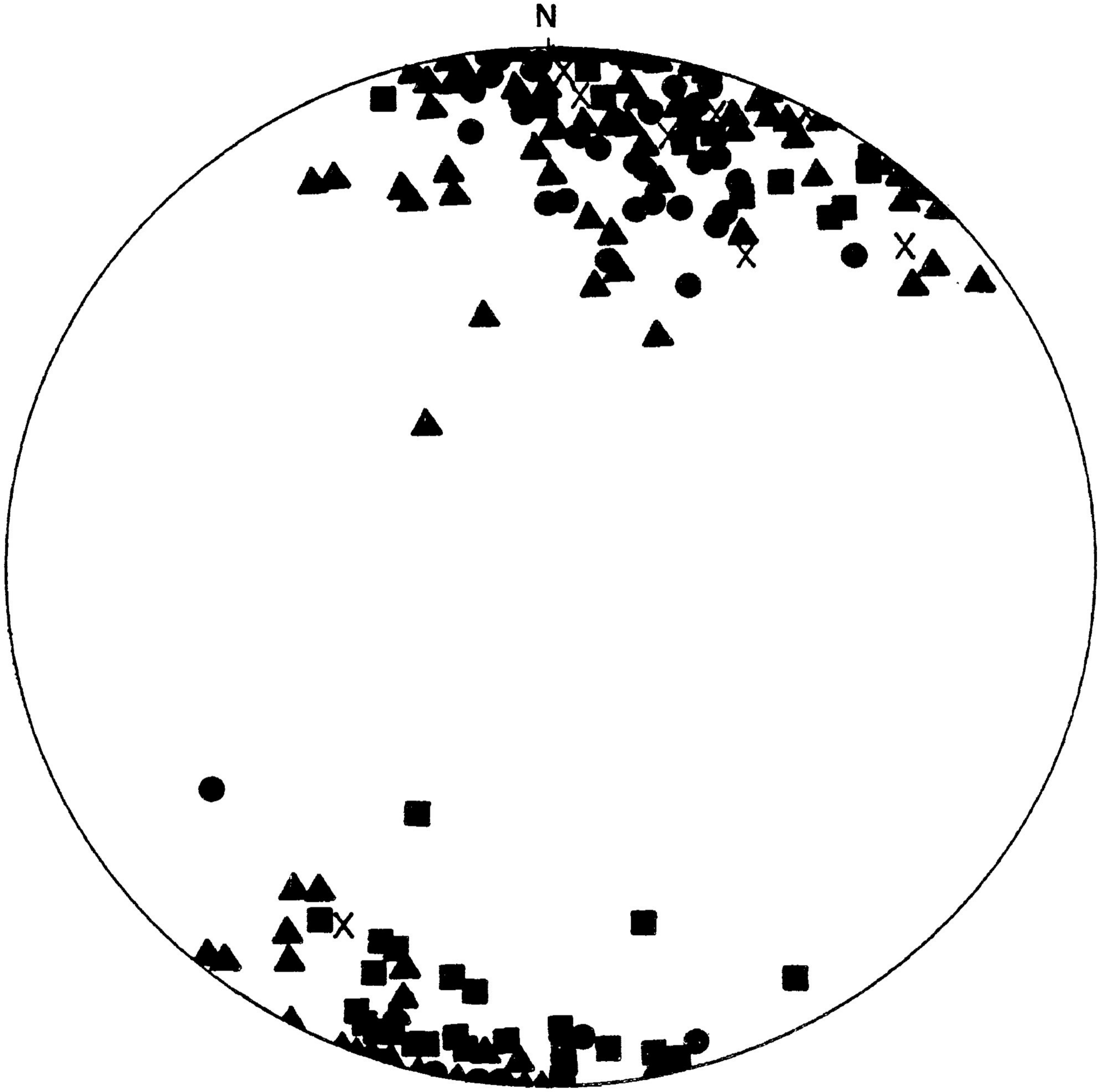
N

Discussion and Conclusions

At the outset of this thesis, three major issues associated with the Keewatin-type and Shebandowan-type rocks of the study area were outlined: 1) the disagreement concerning the age relationship between the two sequences; 2) the difficulty of assigning the peculiar, pigmented breccio-conglomerate unit to either one or the other succession; and 3) the differing opinions on the regional structure of the area. From the evidence in the foregoing chapters, it is felt that these problems can now be resolved.

There have been two views on the age relationship between the Keewatin-type and the Shebandowan-type rocks. Firstly that the latter are probably unconformable upon the former; and secondly that the two are coeval. Most of the field evidence shows that the Shebandowan-type rocks are younger than the Keewatin-type rocks. In physical appearance, the Shebandowan-type rocks seem much less deformed and fresher than the Keewatin-type rocks. Clasts in the rudaceous component of the Shebandowan-type succession generally show little development of a preferred dimensional orientation, whereas pillows in the mafic volcanic flows of the Keewatin-type sequences appear to have been elongated a considerable amount. Delicate, primary sedimentary features, such as load casts, ripple marks and ripple-drift laminations, in the arenaceous rocks of the Shebandowan-type sequence also show virtually no sign of deformation (see Chapter II). The amount of alteration in the two rock sequences appears to differ considerably as well. Intense alteration of the feldspars in the Keewatin-type volcanics is quite common, as is the development of substantial amounts of chlorite, epidote and sericite in the matrix of these rocks. In comparison, the Shebandowan-type rocks contain only minor amounts of sericite and epidote, and the crystals and clasts of feldspar and quartz are relatively unaltered and show few signs of strain (see illustrations in Chapter II). In general, the overall tectonic fabric in the Shebandowan-type rocks is also less well-developed than that in the Keewatin-type rocks. A few outcrops of the former sequence do show a well-developed cleavage and more pronounced elongation of clasts, however these outcrops are very localized. Their fabric is more likely due to proximity to a later fault and therefore can not be used to characterize the typical regional structure of this succession of rocks.

Aside from the general fresher appearance of the Shebandowan-type rocks, other somewhat more conclusive evidence of their age relationship with the Keewatin-type rocks is the presence of clasts of jasper in the conglomerates of the Shebandowan-type sequences. These clasts most likely have as their source the jaspilitic iron formation which is locally interbedded with the Keewatin-type mafic volcanics.

Finally, a recent U-Pb geochronological study of the zircons in the rocks of the Shebandowan Lakes area (Corfu and Stott, 1985) shows that the age of the Keewatin-type rocks is at least 2732^{+10}_{-2} Ma, while the Shebandowan-type rocks have been bracketed at between $2704^{+1.8}_{-1.6}$ Ma, and $2689.3^{+2.5}_{-2.2}$ Ma, in age.

Morton (1982) contended that the Shebandowan-type rocks in the vicinity of the Inco-Shebandowan Mine and the Mine road were coeval with the Keewatin-type rocks in the area. That hypothesis was founded on the correlation of the pigmented breccio-conglomerate (as it is referred to in this study) at the east end of the Mine road with the felsic pyroclastic unit near the west end of the Mine road. Morton proposed that these rocks represented the north and south limbs of a single, folded unit. However, this is not supported by the minor structural evidence and the unit is not a stratified correlatable unit. Also, the author feels that these two units do not represent the same rock (for reasons presented below) therefore it cannot be implied that the Shebandowan-type and Keewatin-type rocks are coeval.

As a result of mapping conducted along the Shebandowan Mine road, as well as further east, plus the study of numerous thin sections and hand samples, the author feels that the peculiar pigmented unit represents rock transitional from a breccio-conglomerate to a breccia whose variable appearance reflects varying distances from a volcanic source as well as differing degrees of hematization and carbonate enrichment. The reasons for calling this a breccio-conglomerate of the Shebandowan-type sequence in the present study centre on the comparison the fragments in the breccio-conglomerate are predominantly sub-angular to angular blocks. The textures of these two rocks seen in thin section (as discussed in Chapter II) are also too dissimilar to be considered as one unit. The breccio-conglomerate, therefore, is not correlative with the felsic pyroclastic unit of the Keewatin-type sequence. Rather it is an integral part of the Shebandowan-type sequence which, based on the criteria outlined previously, is younger than the Keewatin-type succession. This conclusion, plus the author's structural data (as outlined in Chapter V) precludes the theory that a single fold, of which the two units under discussion represent opposite limbs, exists along the Shebandowan Mine road.

A decision may also be reached concerning the regional structure of the area. As shown by the data presented in the previous chapters, the structure of the study area is characterized by isoclinal folds, structurally upwards-facing to the east, with sub-vertical, generally east-west trending axial traces. Local variations exist in the Shebandowan-type rocks in the eastern portion of the study area (as discussed in Chapter V) distinct similarities in clast size, composition, sorting, and degree of roundness between the pigmented unit and some of the regular, unpigmented breccio-conglomerates more typical of the Shebandowan-type sequence. In many instances it is clear that the source for these rocks must be the same.

In light of the proposal that the relationship between the Shebandowan-type and Keewatin-type rocks is coeval (Morton, 1982, as discussed above in Chapter I) it is necessary to distinguish this rock from the felsic pyroclastic unit of the Keewatin-type sequence. The main distinction is the dissimilarity in clast-type and clast-shape. The fragments in the breccio-conglomerate are polymictic and represent at least three distinct mafic to intermediate types of volcanic rocks. The fragments in the felsic agglomerate, on the other hand, are almost entirely composed of a feldspar-and quartz-phyric felsic volcanic rock, most likely representing pumiceous fragments (P. C. Thurston, personal communication, 1985). The shape of the fragments in the felsic agglomerate are usually sub-rounded spindles while in where more open folds are common, structural facing directions are to the west as well as to the east, probably due to the slight variations in primary fold plunge, and in one instance a locally downward-facing macroscopic fold was found. The downward facing fold, however, is considered to be a pre-tectonic structure. The variation in fold plunge in this area may be due to sheath-fold type structure.

The scarcity of visible folds and younging criteria (particularly in the Keewatin-type rocks) lends itself to a simple picture of the regional structure in a cursory study. However, more detailed structural mapping techniques, in particular the use of the cleavage-bedding relationship rule (c.f. Borradaile, 1980), allows the delineation of major fold axial traces in areas of tight folding where the orientation of strata alone would not reveal the presence of major folds. As discussed previously (Chapter III, V), the criteria for the use of cleavage-bedding relationships were satisfied in the present study. Although, due to the lack of available bedding measurements, few fold axial-traces can be outlined in the Keewatin-type rocks using this method, one can infer a similar structure to that in the Shebandowan-type rocks. Due to their proximity and stratigraphic relationships, it is only logical to conclude that the older Keewatin-type rocks will have suffered at least the same intensity of folding as the younger Shebandowan-type rocks, unless the Shebandowan-type rocks represent an allochthonous faulted unit. So far no evidence points to this however.

Morton (1982) and Stott and Schwerdtner (1981) have suggested that two episodes of substantial deformation occurred in the region (their theories are outlined in Chapter I). However, in this study area there is no evidence to support this. The macroscopic and microscopic fabric of the rocks is consistent with a single episode of penetrative deformation throughout (see Chapter III, IV). No secondary folds were seen, crenulations of first cleavage are absent, and the few kink zones observed occur in the same vicinity as the more deformed outcrops of Shebandowan-type rocks. This atypical kinking fabric and locally more intense schistosity, therefore, can perhaps be attributed to the proximity to a fault.

APPENDIX

PART I

Magnetic Susceptibility Anisotropy Data Sheets

Sample No: 7	Location: Shebandowan Mine road	Rock Type: Keewatin-type felsic volcanic

Run No.	Minimum (k_3)			Intermediate (k_2)			Maximum (k_1)			E	L	F
	Dec	Inc	EV ($\times10^{-5}$)	Dec	Inc	EV ($\times10^{-5}$)	Dec	Inc	EV ($\times10^{-5}$)	$(k_2)^2 / k_1 \times k_3$	k_1 / k_2	k_2 / k_3
1	35.5	13.99	1.4659	304.86	2.56	1.4782	24.92	-75.80	1.5033		1.0176	1.0514
2	24.16	-11.19	1.3787	283.84	-42.18	1.4861	305.84	45.66	1.5543		1.0459	1.0779
3	16.03	-11.21	1.4062	273.55	-47.51	1.4925	295.71	40.32	1.5501		1.0386	1.0614
4	12.38	89.98	1.3911	273.05	89.97	1.5041	330.76	-89.99	1.5467		1.028	1.0812
5	9.35	-20.96	1.3628	89.11	24.97	1.5110	314.51	56.45	1.6049		1.062	1.1087
6	23.90	-12.71	1.4135	278.45	-49.75	1.5166	303.83	37.41	1.5786		1.0409	1.0729
Mean	20.22	7.99	1.3930	250.48	-3.66	1.4981	262.59	2.34	1.5563	1.035	1.0388	1.0756
Stan. Dev.			.01778			.0136			.0311		.012	.0019

Sample No: 13	Location: Shebandowan Mine road	Rock Type: Keewatin-type mafic volcanic

Run No.	Minimum (k_3)			Intermediate (k_2)			Maximum (k_1)			E	L	F
	Dec	Inc	EV ($\times10^{-5}$)	Dec	Inc	EV ($\times10^{-5}$)	Dec	Inc	EV ($\times10^{-5}$)	$(k_2)^2 / k_1 \times k_3$	k_1 / k_2	k_2 / k_3
1	14.87	-51.95	6.4485	53.98	31.05	6.5509	311.72	19.34	6.6419		1.0139	1.0159
2	2.94	-48.99	6.5086	50.42	30.84	6.5566	304.55	24.64	6.6379		1.0124	1.0074
3	5.56	-43.45	6.4920	47.02	38.99	6.6164	297.88	22.20	6.6806		1.0097	1.0192
4	15.05	-52.48	6.5026	35.16	34.83	6.6261	297.94	9.24	6.6620		1.0054	1.019
5	18.78	-43.93	6.4762	49.41	42.12	6.5622	304.58	15.93	6.6578		1.0146	1.0133
6	350.15	-52.92	6.4806	40.65	26.05	6.6110	297.75	24.50	6.6786		1.0102	1.0001
Mean	67.99	-48.95	6.4847	46.11	33.98	6.5812	302.40	19.31	6.6598	1.0041	1.011	1.016
Stan. Dev.			.0198			.0311			.0163		.0034	.0157

Sample No: 13'	Location: Shebandowan Mine road	Rock Type: Keewatin-type mafic volcanic

Run No.	Minimum (k_3)			Intermediate (k_2)			Maximum (k_1)			E	L	F
	Dec	Inc	EV ($\times10^{-5}$)	Dec	Inc	EV ($\times10^{-5}$)	Dec	Inc	EV ($\times10^{-5}$)	$(k_2)^2 / k_1 \times k_3$	k_1 / k_2	k_2 / k_3
1	335.39	-8.32	2.0480	62.48	19.11	2.1116	87.82	-69.03	2.2231		1.0531	1.031
2	4.03	-0.92	2.0630	273.72	-18.74	2.1694	276.73	71.24	2.2663		1.0447	1.0516
3	351.48	-2.76	2.0353	80.58	26.91	2.1518	87.39	-62.93	2.2651		1.054	1.057
4	2.33	10.09	2.0816	279.34	-34.27	2.1630	78.20	-53.86	2.2834		1.0557	1.039
5	346.37	-4.29	2.1048	73.41	34.57	2.1599	52.54	-55.09	2.2567		1.044	1.038
6	352.89	-8.50	2.0643	78.99	24.50	2.1615	280.63	63.88	2.2984		1.0634	1.047
Mean	232.17	-2.45	2.0670	141.42	8.68	2.1579	148.88	-17.63	2.2712	.9919	1.0525	1.044
Stan. Dev.			.0239			.0237			.0238		.0066	.0088

Sample No: 14	Location: Shebandowan Mine road	Rock Type: Keewatin-type mafic volcanic

Run No.	Minimum (k_3)			Intermediate (k_2)			Maximum (k_1)			E	L	F
	Dec	Inc	EV ($\times10^{-5}$)	Dec	Inc	EV ($\times10^{-5}$)	Dec	Inc	EV ($\times10^{-5}$)	$(k_2)^2 / k_1 \times k_3$	k_1 / k_2	k_2 / k_3
1	17.93	13.25	5.9285	288.12	-0.82	6.0019	21.77	-76.78	6.0865		1.0141	1.0124
2	348.25	8.79	5.9022	77.82	-3.13	5.9973	327.17	-80.88	6.1055		1.0180	1.0161
3	352.57	14.63	5.9243	82.82	2.99	6.0216	57.21	88.20	6.0951		1.0122	1.0164
4	341.99	12.82	5.9193	71.51	-2.29	6.0004	330.91	-77.13	6.0971		1.0161	1.0137
5	353.48	7.01	5.9529	84.53	4.26	6.0082	19.56	-78.86	6.1051		1.0162	1.0093
6	18.10	3.36	5.9315	288.35	-7.28	5.9733	85.69	-81.98	6.1051		1.0221	1.0070
Mean	238.12	9.987	5.9264	148.86	-1.045	6.0004	140.38	-51.24	6.0992	.9961	1.0164	1.0125
Stan. Dev.			.015			.0144			.0076		.0031	.0034

Sample No: 24	Location: Shebandowan Mine road	Rock Type: Sheb. type breccia-conglom.

Run No.	Minimum (k_3) Dec	Inc	EV ($\times 10^{-5}$)	Intermediate (k_2) Dec	Inc	EV ($\times 10^{-5}$)	Maximum (k_1) Dec	Inc	EV ($\times 10^{-5}$)	E $(k_2)^2 / k_1 \times k_3$	L k_1/k_2	F k_2/k_3
1	354.39	-5.19	6.7964	60.21	77.75	7.0510	85.38	-10.95	7.0667		1.0022	1.0375
2	343.62	-0.96	6.8971	78.73	-83.17	7.0249	73.53	7.01	7.0883		1.009	1.0185
3	342.81	3.51	6.9553	65.03	-65.05	7.0344	74.44	24.65	7.1150		1.011	1.0114
4	347.07	-5.15	6.9405	54.52	76.66	7.0655	78.14	-12.28	7.1209		1.0078	1.018
5	348.21	4.69	6.9764	59.64	-75.84	7.1248	79.30	13.35	7.1524		1.0039	1.0213
6	347.83	-15.49	6.9646	296.01	65.66	7.1029	72.60	18.05	7.1539		1.0072	1.0198
Mean	347.32	-3.10	6.9217	102.36	-0.61	7.0672	77.23	-6.621	7.1163	1.014	1.0069	1.0209
Stan. Dev.			.0614			.0354			.0317		.003	.0079

Sample No: 24'	Location: Shebandowan Mine road	Rock Type: Sheb-type breccia-conglom.

Run No.	Minimum (k_3) Dec	Inc	EV ($\times 10^{-4}$)	Intermediate (k_2) Dec	Inc	EV ($\times 10^{-4}$)	Maximum (k_1) Dec	Inc	EV ($\times 10^{-4}$)	E $(k_2)^2 / k_1 \times k_3$	L k_1/k_2	F k_2/k_3
1	16.34	-14.77	2.5544	296.74	34.29	2.6094	50.84	51.80	2.6326		1.0059	1.0215
2	57.23	-43.34	2.6008	293.46	-30.16	2.6215	8.58	39.27	2.6405		1.0051	1.010
3	56.04	-42.36	2.5964	300.27	-25.76	2.6251	7.26	34.77	2.6372		1.0046	1.011
4	51.83	-41.48	2.6020	281.52	-32.68	2.6294	355.31	32.95	2.6457		1.0062	1.01
5	53.28	-40.75	2.6015	289.20	-33.31	2.6338	0.43	37.55	2.6439		1.0038	1.0124
Mean	53.05	-36.99	2.5910	285.57	-28.07	2.6250	355.37	32.83	2.6400	1.0074	1.0051	1.013
Stan. Dev.			0.55			.081			.187		.298	.0044

Sample No: 58 | Location: Shebandowan Mine road | Rock Type: Shebandowan-type slate

Run No.	Minimum (k_3)			Intermediate (k_2)			Maximum (k_1)			E	L	F
	Dec	Inc	EV ($x10^{-5}$)	Dec	Inc	EV ($x10^{-5}$)	Dec	Inc	EV ($x10^{-5}$)	$(k_2)^2 / k_1 \times k_3$	k_1 / k_2	k_2 / k_3
1	20.69	20.32	2.0307	283.39	18.94	2.3793	333.95	-61.62	2.4762		1.0407	1.1717
2	21.44	21.25	1.9448	283.22	20.18	2.3360	333.73	-59.97	2.4353		1.0425	1.201
3	23.00	18.76	2.0157	289.77	9.43	2.3855	354.37	-68.85	2.4662		1.0338	1.183
4	22.13	20.71	2.0226	255.14	17.56	2.3717	337.68	-62.09	2.5280		1.0659	1.1726
5	24.52	21.56	2.0297	288.61	15.32	2.4090	345.94	-63.09	2.4905		1.0338	1.1569
6	22.18	22.93	2.0268	286.44	13.30	2.4114	348.67	-63.09	2.5270		1.0479	1.1897
Mean	22.38	20.92	2.0117	286.09	15.84	2.3821	342.39	-63.12	2.4812	1.1341	1.044	1.1842
Stan. Dev.			.030			.0253			.0329		.0109	.0101

Sample No: 58' | Location: Shebandowan Mine road | Rock Type: Shebandowan-type slate

Run No.	Minimum (k_3)			Intermediate (k_2)			Maximum (k_1)			E	L	F
	Dec	Inc	EV ($x10^{-5}$)	Dec	Inc	EV ($x10^{-5}$)	Dec	Inc	EV ($x10^{-5}$)	$(k_2)^2 / k_1 \times k_3$	k_1 / k_2	k_2 / k_3
1	15.40	8.05	2.0455	280.68	30.19	2.4485	298.76	-58.53	2.5262		1.0317	1.197
2	13.37	6.80	2.0654	277.91	38.58	2.4149	291.72	-50.60	2.5261		1.046	1.1692
3	11.23	4.36	2.0586	277.81	38.05	2.4816	286.74	51.64	2.5024		1.0084	1.2055
4	16.20	4.27	2.0556	283.50	32.24	2.4481	292.90	-57.41	2.4840		1.0147	1.1909
5	17.30	7.01	2.0692	282.18	36.00	2.4623	296.72	-53.15	2.4990		1.0149	1.1899
6	16.50	7.22	2.0463	281.93	32.16	2.4654	297.69	-56.85	2.5446		1.0321	1.2048
Mean	15.00	6.28	2.0568	280.67	34.54	2.4535	294.09	-54.70	2.5137	1.1643	1.0246	1.193
Stan. Dev.			.0088			.0206			.0204		.013	.0122

Sample No: 63	Location: Shebandowan Mine road	Rock Type: Sheb-type breccio-conglom.

Run No.	Minimum (k_3)			Intermediate (k_2)			Maximum (k_1)			E	L	F
	Dec	Inc	EV (x10^{-5})	Dec	Inc	EV (x10^{-5})	Dec	Inc	EV (x10^{-5})	$(k_2)^2 / k_1 \times k_3$	k_1 / k_2	k_2 / k_3
1	356.51	6.37	2.1132	84.49	31.89	2.2828	70.48	-57.34	2.3424		1.0261	1.0502
2	1.87	2.58	2.1738	272.48	-13.24	2.3351	80.98	-76.50	2.3678		1.0124	1.0763
3	7.74	12.64	2.1934	252.45	-20.10	2.3726	67.54	-65.96	2.4078		1.0148	1.0817
4	357.44	10.94	2.2157	275.44	-34.13	2.3371	72.71	-53.69	2.4332		1.0411	1.0548
5	0.47	7.91	2.1611	275.38	-31.92	2.2493	78.26	-56.90	2.3158		1.0333	1.0639
6	9.04	9.07	2.1865	286.99	-40.89	2.3388	88.95	-47.67	2.4148		1.0323	1.0696
Mean	121.26	8.25	2.1738	246.21	-18.06	2.3252	76.49	-59.68	2.3402	1.0432	1.0267	1.0711
Stan. Dev.			.032			.029			.0309		.0102	.0095

Sample No: 63'	Location: Shebandowan Mine road	Rock Type: Sheb-type breccio-conglom.

Run No.	Minimum (k_3)			Intermediate (k_2)			Maximum (k_1)			E	L	F
	Dec	Inc	EV (x10^{-5})	Dec	Inc	EV (x10^{-5})	Dec	Inc	EV (x10^{-5})	$(k_2)^2 / k_1 \times k_3$	k_1 / k_2	k_2 / k_3
1	40.49	-46.26	3.0106	21.95	38.11	3.0310	297.14	-13.31	3.0412		1.0034	1.0068
2	303.03	-1.89	2.9941	33.43	-19.35	3.0301	28.69	73.21	3.0483		1.006	1.012
3	76.81	-42.10	2.9953	290.69	18.80	3.0101	284.21	-44.57	3.0319		1.009	1.0049
4	318.57	-11.14	2.9841	65.35	-44.80	3.0303	33.14	42.67	3.0514		1.007	1.0138
5	39.77	-4.55	2.9685	314.21	44.25	3.0465	305.15	-45.36	3.0747		1.009	1.0263
6	35.61	20.53	2.9992	336.44	-53.88	3.0497	293.99	28.29	3.0785		1.009	1.0168
Mean	135.72	-15.23	2.993	177.02	-2.81	3.033	207.05	-6.832	3.0553	1.006	1.0074	1.0134
Stan. Dev.			.0127			.0129			.0157		.002	.007

Sample No: 610	Location: Shebandowan Mine road	Rock Type: Shebandowan-type arkose

Run No.	Minimum (k_3) Dec	Minimum (k_3) Inc	Minimum (k_3) EV ($x10^{-5}$)	Intermediate (k_2) Dec	Intermediate (k_2) Inc	Intermediate (k_2) EV ($x10^{-5}$)	Maximum (k_1) Dec	Maximum (k_1) Inc	Maximum (k_1) EV ($x10^{-5}$)	E $(k_2)^2 / k_1 \times k_3$	L k_1 / k_2	F k_2 / k_3
1	21.54	7.15	2.2541	295.30	-27.58	2.4571	278.26	61.35	2.5300		1.0291	1.090
2	22.73	11.28	2.2493	298.21	-25.57	2.4745	270.98	61.71	2.5250		1.0204	1.100
3	17.52	6.94	2.2250	289.73	-17.55	2.4390	86.77	-71.04	2.5144		1.0309	1.0962
4	26.04	12.90	2.2509	301.77	-23.55	2.4344	89.63	-62.76	2.5223		1.0361	1.0515
5	14.35	7.40	2.2362	286.43	-15.63	2.4447	79.51	-72.63	2.5108		1.0279	1.0932
6	20.73	10.45	2.2345	294.71	-20.63	2.4170	85.43	-66.65	2.5509		1.0554	1.0817
Mean	20.48	9.35	2.2418	294.36	-21.75	2.4444	148.48	-25.0	2.5259	1.0552	1.0334	1.0904
Stan. Dev.			.0106			.018			.0126		.011	.007

Sample No: 264A	Location: Shabaqua	Rock Type: Shebandowan-type slate

Run No.	Minimum (k_3) Dec	Minimum (k_3) Inc	Minimum (k_3) EV ($x10^{-5}$)	Intermediate (k_2) Dec	Intermediate (k_2) Inc	Intermediate (k_2) EV ($x10^{-5}$)	Maximum (k_1) Dec	Maximum (k_1) Inc	Maximum (k_1) EV ($x10^{-5}$)	E $(k_2)^2 / k_1 \times k_3$	L k_1 / k_2	F k_2 / k_3
1	355.95	2.10	2.2604	82.61	-57.83	2.9123	81.27	32.09	2.9774		1.0223	1.2884
2	357.34	3.03	2.2648	59.00	-83.62	2.8865	87.64	5.60	2.9422		1.0193	1.2745
3	356.53	0.18	2.2465	55.60	-79.45	2.9132	86.57	10.54	2.9317		1.0098	1.2923
4	357.44	3.29	2.2541	274.03	-63.41	2.8968	85.81	-26.36	2.9355		1.0134	1.2851
5	355.65	1.88	2.2405	63.18	-85.09	2.9252	85.80	4.53	2.9476		1.0076	1.3054
6	354.95	3.07	2.2744	277.67	-73.89	2.9333	86.08	-15.80	2.9800		1.0154	1.2897
Mean	356.64	2.26	2.2568	140.35	-73.88	2.9095	86.53	1.77		1.27	1.0147	1.2892
Stan. Dev.			.0112			.0161					.0051	.0092

Sample No: 206A	Location: Finmark	Rock Type: Sheb.-type sandstone

Run No.	Minimum (k_3)			Intermediate (k_2)			Maximum (k_1)			E	L	F
	Dec	Inc	EV ($x10^{-5}$)	Dec	Inc	EV ($x10^{-5}$)	Dec	Inc	EV ($x10^{-5}$)	$(k_2)^2 / k_1 \times k_3$	k_1 / k_2	k_2 / k_3
1	321.82	-16.92	3.3776	330.83	12.91	3.7770	60.41	-1.99	3.7980		1.0056	1.1182
2	326.92	-77.96	3.3573	332.41	11.46	3.7831	62.66	-1.23	3.8297		1.0123	1.1268
3	320.26	-76.06	3.3343	7.97	9.47	3.7438	276.31	10.13	3.7576		1.0037	1.1228
4	307.36	-81.00	3.3686	15.23	3.42	3.7467	284.73	8.32	3.8081		1.0164	1.1122
5	333.65	-79.61	3.3884	6.54	8.72	3.7864	275.98	5.60	3.8192		1.0087	1.1174
6	338.94	-78.14	3.4074	34.59	6.71	3.8021	303.73	9.74	3.8567		1.0144	1.1158
Mean	324.82	-78.28	3.3723	121.44	8.86	3.7798	210.64	5.09	3.8115	1.1116	1.0102	1.1190
Stan. Dev.			.023			.0212			.0304		.0046	.0046

Sample No: 206B	Location: Finmark	Rock Type: Sheb.-type sandstone

Run No.	Minimum (k_3)			Intermediate (k_2)			Maximum (k_1)			E	L	F
	Dec	Inc	EV ($x10^{-5}$)	Dec	Inc	EV ($x10^{-5}$)	Dec	Inc	EV ($x10^{-5}$)	$(k_2)^2 / k_1 \times k_3$	k_1 / k_2	k_2 / k_3
1	311.96	-87.65	2.9932	317.33	2.33	3.5564	47.33	-0.23	3.5795		1.0065	1.1881
2	337.64	-88.07	3.1035	308.65	1.68	3.6443	38.68	0.92	3.6614		1.0047	1.1742
3	342.33	-86.03	3.1289	73.06	-0.05	3.6632	343.06	3.99	3.7030		1.0109	1.1708
4	323.55	-83.73	3.1108	74.31	-2.20	3.6893	344.51	5.89	3.7159		1.0072	1.1860
5	308.42	-87.43	3.1512	48.88	-0.47	3.6620	318.90	2.52	3.6977		1.0097	1.1621
6	3.83	-87.80	3.1137	284.89	0.35	3.6419	14.89	1.91	3.6765		1.0095	1.1696
Mean	271.34	-86.78	3.0942	184.52	-0.273	3.6428	184.56	-2.5	3.6723	1.1679	1.0081	1.1751
Stan. Dev.			.0503			.0417			.0452		.0021	.0092

Sample No: 2060 | Location: Finmark | Rock Type: Sheb.-type slate

Run No.	Minimum (k_3)			Intermediate (k_2)			Maximum (k_1)			E $(k_2)^2 / k_1 \times k_3$	L k_1/k_2	F k_2/k_3
	Dec	Inc	EV ($\times 10^{-5}$)	Dec	Inc	EV ($\times 10^{-5}$)	Dec	Inc	EV ($\times 10^{-5}$)			
1	30.15	5.10	2.6626	337.17	-81.56	3.1084	299.54	6.79	3.1338		1.008	1.1674
2	28.84	5.70	2.6776	294.61	36.53	3.1568	306.43	-52.93	3.1803		1.0074	1.1790
3	26.88	5.07	2.7372	300.54	-35.72	3.2046	289.91	53.51	3.2397		1.0109	1.1705
4	28.14	5.03	2.7365	297.06	12.14	3.2268	320.31	-76.89	3.2475		1.0064	1.1792
5	25.00	5.29	2.7147	286.31	58.49	3.1535	298.19	-30.94	3.1929		1.0125	1.1616
6	30.72	4.46	2.6698	288.60	69.63	3.1622	302.36	-20.06	3.1708		1.0027	1.1844
Mean	28.29	5.12	2.6997	300.71	-9.92	3.1681	302.79	-20.04	3.1942	1.1643	1.0080	1.1737
Stan. Dev.			.0304			0381			.0394		.029	.0078

Sample No: 2061 | Location: Finmark | Rock Type: Sheb.-type sandstone

Run No.	Minimum (k_3)			Intermediate (k_2)			Maximum (k_1)			E $(k_2)^2 / k_1 \times k_3$	L k_1/k_2	F k_2/k_3
	Dec	Inc	EV ($\times 10^{-5}$)	Dec	Inc	EV ($\times 10^{-5}$)	Dec	Inc	EV ($\times 10^{-5}$)			
1	15.13	-2.35	2.9363	285.32	4.51	3.3138	77.68	84.91	3.5012		1.0378	1.1412
2	12.82	-3.16	2.9249	281.64	-17.42	3.3579	294.62	72.14	3.4403		1.0245	1.1480
3	13.93	-5.43	2.9365	282.85	-11.23	3.3615	309.32	77.48	3.4703		1.0324	1.1370
4	15.58	-3.97	2.9306	285.52	-0.88	3.3712	3.18	85.44	3.4677		1.0286	1.1503
5	13.87	-1.21	2.9269	283.57	-14.05	3.3635	288.67	75.86	3.4498		1.0256	1.1492
6	11.44	-4.59	2.9205	281.18	-3.21	3.3816	336.33	84.42	3.4792		1.0284	1.1578
Mean	13.795	-3.55	2.9360	283.35	-7.05	3.3682	218.30	80.12	3.4681	1.1142	1.0246	1.1472
Stan. Dev.			.0147			.0081			0197		.0044	.0066

Sample No: 207B	Location: Finmark	Rock Type: Sheb.- type sandstone.

Run No.	Minimum (k_3)			Intermediate (k_2)			Maximum (k_1)			E	L	F
	Dec	Inc	EV ($x10^{-5}$)	Dec	Inc	EV ($x10^{-5}$)	Dec	Inc	EV ($x10^{-5}$)	$(k_2)^2 / k_1 \times k_3$	k_1 / k_2	k_2 / k_3
1	349.06	6.24	1.4261	76.84	-19.56	1.5225	276.02	-69.45	1.5741		1.0339	1.0676
2	356.66	9.07	1.4601	82.56	-24.16	1.5482	285.73	-63.99	1.6141		1.0426	1.0603
3	346.60	13.14	1.4409	71.84	-19.57	1.5708	288.42	-66.13	1.6108		1.0255	1.0901
4	343.08	8.56	1.4868	80.91	42.23	1.5716	63.96	-46.52	1.5951		1.0149	1.0570
5	349.85	10.54	1.4232	75.43	-22.52	1.5365	283.26	-64.89	1.5821		1.0297	1.0796
6	333.84	13.30	1.3999	55.35	-32.00	1.5360	83.36	54.72	1.5954		1.0387	1.0972
Mean	346.51	10.14	1.4395	73.82	-12.59	1.5476	213.46	-42.71	1.5953	1.0430	1.0309	1.0753
Stan. Dev.			.028			.0183			.0142		.009	.015

AI – 10

Sample No: 207B'	Location: Finmark	Rock Type: Sheb - type sand stone

Run No.	Minimum (k_3)			Intermediate (k_2)			Maximum (k_1)			E	L	F
	Dec	Inc	EV ($x10^{-5}$)	Dec	Inc	EV ($x10^{-5}$)	Dec	Inc	EV ($x10^{-5}$)	$(k_2)^2 / k_1 \times k_3$	k_1 / k_2	k_2 / k_3
1	76.35	-59.36	1.2670	44.29	26.65	1.3316	321.47	-13.99	1.4147		1.0576	1.0557
2	61.78	-69.68	1.3017	65.09	20.29	1.3748	334.70	1.08	1.4187		1.0319	1.0562
3	88.51	-73.77	1.3120	43.62	11.65	1.3939	315.95	-11.14	1.4614		1.0484	1.0624
4	282.94	78.76	1.3550	38.89	4.98	1.4061	309.78	-10.05	1.4646		1.0416	1.0377
5	75.93	-62.63	1.3261	25.26	18.16	1.4390	302.02	-19.75	1.5156		1.0532	1.0851
6	60.15	-81.28	1.3689	22.58	6.93	1.4353	293.23	-5.26	1.4765		1.0287	1.0485
Mean	107.61	-44.66	1.3218	39.95	14.78	1.3978	312.86	-9.85	1.4586	1.0347	1.0436	1.0576
Stan. Dev.			.0338			.035			.0345		.0106	.0145

Sample No: 207B"	Location: Finmark	Rock Type: Sheb.-type sandstone

Run No.	Minimum (k_3)			Intermediate (k_2)			Maximum (k_1)			E	L	F
	Dec	Inc	EV ($\times10^{-5}$)	Dec	Inc	EV ($\times10^{-5}$)	Dec	Inc	EV ($\times10^{-5}$)	$(k_2)^2 / k_1 \times k_3$	k_1 / k_2	k_2 / k_3
1	301.26	46.17	1.1057	331.56	-39.65	1.1294	48.17	15.60	1.2639		1.1191	1.0214
2	281.37	56.19	1.1460	346.54	-15.70	1.2358	67.54	29.09	1.2544		1.0150	1.0783
3	294.59	56.13	1.1585	314.55	-32.25	1.2133	38.64	9.26	1.2576		1.0365	1.0473
4	298.54	49.52	1.1324	346.42	-29.78	1.2160	61.16	24.71	1.2672		1.0421	1.0738
5	293.89	45.59	1.1166	318.39	-41.72	1.1849	36.48	12.51	1.2347		1.0437	1.0612
6	316.80	57.09	1.1331	311.82	-32.81	1.1811	43.28	-2.27	1.2256		1.0317	1.0424
Mean	297.74	51.78	1.1320	328.21	-31.98	1.1934	49.29	14.82	1.2509	1.0058	1.0490	1.0541
Stan. Dev.			.0174			.0342			.015		.033	.0195

Sample No: 2110	Location: Finmark	Rock Type: Sheb.-type sandstone

Run No.	Minimum (k_3)			Intermediate (k_2)			Maximum (k_1)			E	L	F
	Dec	Inc	EV ($\times10^{-5}$)	Dec	Inc	EV ($\times10^{-5}$)	Dec	Inc	EV ($\times10^{-5}$)	$(k_2)^2 / k_1 \times k_3$	k_1 / k_2	k_2 / k_3
1	315.66	5.50	2.5748	55.75	61.21	2.9475	42.70	-28.16	2.9990		1.0175	1.1447
2	312.98	5.29	2.5775	43.61	6.80	2.9912	12.02	-79.73	3.0023		1.0037	1.1605
3	309.76	1.40	2.6203	40.43	25.72	2.9880	36.85	-64.21	3.0246		1.0122	1.1403
4	312.34	2.73	2.6010	46.53	56.73	3.0191	40.56	-33.06	3.0746		1.0184	1.1607
5	314.21	2.04	2.6188	44.76	14.99	3.0482	36.67	-74.79	3.0636		1.0050	1.1640
6	314.09	5.47	2.6576	334.23	-84.17	3.0797	44.29	2.11	3.0949		1.0049	1.1588
7	313.77	1.53	2.6567	44.55	26.85	3.0822	40.74	-63.10	3.1070		1.0080	1.1602
Mean	313.26	3.42	2.6152	57.12	15.45	3.0223	36.26	-48.71	3.0523	1.144	1.0099	1.1556
Stan. Dev.			.0312			.0505			.0406		.0057	.0085

Sample No: 211'	Location: Finmark	Rock Type: Sheb.-type sandstone

Run No.	Minimum (k_3)			Intermediate (k_2)			Maximum (k_1)			E	L	F
	Dec	Inc	EV ($\times 10^{-5}$)	Dec	Inc	EV ($\times 10^{-5}$)	Dec	Inc	EV ($\times 10^{-5}$)	$(k_2)^2 / k_1 \times k_3$	k_1 / k_2	k_2 / k_3
1	0.93	4.62	2.7645	276.49	-52.75	3.1858	87.48	-36.86	3.2385		1.0165	1.1503
2	2.63	6.33	2.7512	283.10	-58.61	3.1545	88.87	-30.60	3.2246		1.022	1.1466
3	0.67	4.34	2.7630	250.24	-65.65	3.1640	88.76	-23.92	3.2377		1.0217	1.1469
4	5.45	6.69	2.7717	283.80	-51.06	3.1762	270.16	38.14	3.2765		1.0317	1.1459
5	3.25	6.56	2.8051	279.31	-42.57	3.2114	86.25	-46.69	3.2786		1.0209	1.1448
6	0.41	2.61	2.8178	274.32	-56.03	3.2138	88.64	-33.84	3.2841		1.0219	1.1405
Mean	2.22	5.19	2.7797	279.63	-54.44	3.1851	118.36	-23.34	3.2567	1.1207	1.0225	1.1459
Stan. Dev.			.0236			.0216			.0236		.0045	.0029

Sample No: 211''	Location: Finmark	Rock Type: Sheb.-type sandstone

Run No.	Minimum (k_3)			Intermediate (k_2)			Maximum (k_1)			E	L	F
	Dec	Inc	EV ($\times 10^{-5}$)	Dec	Inc	EV ($\times 10^{-5}$)	Dec	Inc	EV ($\times 10^{-5}$)	$(k_2)^2 / k_1 \times k_3$	k_1 / k_2	k_2 / k_3
1	279.39	-82.53	2.7731	40.03	-3.82	3.2027	310.46	6.41	3.2685		1.0205	1.1549
2	323.34	-86.01	2.7909	60.82	-0.51	3.2215	330.85	3.97	3.2522		1.0095	1.1543
3	280.27	-85.98	2.7822	73.66	-3.59	3.2265	343.77	1.79	3.2730		1.0144	1.1597
4	64.37	83.48	2.7899	53.53	-6.28	3.1616	323.73	1.77	3.2701		1.0343	1.1332
5	75.13	85.28	2.7798	64.70	-4.65	3.2109	334.77	0.85	3.2447		1.0105	1.1551
6	84.06	84.44	2.7870	61.99	-5.16	3.2303	332.19	2.07	3.2627		1.010	1.1590
Mean	185.26	-0.22	2.7838	54.12	-4.00	3.2084	329.29	2.81	3.2619	1.1339	1.0165	1.1527
Stan. Dev.			0062			.023			.0102		.0058	0090

Sample No: KD.	Location: Kashabowie ; D_1 area	Rock Type: Gabbro

Run No.	Minimum (k_3)			Intermediate (k_2)			Maximum (k_1)			E	L	F
	Dec	Inc	EV ($x10^{-5}$)	Dec	Inc	EV ($x10^{-5}$)	Dec	Inc	EV ($x10^{-5}$)	$(k_2)^2 / k_1 \times k_3$	k_1 / k_2	k_2 / k_3
1	309.81	-26.42	5.5510	329.83	62.15	5.8048	43.88	-8.12	5.8548		1.0086	1.046
2	309.18	-22.54	5.5345	316.63	67.31	5.7854	40.24	-2.52	5.8328		1.0082	1.0453
3	309.63	-19.85	5.5392	348.36	64.94	5.7741	44.50	-14.79	5.8232		1.0085	1.0424
4	310.99	-22.42	5.5445	347.45	62.83	5.7508	47.14	-14.54	5.8276		1.0132	1.0372
5	311.93	-21.81	5.5718	319.64	68.00	5.7848	43.02	-2.73	5.8309		1.0079	1.0382
6	310.03	-24.26	5.5575	301.06	65.47	5.7890	38.51	3.35	5.8760		1.015	1.0416
Mean	310.16	-22.88	5.5497	327.16	65.12	5.7815	42.88	-6.56	5.8408	1.0312	1.0102	1.0417
Stan. Dev.			.012			.0164			.0187		.0028	.0033

AI - 13

Sample No: KD.	Location: Kashabowie ; D_1 area	Rock Type: Gabbro

Run No.	Minimum (k_3)			Intermediate (k_2)			Maximum (k_1)			E	L	F
	Dec	Inc	EV ($x10^{-5}$)	Dec	Inc	EV ($x10^{-5}$)	Dec	Inc	EV ($x10^{-5}$)	$(k_2)^2 / k_1 \times k_3$	k_1 / k_2	k_2 / k_3
1	55.66	20.57	5.6899	341.75	-36.45	5.7950	302.48	46.36	5.8482		1.0092	1.0185
2	46.30	-11.82	5.6862	305.45	-42.49	5.7469	328.89	45.41	5.8159		1.0116	1.0107
3	65.89	16.82	5.6858	342.86	-21.64	5.7563	301.08	62.07	5.8349		1.0136	1.0124
4	62.16	22.40	5.6838	358.01	-42.59	5.6945	313.45	31.86	5.7950		1.0176	1.0019
5	69.94	25.92	5.6830	350.98	-22.60	5.7297	297.55	54.28	5.8059		1.0133	1.008
6	38.08	-6.06	5.7050	302.55	-40.39	5.7502	315.25	48.61	5.8040		1.009	1.0019
Mean	56.34	11.3	5.6889	333.60	-34.42	5.7454	309.61	49.10	5.8170	.9975	1.0125	1.0099
Stan. Dev.			.0075			.0301			.0172		.0029	.0050

Sample No: KO₂	Location: Kashabowie ; O₂ area	Rock Type: Gabbro

Run No.	Minimum (k_3)			Intermediate (k_2)			Maximum (k_1)			E	L	F
	Dec	Inc	EV ($\times 10^{-5}$)	Dec	Inc	EV ($\times 10^{-5}$)	Dec	Inc	EV ($\times 10^{-5}$)	$(k_2)^2 / k_1 \times k_3$	k_1 / k_2	k_2 / k_3
1	358.61	6.71	1.6492	89.11	35.16	2.1147	87.60	-54.83	2.1648		1.0260	1.282
2	358.46	2.14	1.6658	86.76	-38.35	2.1314	271.17	-51.58	2.1380		1.0078	1.273
3	358.67	1.29	1.6491	87.84	-32.61	2.0986	270.65	-57.36	2.1396		1.019	1.2726
4	356.93	4.01	1.6579	272.21	-52.74	2.1056	83.90	-36.97	2.1342		1.0136	1.270
5	359.97	5.83	1.6563	279.49	56.19	2.1201	89.95	3.74	2.1465		1.0122	1.280
6	355.67	1.85	1.6463	84.91	-22.18	2.1261	270.20	-67.74	2.1423		1.0076	1.291
Mean	358.05	2.64	1.6541	150.05	-4.088	2.1145	178.92	-44.12	2.1451	1.26	1.0145	1.2784
Stan. Dev.			.0066			.0096			.0117		.0065	.0071

Sample No: KO₂'	Location: Kashabowie ; O₂ area	Rock Type: Gabbro

Run No.	Minimum (k_3)			Intermediate (k_2)			Maximum (k_1)			E	L	F
	Dec	Inc	EV ($\times 10^{-5}$)	Dec	Inc	EV ($\times 10^{-5}$)	Dec	Inc	EV ($\times 10^{-5}$)	$(k_2)^2 / k_1 \times k_3$	k_1 / k_2	k_2 / k_3
1	340.25	-15.05	2.1156	82.38	-37.99	2.4010	52.82	48.09	2.4230		1.0091	1.1349
2	337.54	-8.95	2.1720	40.63	70.85	2.4096	70.31	-16.79	2.4952		1.0355	1.1094
3	335.37	-10.28	2.2044	314.82	79.03	2.4460	64.68	3.76	2.5419		1.0392	1.1096
4	337.50	-12.71	2.2414	83.05	-49.93	2.4895	57.64	37.23	2.5522		1.0252	1.1107
5	340.85	-9.88	2.2324	286.95	73.68	2.4737	68.55	13.06	2.5308		1.0231	1.1081
6	341.84	-14.83	2.1967	35.64	65.86	2.4736	76.95	-18.54	2.4944		1.0084	1.1260
Mean	338.90	-11.95	2.1937	140.58	-33.58	2.4489	65.16	-11.13	2.5062	1.0908	1.0234	1.1164
Stan. Dev.			.0418			.0335			.0432		.0117	.0102

PART II

Equal area stereonet plots of the maximum (●), intermediate (▲), and minimum (■) susceptibility directions. Average plane of cleavage in sample is denoted by solid line.

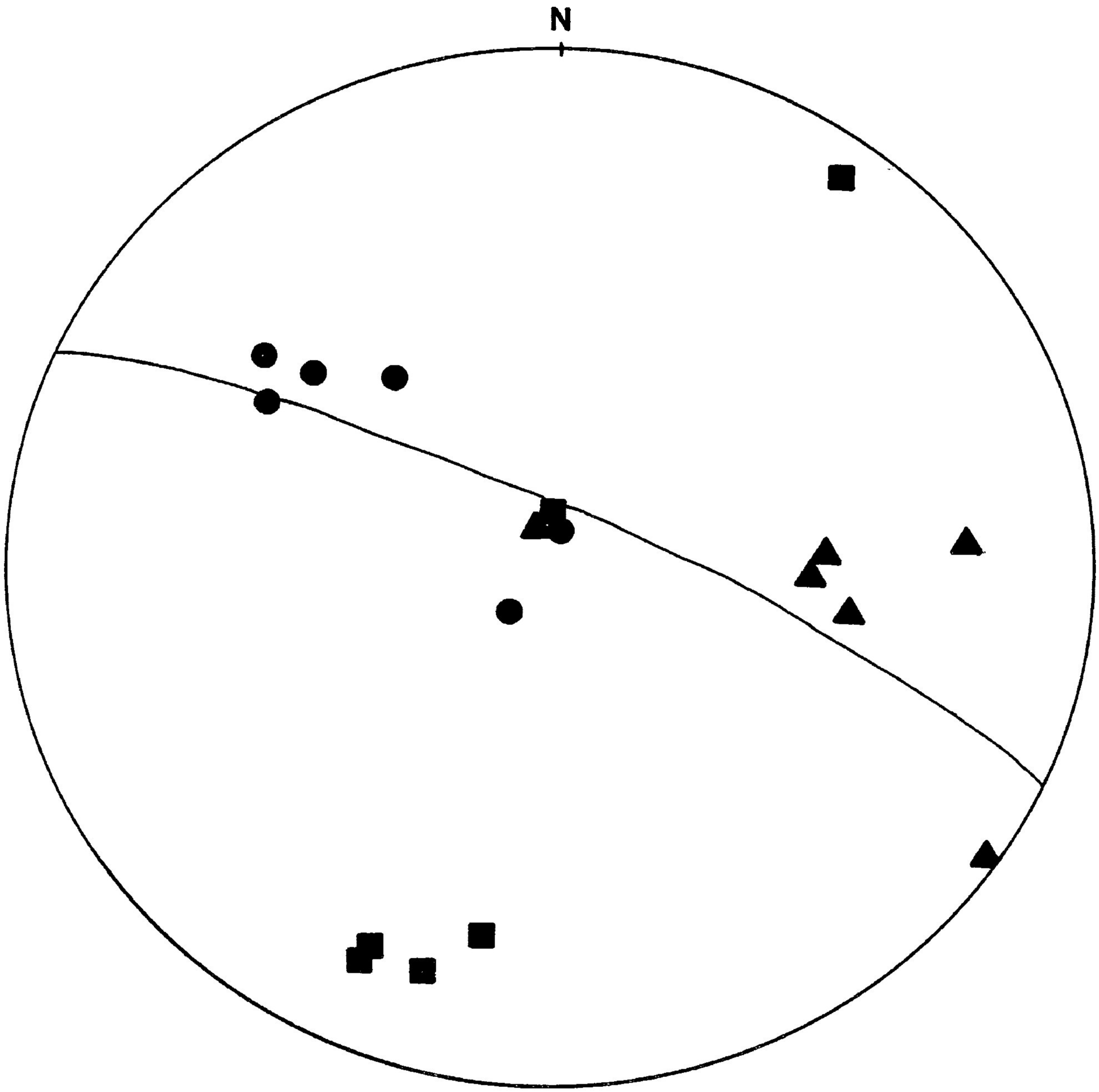

Keewatin-type felsic volcanic.

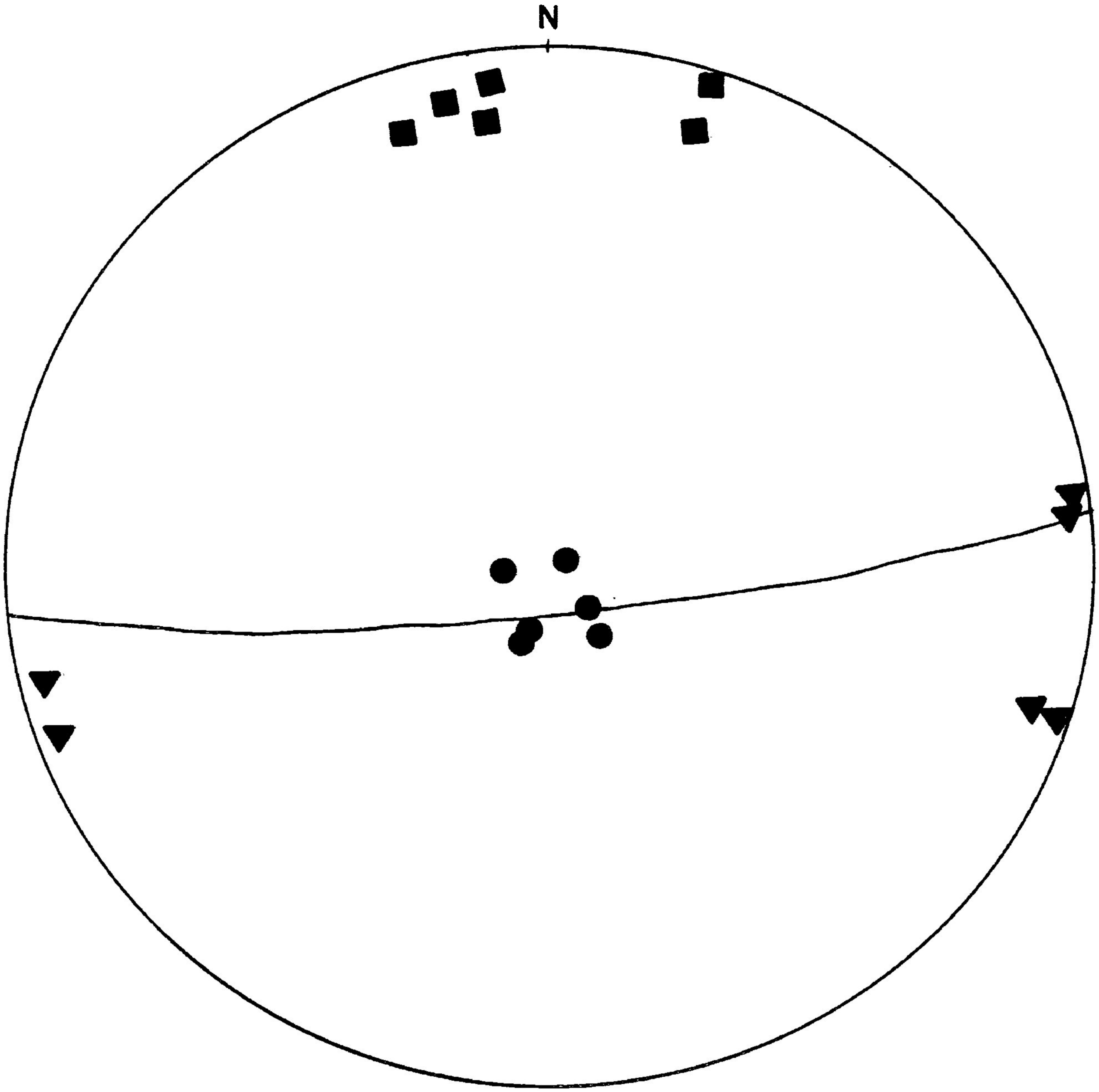

Keewatin-type mafic volcanic.

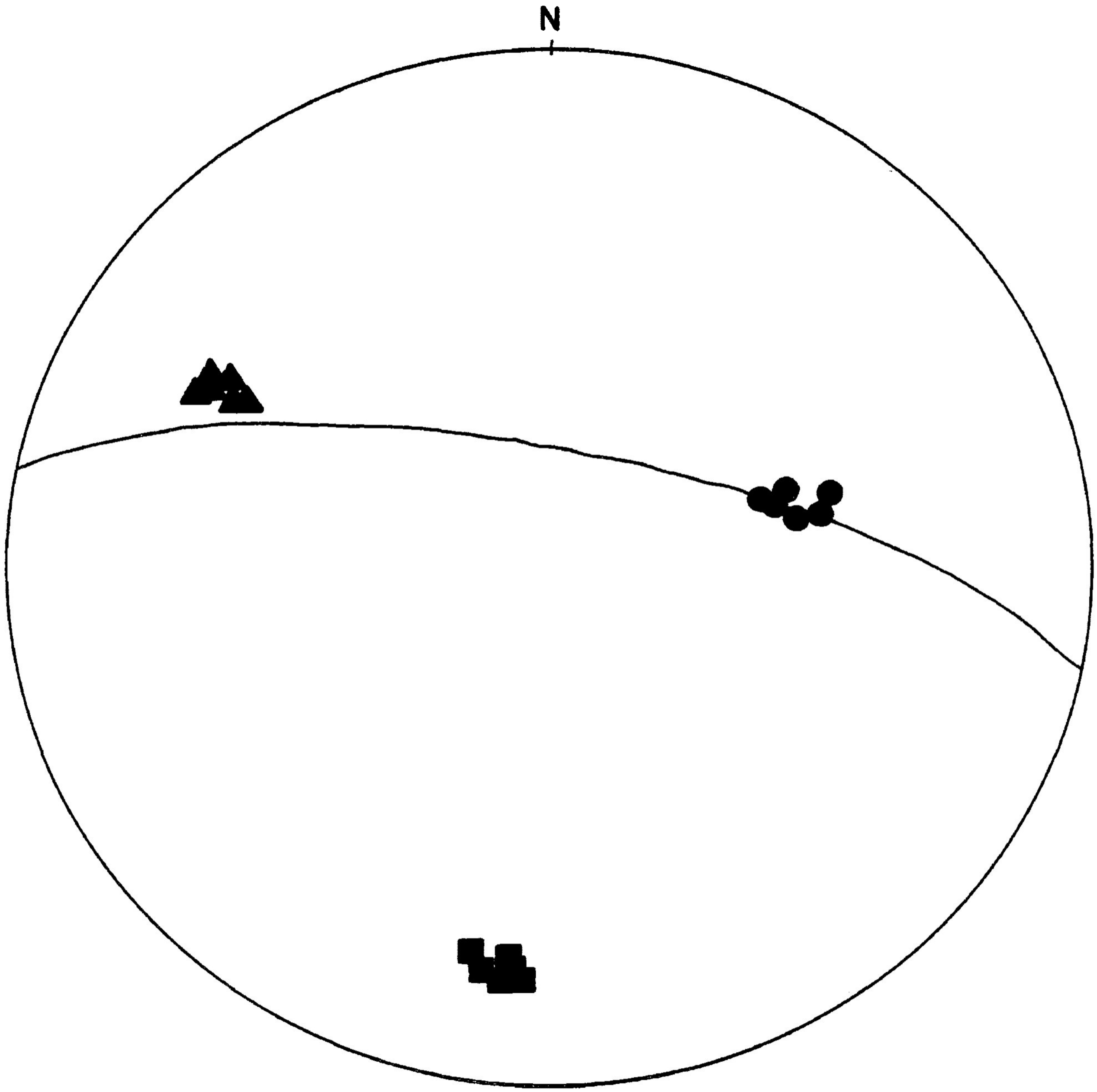

Shebandowan-type slate.

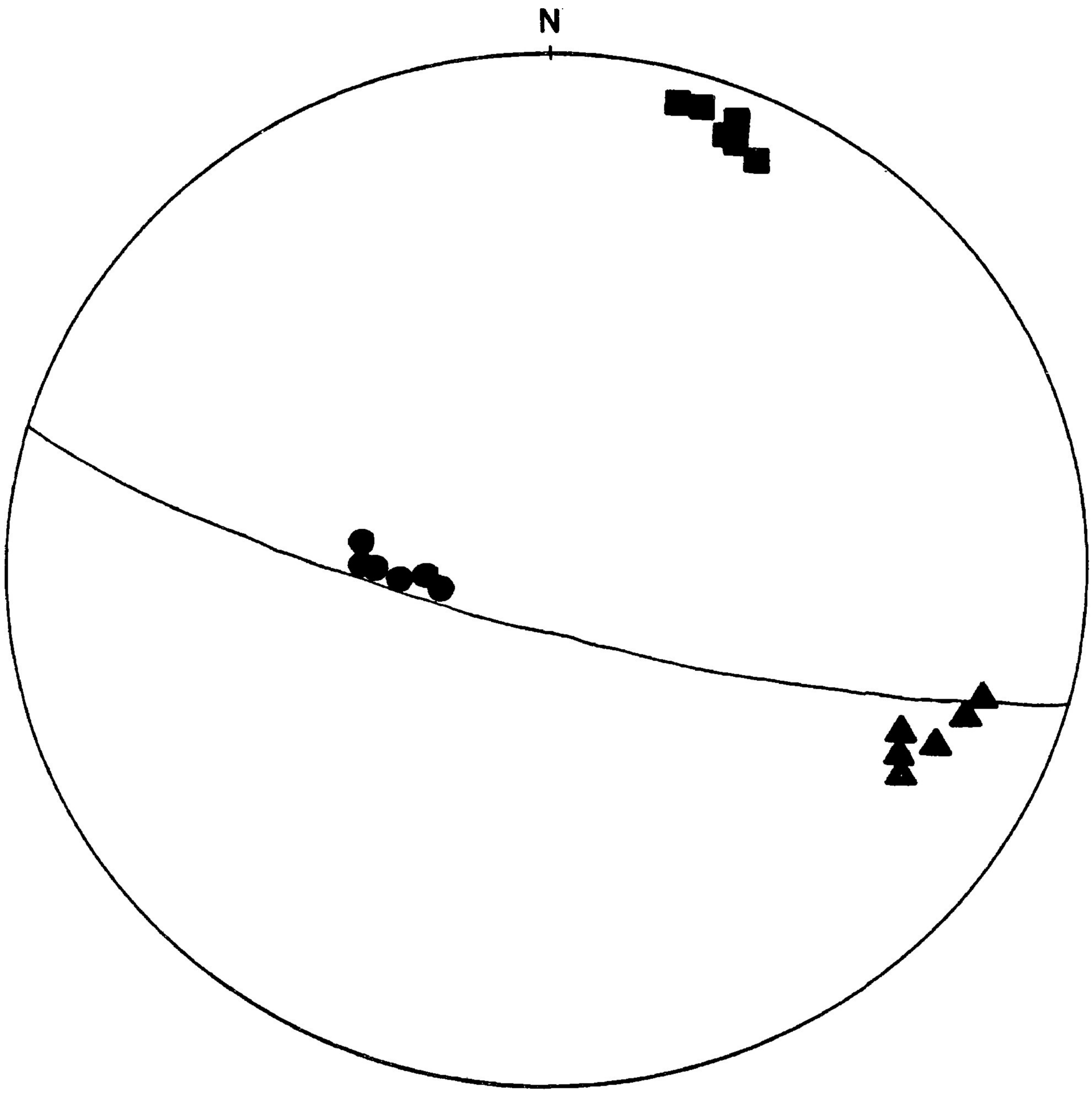

Shebandowan-type arkose.

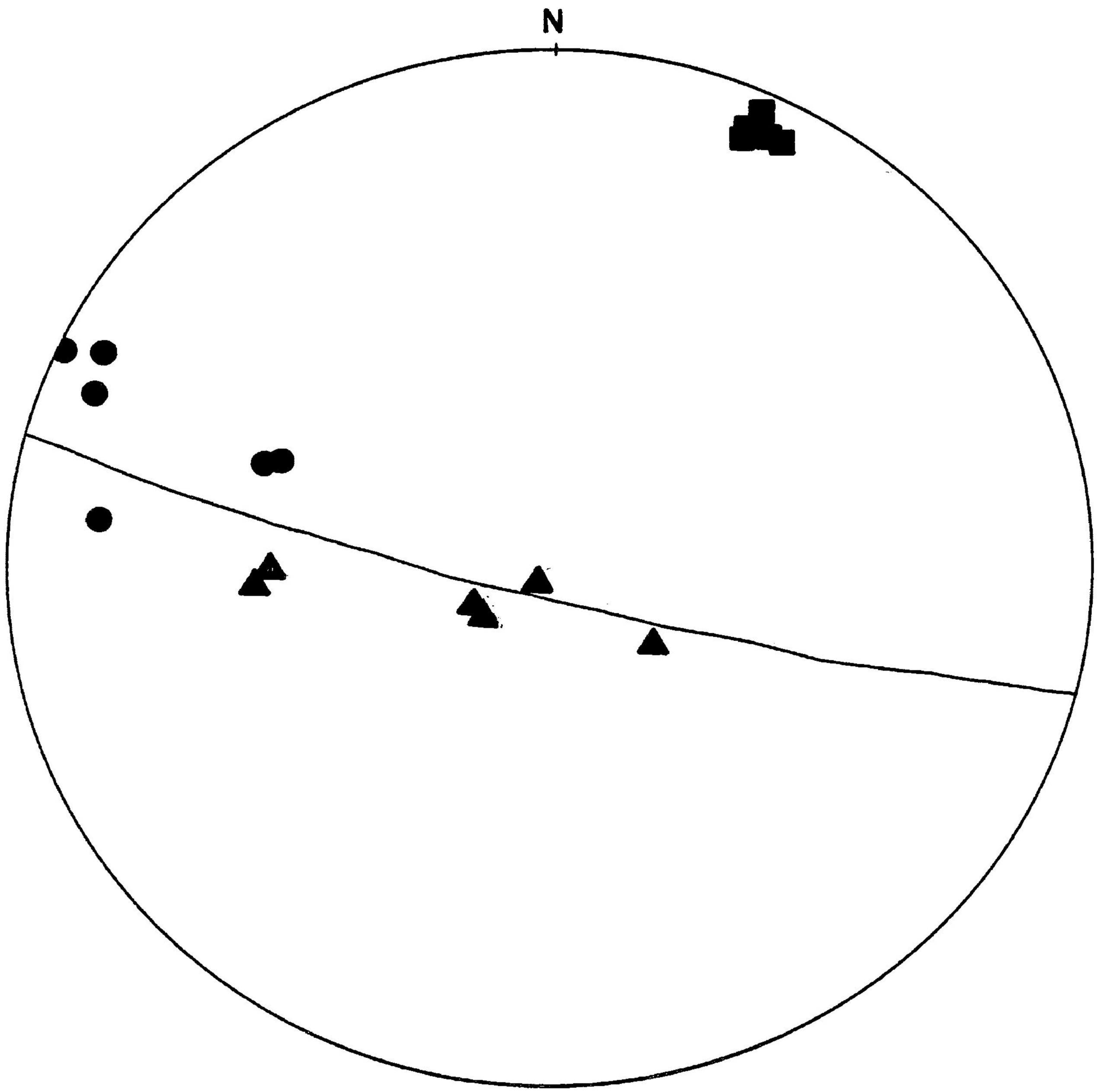

Shebandowan-type sandstone.

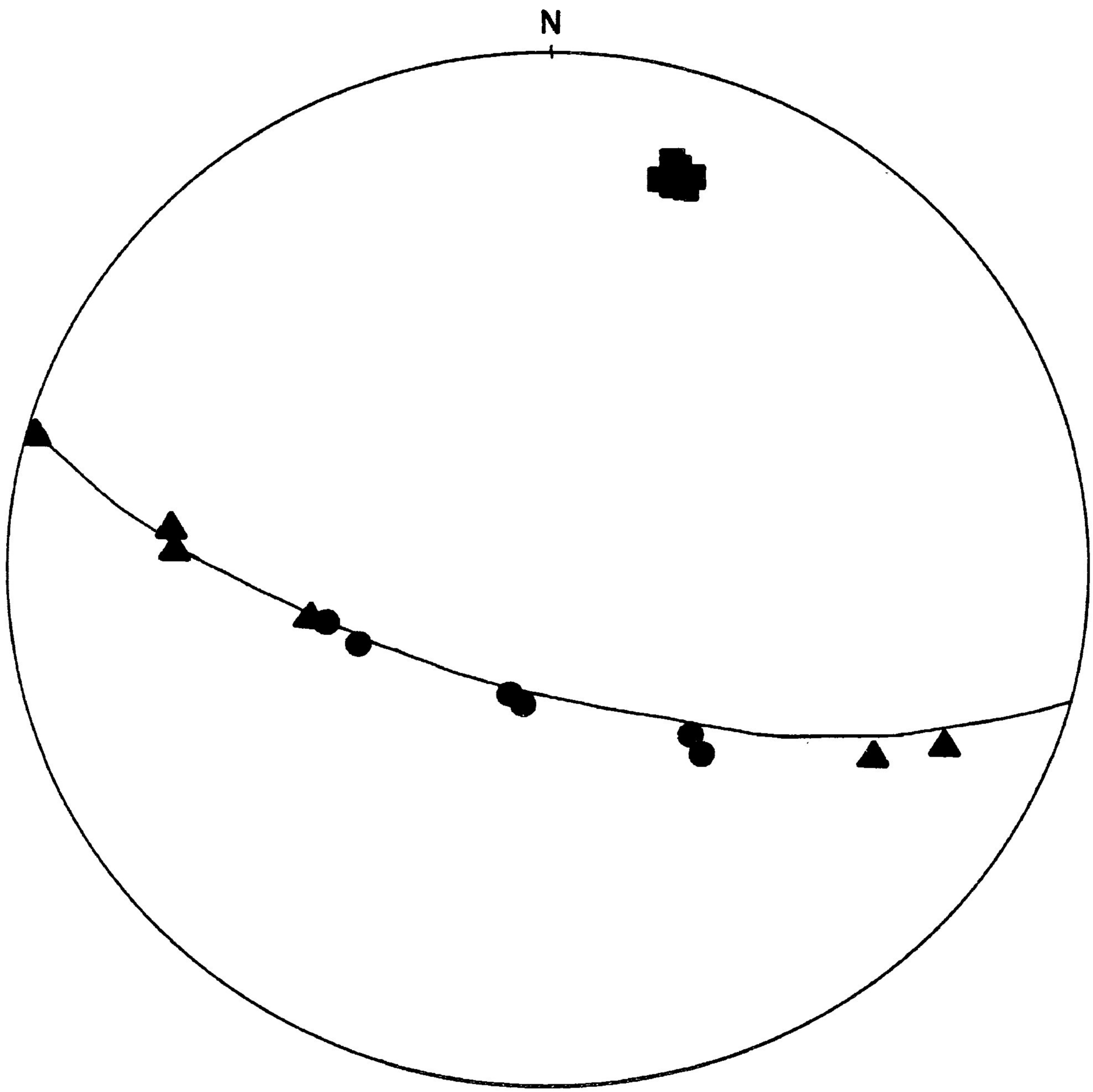

Shebandowan-type sandstone.

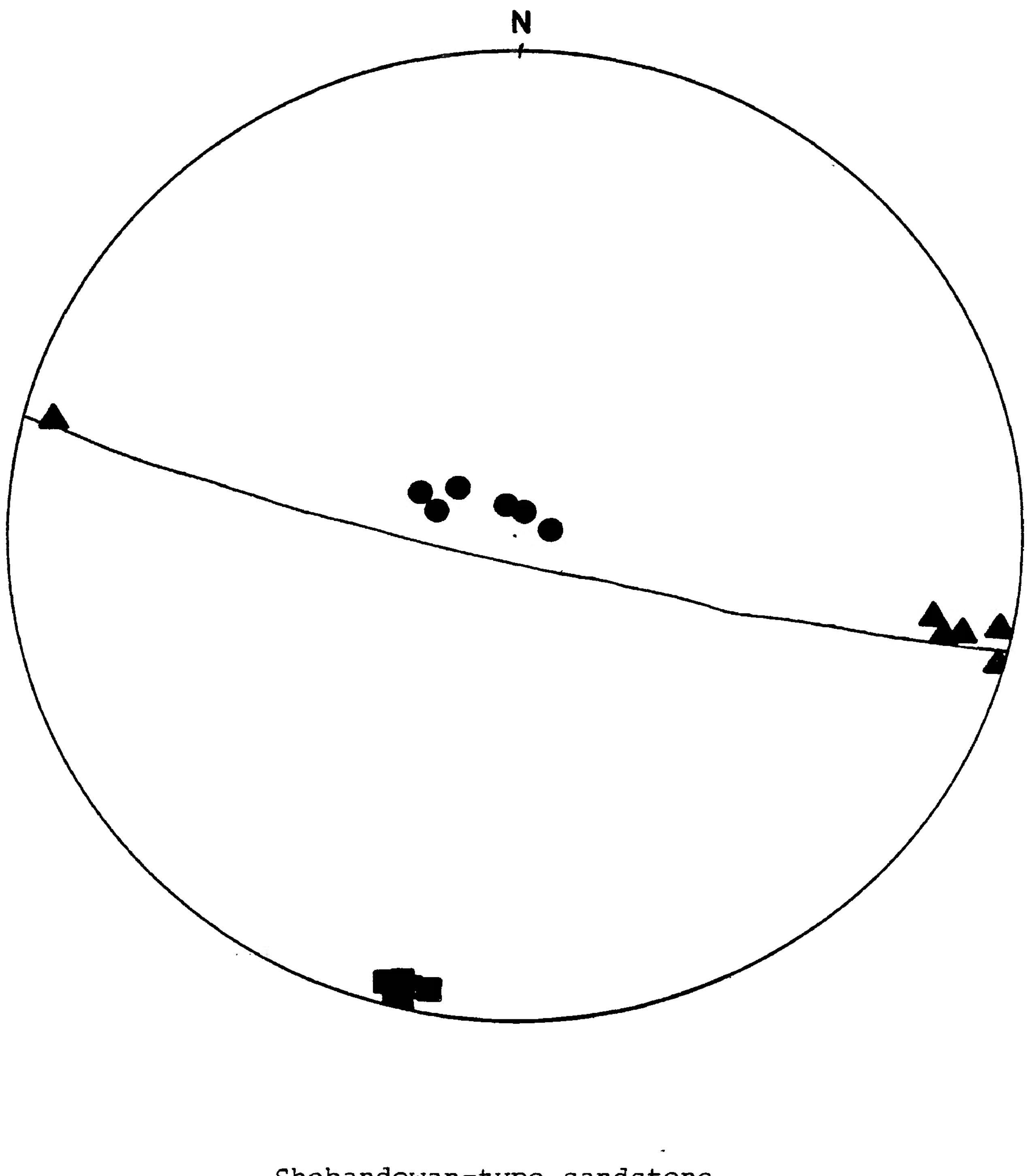

Shebandowan-type sandstone.

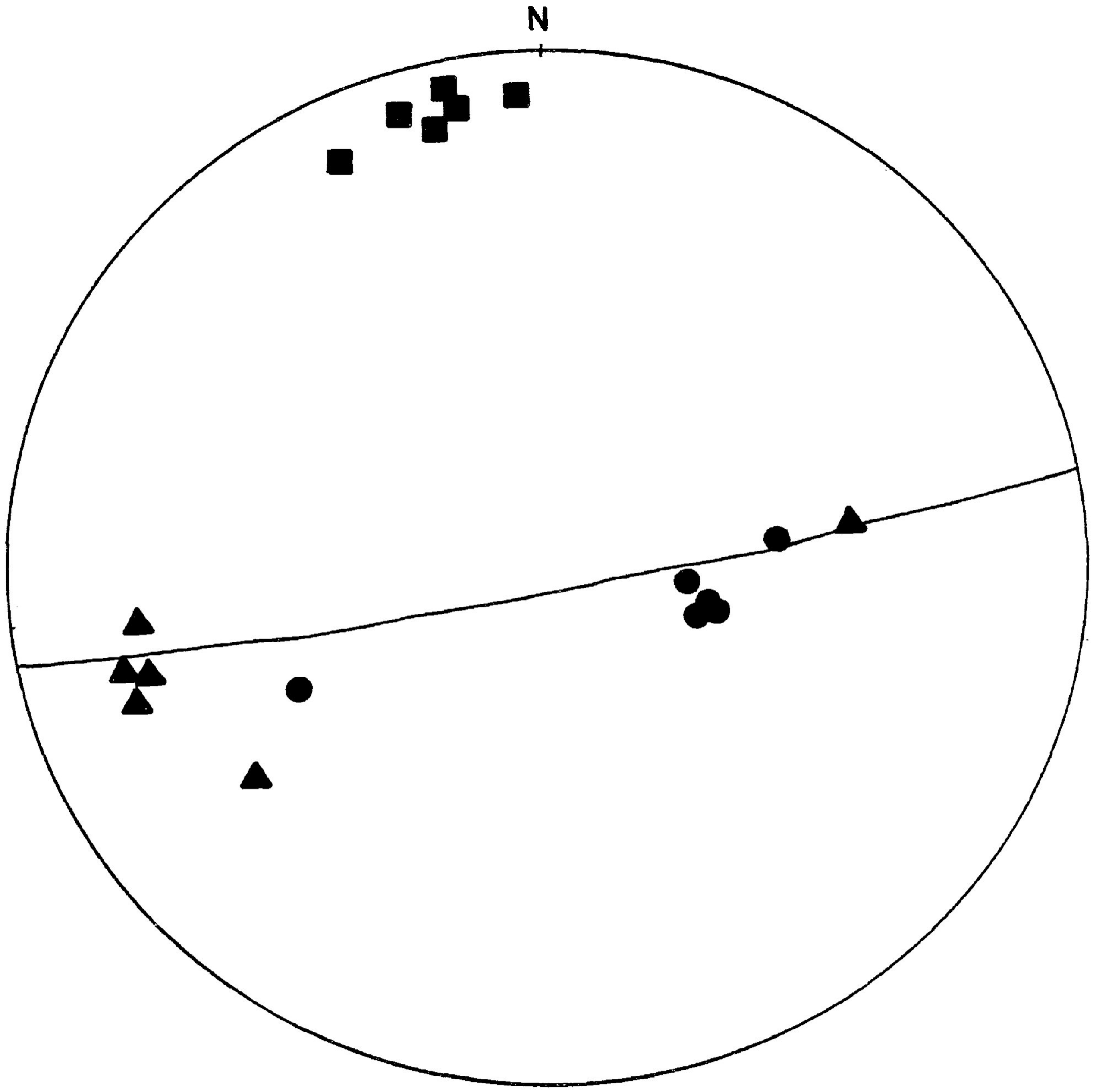

Shebandowan-type sandstone.

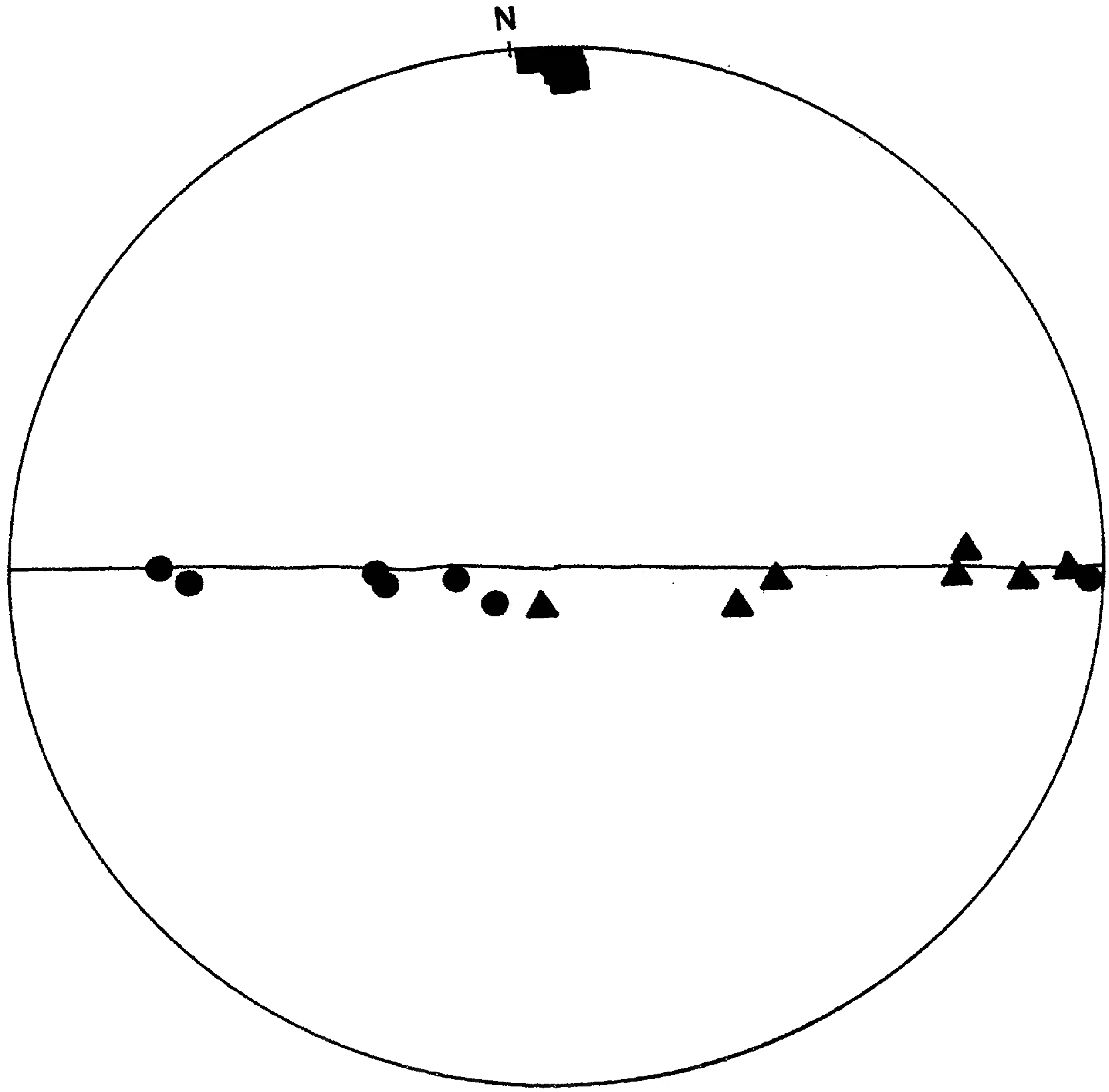

Shebandowan-type sandstone.

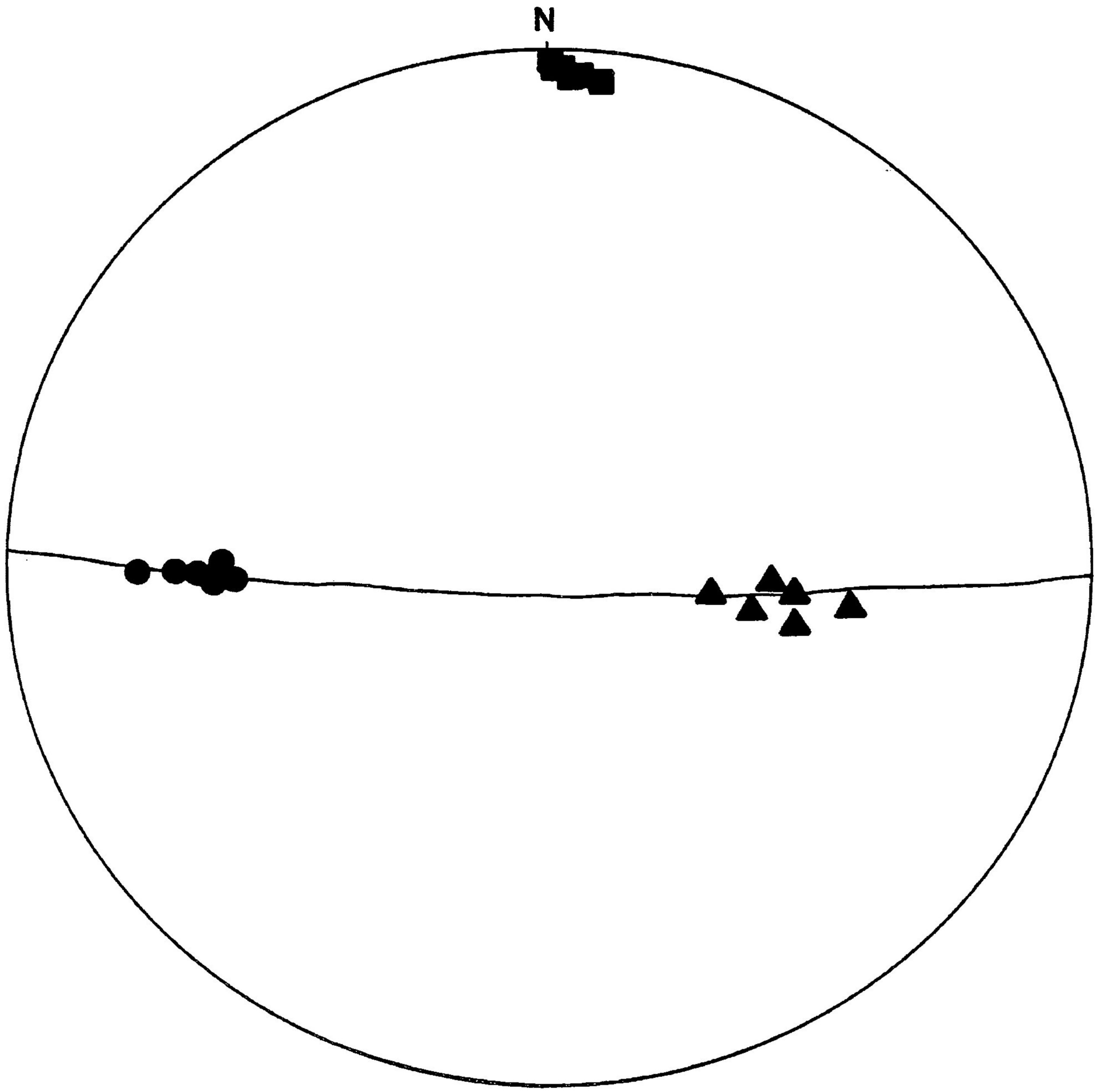

Shebandowan-type sandstone.

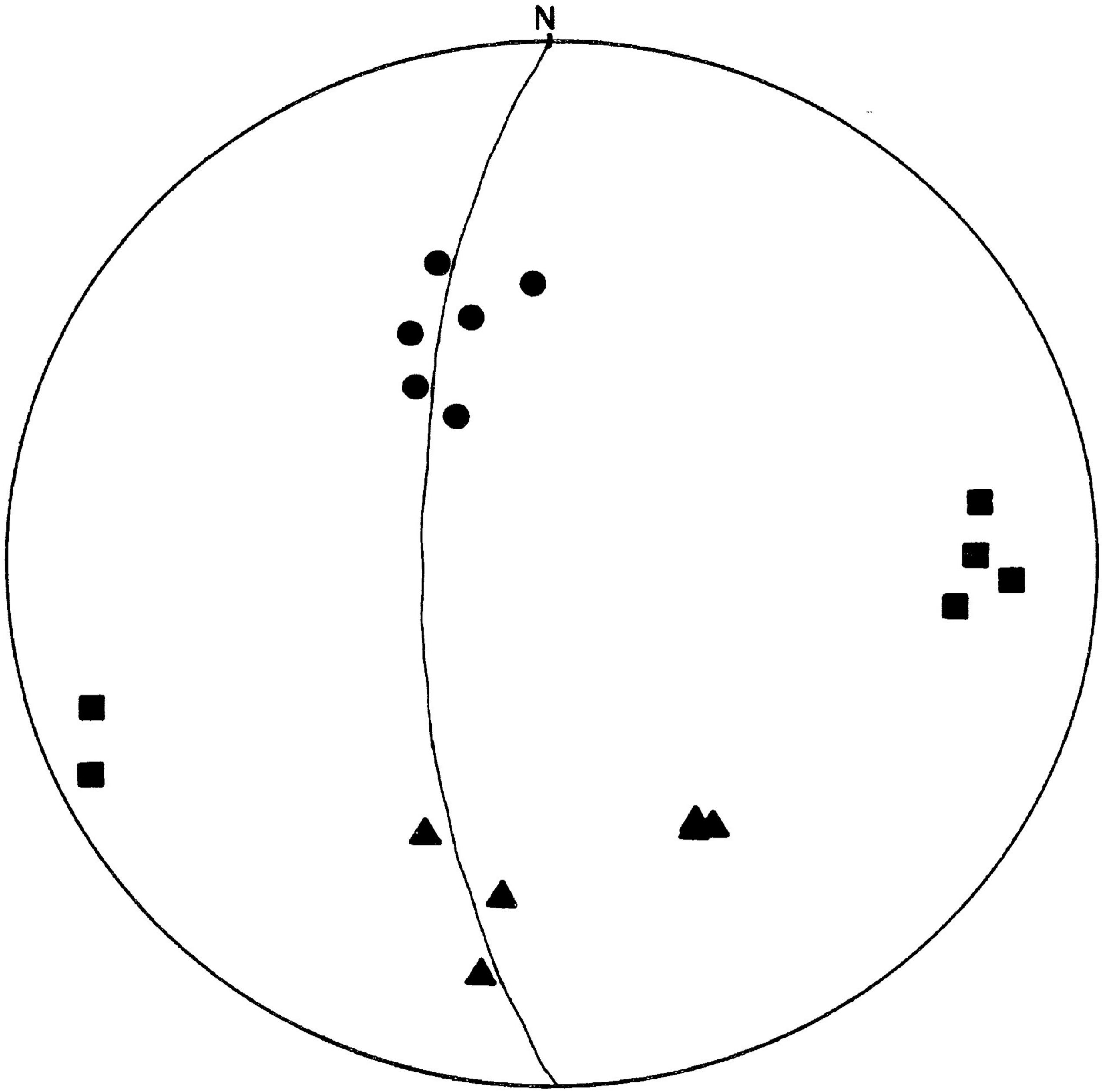

Gabbro from the Kashabowie area; outside of present study area.

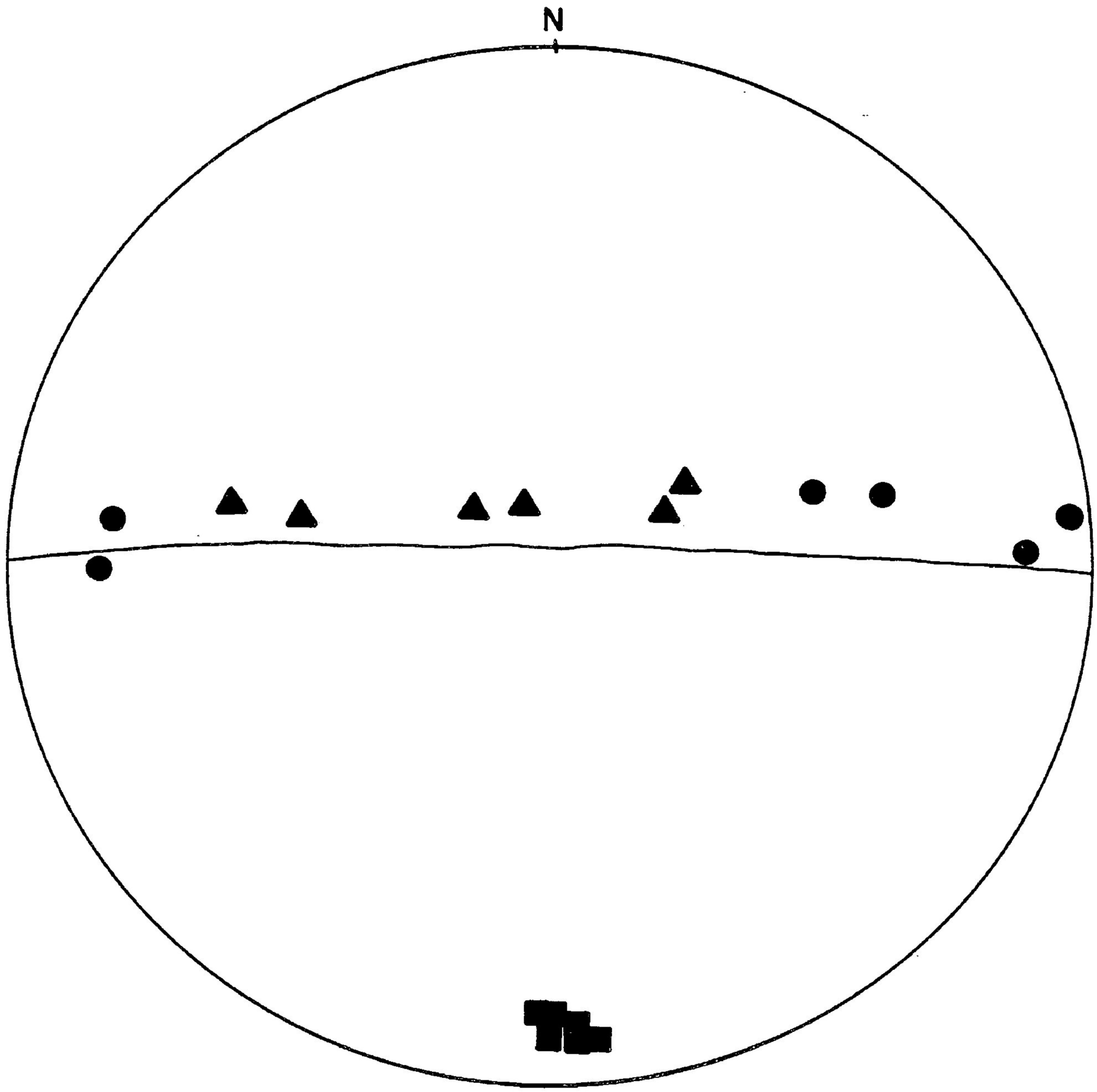

Gabbro from the Kashabowie area;
outside of the present study area.

REFERENCES

BAYLY, B. 1974. Cleavage not parallel to finite-strain ellipsoid's XY-plane: Discussion. Tectonophysics, v.23, p.205-207.

BEAKHOUSE, G. P. 1974. Volcanic stratigraphy in the Greenwater-Upper Shebandowan Lakes area, Northwestern Ont. In - Centre for Precambrian Studies, Univ. of Man., Ann. Rep. for 1974, Pt.2, p.89-99.

BORRADAILE, G. J. 1978. Transected folds - A study illustrated with examples from Canada and Scotland. Geol. Soc. Am. Bull., v.89, p.481-493.

BORRADAILE, G. J. 1980. Structural Mapping Techniques, 1979-80 Edition, Unpub. teaching manual, Lakehead Univ. 221 pages.

BORRADAILE, G. J. 1981. Particulate flow of rock and the formation of cleavage. Tectonophysics, v.72 p.305-321.

BORRADAILE, G. J. 1982. Tectonically deformed pillow lava as an indicator of bedding and way-up. Journal Struc. Geol. v.4, No.4, p.469-479.

BORRADAILE, G. J. and TARLING, D. H. 1981. The influence of deformation mechanisms on magnetic fabrics in weakly deformed rocks. Tectonophysics, v.77, p.151-168.

CORFU, F. and STOTT, G. M. 1985. U-Pb geochronology and tectonic history of the Shebandowan belt, Northwestern Ontario. 31st Ann. Inst. on Lake Superior Geology, Kenora, Ont., p.15-16.

DIETERICH, J. H. 1969. Origin of cleavage in folded rocks. Am. Journ. Sci., v.267, p.155-165.

DURNEY, D. W. 1972. Solution-transfer, an important geological deformation mechanism. Nature, v.235, p.315-317.

ETHERIDGE, M. A., PATERSON, M. S. and HOBBS, B. E. 1974. Experimentally produced preferred orientation in synthetic mica aggregates. Contr. Mineral. and Petrol., v.44, p.275-294.

GRAHAM, R. W. 1954. Magnetic susceptibility anisotropy, an unexploited petrofabric element. Geol. Soc. Am. Bull., v.65, p.1257-1258.

HAMILTON, N. and REES, A. I. 1971. The anisotropy of magnetic susceptibility of the Franciscan rocks of the Diablo Range, Central California. Geol. Runds., v.60, p.1103-1124.

HENDERSON, J.R. 1981. Structural analysis of sheath folds with horizontal X-axes, northeast Canada. Journ. Struct. Geol., v. 3, p. 203-210.

HOBBS, B. E., MEANS, W. D., WILLIAMS, P. F. 1976. An outline of Structural Geology. John Wiley and Sons, pub. 571 pp.

HROUDA, F. 1976a. The origin of cleavage in the light of magnetic anisotropy investigations. Physics of the Earth and Planetary Interiors, v.13, p.132-142.

HROUDA, F. 1976b. A model for the orientation process of the ferromagnetic minerals in slates. Earth and Planet. Sci. Lett., v.33, p.107-110.

HROUDA, F. 1982. Magnetic anisotropy of rocks and its application in geology and geophysics. Geophysical Surveys, v.5, p.37-82.

HROUDA, F., JANAK, F., REJL, L. and WEISS, J. 1971. The use of magnetic susceptibility anisotropy for estimating the ferromagnetic mineral fabrics of metamorphic rocks. Geol. Runds., v.60, p.1124-1142.

IRVING, E. 1964. Paleomagnetism and its application to geological and geophysical problems. John Wiley and Sons, pub. 440 pp.

KEHLENBECK, M. M. 1983. Use of stratigraphic and structural-facing directions to delineate the geometry of refolded folds near Thunder Bay, Ontario. Geoscience Canada, v.11, No.1, p.23-32.

KLIGFIELD, R., LOWRIE, W., and DALZIEL, I. W. D. 1977. Magnetic susceptibility anisotropy as a strain indicator in the Sudbury Basin, Ontario. Tectonophysics, v.40, p.287-308.

MCINNES, W. 1899. Report on the geology of the area covered by the Seine River and Lake Shebandowan map sheets. GSC Ann. Rep., v.10, 1899, pt.H.

MOON, C. F. 1972. The microstructure of clay sediments. Earth Sci. Rev., v.8, p.303-321.

MORIN, J. A. 1973. Geology of the Lower Shebandowan Lake area, District of Thunder Bay. ODM Geol. Rep. 110, 45 p.

MORTON, P. 1979. Volcanic stratigraphy in the Shebandowan Ni-Cu Mine area, Ontario. In - Current Research, Geol. Surv. Can., Paper 79-1B, p.39-43.

MORTON, P. 1982. Archean volcanic stratigraphy, and petrology and chemistry of mafic and ultramafic rocks, chromite and the Shebandowan Ni-Cu Mine, Shebandowan, Northwestern Ontario. Unpub. PhD thesis, Carleton Univ., 346 p.

O'BRIAN, N. R. 1970. The fabric of shale - an electron microscope study. Sedimentology, v.15, p.229-246.

PETTIJOHN, F. J. 1975. Sedimentary Rocks, Third edition. Harper and Row., 628 p.

POULSEN, K. H., BORRADAILE, G. J. and KEHLENBECK, M. M. 1980. An inverted Archean succession at Rainy Lake. Can. Journ. Earth Sci., v.17, p.1358-1369.

POWELL, C. McA. 1974. Timing of slaty cleavage during folding of Precambrian rocks, northwest Tasmania. Geol. Soc. Am. Bull., v.85, p.1043-1060.

PYE, E. G. and FENWICK, K. G. 1965. Atikokan-Lakehead Sheet, District of Thunder Bay. ODM Geol. Comp. Series, Map 2065, scale 1 inch to 4 miles.

RAMSAY, J. G. 1967. Folding and fracturing of rocks. McGraw-Hill, New York, 568 p.

RATHORE, J. S. 1979. Magnetic susceptibiltiy anisotropy in the Cambrian Slate Belt of North Wales and correlation with strain. Tectonophysics, v.53, p.83-97.

SHEGELSKI, R. J. 1980. Archean cratonization, emergence and red bed development, Lake Shebandowan Area, Canada. Precam. Res., v.12, p.331-347.

SIDDANS, A. W. B. 1972. Slaty Cleavage - A review of research since 1815. Earth Sci. Rev., v.8, p.205-232.

STOTT, G. M. and SCHNIEDERS, B. R. 1983. Gold mineralization in the Shebandowan belt and its relation to regional deformation patterns, p.181-193 in-The Geology of Gold in Ontario, edited by A. C. Colvine, Ont. Geol. Surv. Misc. Paper 110, 278 p.

STOTT, G. M., and SCHWERDTNER, W. M. 1981. A structural analysis of the central part of the Shebandowan metavolcanic-metasedimentary belt. OGS, Open File Rep. 5349, 44 p.

TANTON, T. L. 1922. Palladium-bearing nickel deposit at Shebandowan Lake, Thunder Bay District, Ontario. GSC Summ. Rept., Pt.D, p.1-8.

TANTON, T. L. 1938. Quetico-Sheet (East Half) Thunder Bay and Rainy River Districts, Ontario. Geol. Surv. Can., Map 432A.

WATSON, R. J. 1928. Platinum-bearing nickel-copper deposit on Lower Shebandowan Lake, District of Thunder Bay. ODM Annual Reprt, v.37, Pt.4, p.128-149.

WEBER, K. 1982. Scanning electron microscope study of slates from the Rheinische Schiefergebirge, in-Atlas of defôrmational and metamorphic rock fabrics. Borradaile, G. J., Bayly, B., and Powell, C. McA., (eds.). Springer Verlag, Heidelber. 450 pp.

WHITTEN, D. G. A. and BROOKS, J. R. V. 1972. A dictionary of geology. Penguin Books. 519 pp.

WILLIAMS, P. F. 1976. Relationship between axial-plane foliations and strain. Tectonophysics, v.30, p.181-196.

WILLIAMS, P. F. 1977. Foliation; a review and discussion. Tectonophysics, v.39, No.1-3, p.305-328.

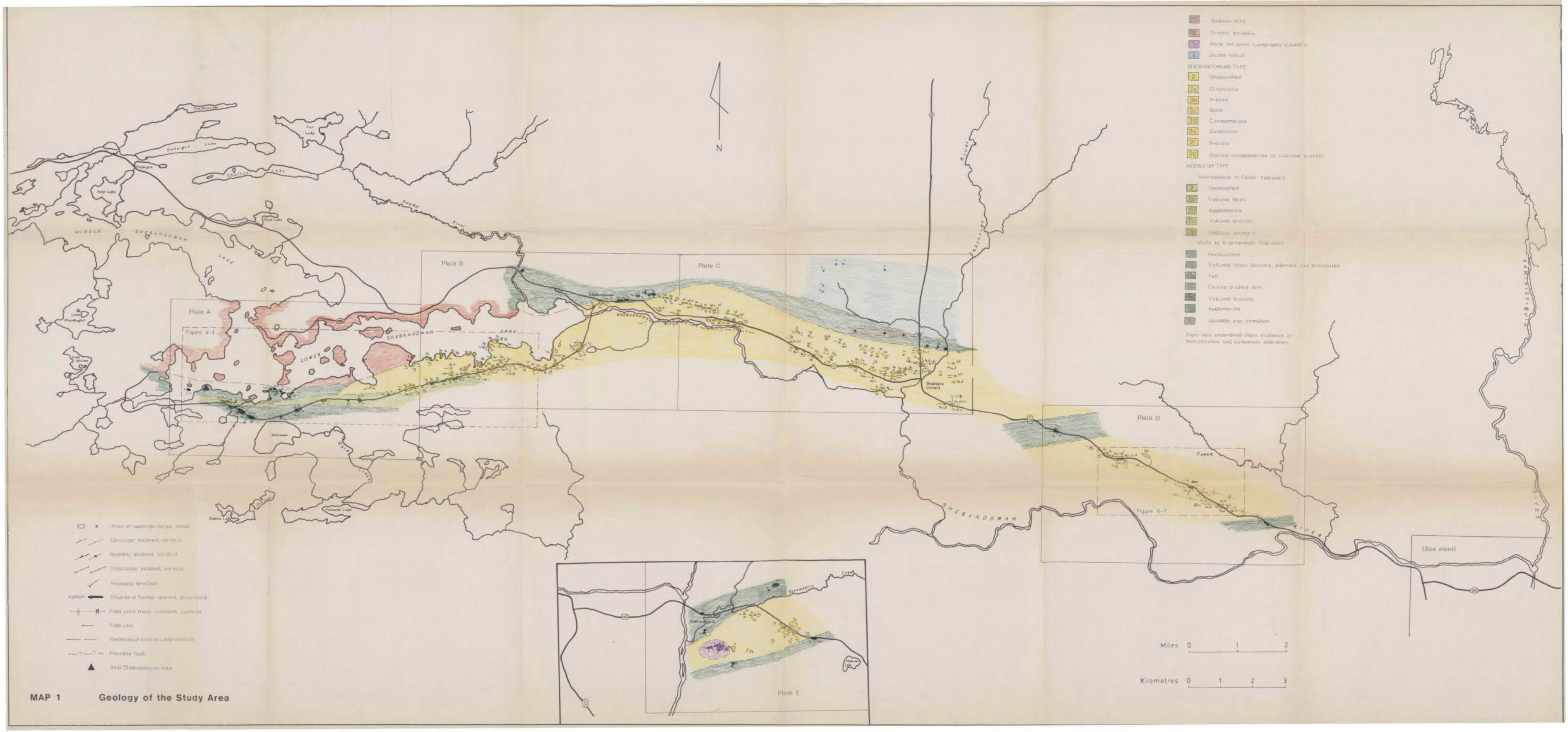

MAP 1 **Geology of the Study Area**

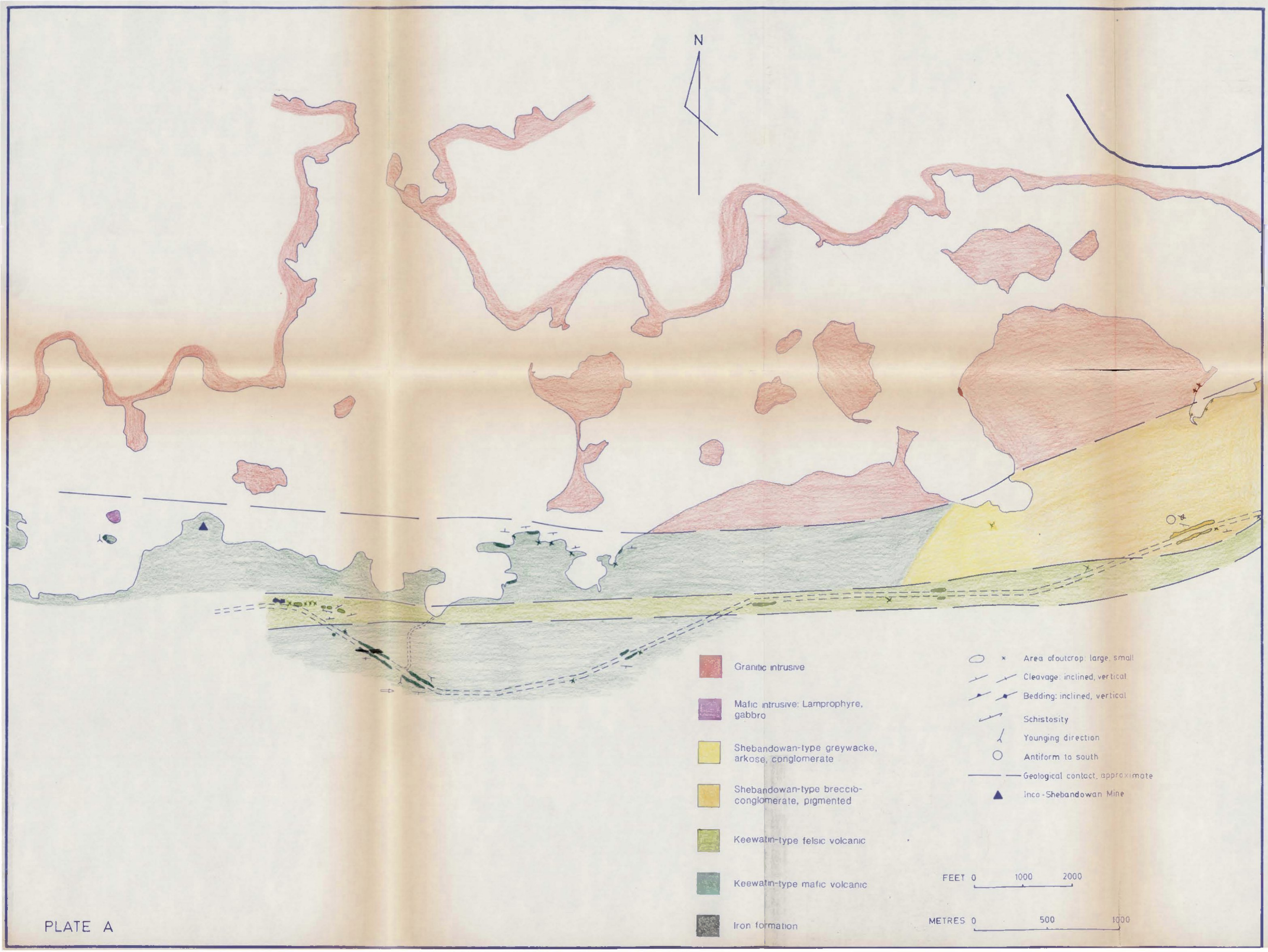
N
Granitic intrusive
Mafic intrusive: Lamprophyre, gabbro
Shebandowan-type greywacke, arkose, conglomerate
Shebandowan-type breccio-conglomerate, pigmented
Keewatin-type felsic volcanic
Keewatin-type mafic volcanic
Iron formation
Area of outcrop: large, small
Cleavage: inclined, vertical
Bedding: inclined, vertical
Schistosity
Younging direction
Antiform to south
Geological contact, approximate
Inco-Shebandowan Mine
FEET 0 1000 2000
METRES 0 500 1000

PLATE A


N
Granitic intrusive
Shebandowan-type greywacke, arkose, conglomerate
Shebandowan-type breccio-conglomerate, pigmented
Keewatin-type felsic volcanic
Keewatin-type mafic volcanic
Area of outcrop: large, small
Cleavage: inclined, vertical
Bedding: inclined, vertical
Schistosity, inclined, vertical
Younging direction
Structural facing, upward
Antiform to south
Antiform to north
Fold axial trace: antiform, synform
Geological contact, approximate
Possible fault
Hydroelectrical and telephone lines
FEET 0 1000 2000
METRES 0 500 1000

PLATE B

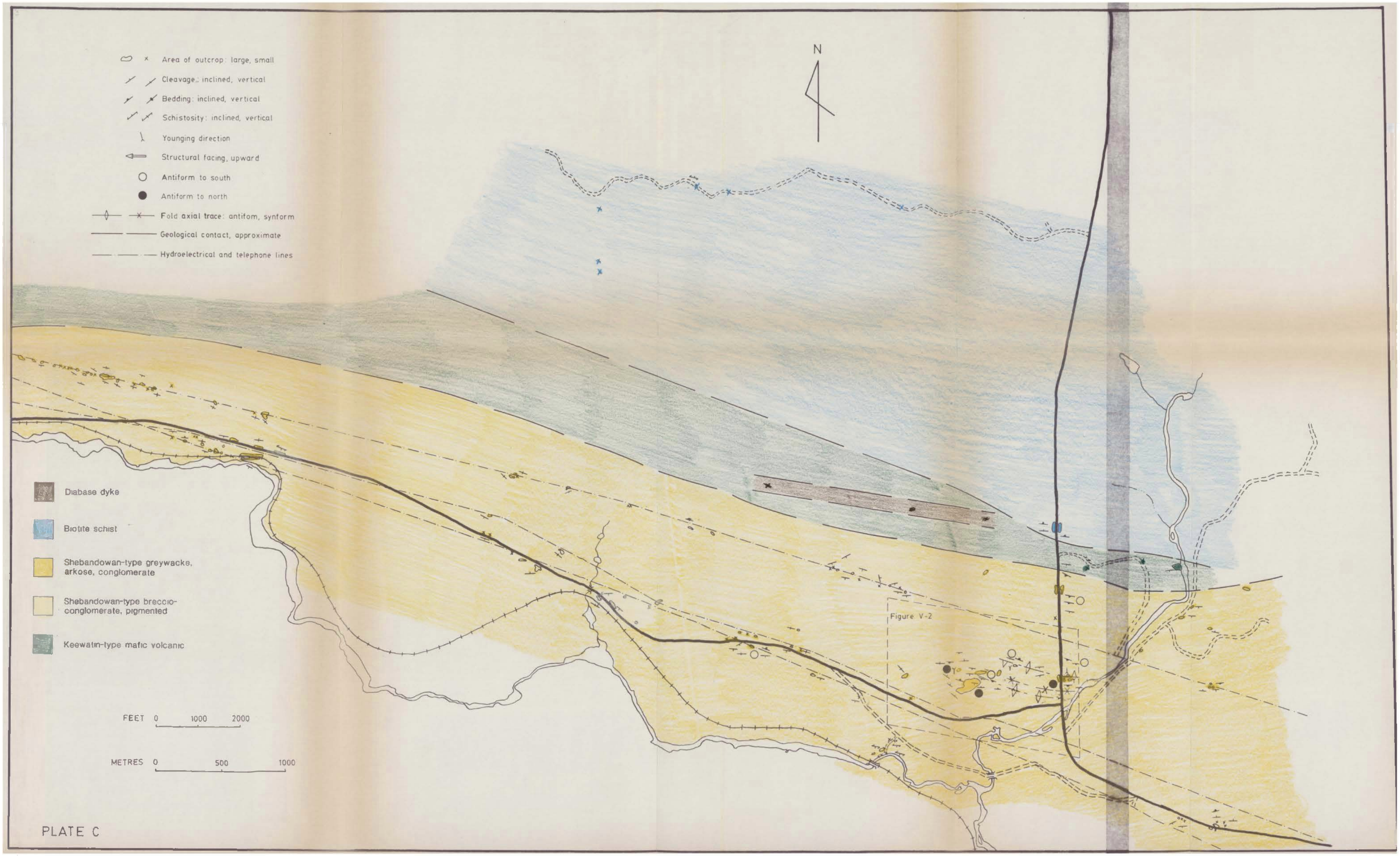
N
Area of outcrop: large, small
Cleavage: inclined, vertical
Bedding: inclined, vertical
Schistosity: inclined, vertical
Younging direction
Structural facing, upward
Antiform to south
Antiform to north
Fold axial trace: antifom, synform
Geological contact, approximate
Hydroelectrical and telephone lines
Diabase dyke
Biotite schist
Shebandowan-type greywacke, arkose, conglomerate
Shebandowan-type breccio-conglomerate, pigmented
Keewatin-type mafic volcanic
FEET 0 1000 2000
METRES 0 500 1000
Figure V-2

PLATE C

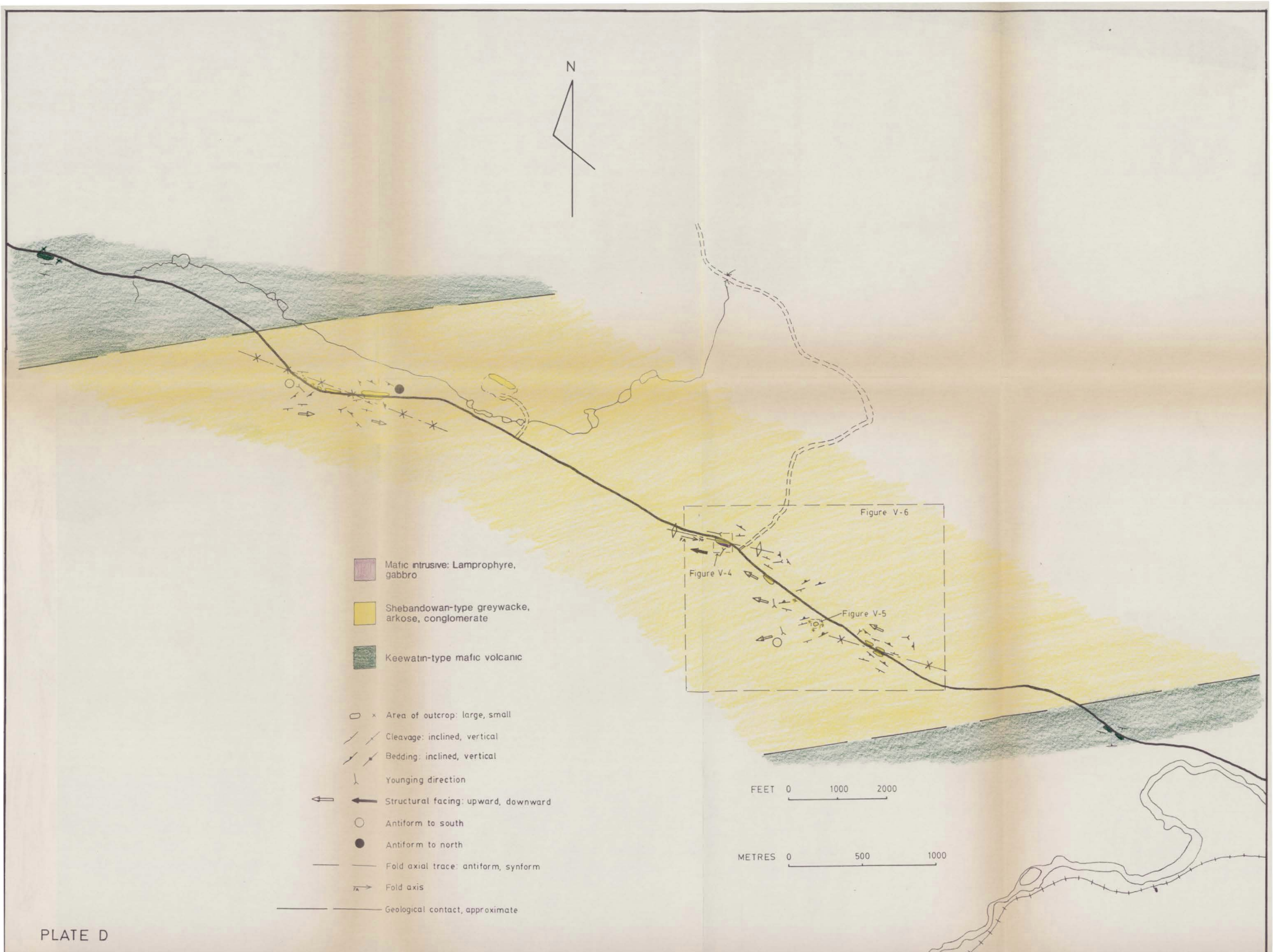
N
Figure V-6
Figure V-4
Figure V-5
Mafic intrusive: Lamprophyre, gabbro
Shebandowan-type greywacke, arkose, conglomerate
Keewatin-type mafic volcanic
Area of outcrop: large, small
Cleavage: inclined, vertical
Bedding: inclined, vertical
Younging direction
Structural facing: upward, downward
Antiform to south
Antiform to north
Fold axial trace: antiform, synform
Fold axis
Geological contact, approximate
FEET 0 1000 2000
METRES 0 500 1000

PLATE D


N
Mafic intrusive: Lamprophyre, gabbro
Shebandowan-type greywacke, arkose, conglomerate
Shebandowan-type breccio-conglomerate, pigmented
Keewatin-type mafic volcanic
Iron formation
Area of outcrop: large, small
Cleavage: inclined, vertical
Bedding: inclined, vertical
Minor fold axis
Geological contact, approximate
Hydroelectrical and telephone line
Gravel pit
FEET 0 1000 2000
METRES 0 500 1000

PLATE E